University of Strathclyde

Strathclyde Institute of Pharmacy and Biomedical Sciences (SIPBS)

Biodegradable nanoparticles as a potential oral delivery system for oestradiol: Pharmacokinetic and pharmacodynamic evaluations

by

Girish Mittal

A thesis presented in fulfilment of the requirements for the degree of Doctor of Philosophy

2010

This thesis is the result of the author's original research. It has been composed by the author and has not been previously submitted for examination which has led to the award of a degree.

Signed:

Date:

Acknowledgements

My supervisor, Prof. MNV Ravi Kumar and co-supervisors, Dr. Hilary Carswell and Dr. Ros Brett for the guidance, support and encouragement during the project.

PhD studentship by the Faculty of Science, University of Strathclyde is gratefully acknowledged.

Dr. Susan Currie and Dr. Marie-Ann Ewart for the kind help in Western blotting studies.

A special mention to Shalmali Patkar, Tamara Martin, Dr. Paul Coats and Dr. Brendan Clarke for all the invaluable guidance and support in the cardiovascular lab.

Mark Thomson for demonstrating the prepulse inhibition (PPI) behavioural apparatus and for analyzing the data.

John, Stevie and all other members of BPU for taking care of the animals and for being immensely helpful.

Chandu for his great help during the animal experiments performed in India.

Nano-group members Dhawal Ankola, Gaurav Sharma, Jagdish Italia, Venkat Ratnam and Vivekanand Bhardwaj for sharing a great time throughout my PhD duration.

All the members of the drug delivery and cardiovascular lab for making my time at Strathclyde enjoyable and memorable.

Most importantly, a limitless gratitude to '*my family*' for the love, care, motivation and support.

Table of Contents

Chapter-2
A dose-dependent pharmacokinetic study of oral oestradiol nanoparticles

Chapter-3
Evaluating the potential of oral oestradiol nanoparticles in a rat model of hyperlipidaemia

Chapter-4
Oral delivery of oestradiol to brain aided by biodegradable nanoparticles

Chapter-5
Evaluation of oral oestradiol nanoparticles in a rat model of Alzheimer's disease

Abstract

The present dissertation was aimed at realizing the therapeutic potential of oestradiol by oral dosing aided by a nanoparticulate delivery system with a view to improving the bioavailability and minimizing the possible toxic effects of oestradiol. The most widely used polyester; poly(lactide-co-glycolide) (PLGA) was chosen to develop oestradiol entrapped nanoparticles by the emulsion-diffusion-evaporation method. The nanoparticles were in the size range of 100-150 nm and ideal for oral dosing. A detailed pharmacokinetic study of oestradiol as a function of dose and nanoparticle characteristics was carried out in rats, which demonstrated improved bioavailability and sustained release of oestradiol with the nanoparticulate formulations. These polymeric nanoparticles (given once in 3 days against daily administration of suspension) were subsequently evaluated in the ovariectomized (OVX) rat model of hyperlipidaemia, where they were found effective in treating post-menopausal hyperlipidaemia at a dose 3 times less than simple oral drug suspension. Further, attempts were also made to improve brain delivery of oestradiol by oral administration aided by Tween 80 (T-80) coated nanoparticles. The process of T-80 coating on the nanoparticles was optimized and the pharmacokinetics of oestradiol nanoparticles was studied as a function of T-80 coating. *In vitro* data in simulated gastric fluid (SGF) and simulated intestinal fluid (SIF) confirmed the stability of T-80 coating and the amount of the T-80 remaining on the surface was proportional to the initial coating concentration. Nanoparticles coated with 4% T-80 showed significantly higher brain oestradiol levels as compared to uncoated ones. Finally, these surface coated oestradiol nanoparticles were evaluated in the OVX rat model of Alzheimer's disease (AD) and were successful in preventing the expression of amyloid beta-42

(Aβ42) immunoreactivity in hippocampus. Together, the data indicates that nanoparticles can be tailored appropriately to achieve different target tissue drug levels that are not possible by conventional means, which can make the treatment/prevention of a variety of diseases possible.

Publications

1) Mittal, G., Kumar, M.N.V.R., 2009. Impact of polymeric nanoparticles on oral pharmacokinetics: a dose-dependent case study with estradiol. J. Pharm. Sci., 98, 3730-3734.

2) Mittal, G., Chandraiah, G., Ramarao, P., Kumar M.N.V.R., 2009. Pharmacodynamic evaluation of oral estradiol nanoparticles in estrogen deficient (ovariectomized) high-fat diet induced hyperlipidemic rat model. Pharm. Res., 26, 218-223.

List of abbreviations

AD	Alzheimer's Disease
AF	Activation Function
AUC	Area Under The Curve
Aβ	Amyloid Beta
BBB	Blood–Brain Barrier
BMD	Bone Mineral Density
cAMP	Cyclic Adenosine Monophosphate
CNS	Central Nervous System
CVD	Cardiovascular Disease
DAB	Diaminobenzidine
dB	Decibel
DBD	DNA-Binding Domain
DG	Dentate Gyrus
D-gal	D-Galactose
DMAB	Didodecyl Dimethyl Ammonium Bromide
E1	Oestrone
E2	Oestradiol
E3	Oestriol
ELISA	Enzyme-Linked Immunosorbent Assay
EREs	Oestrogen-Response-Elements
ERs	Oestrogen Receptors
ERT	Oestrogen Replacement Therapy

ERα	Oestrogen Receptor Alpha
ERβ	Oestrogen Receptor Beta
FAE	Follicle-Associated Epithelium
FSH	Follicle-Stimulating Hormone
GALT	Gut Associated Lymphoid Tissue
GAPDH	Glyceraldehyde 3 Phosphate Dehydrogenase
GFAP	Glial Fibrillary Acidic Protein
GI	Gastrointestinal
GnRH	Gonadotrophin Releasing Hormone
hCG	Human Chorionic Gonadotrophin
HDL	High-Density Lipoproteins
HDL-C	High-Density Lipoprotein Cholesterol
HERS	Heart And Estrogen/Progestin Replacement Study
HFD	High-Fat Diet
HPLC	High-Performance Liquid Chromatography
HRP	Horseradish Peroxidase
HRT	Hormone Replacement Therapy
i.v.	Intravenous
ICH	International Conference On Harmonization
IUDs	Intrauterine Devices
LBD	Ligand-Binding Domain
LDL	Low-Density Lipoproteins
LDL-C	Low-Density Lipoprotein Cholesterol

LH	Luteinizing Hormone
MAT	Mean Absorption Time
MDA	Malondialdehyde
MPS	Mononuclear Phagocytic System
MRT	Mean Residence Time
NFTs	Neurofibrillary Tangles
NGS	Normal Goat Serum
NP	Nanoparticles
NPD	Normal Pellet Diet
OVX	Ovariectomized
PBCA	Poly(Butylcyanoacrylate)
PDA	Photodiode Array
PDI	Polydispersity Index
PEG	Poly(Ethylene Glycol)
PGA	Poly(Glycolic Acid)
Pgp	P-Glycoprotein
PK	Pharmacokinetic
PLA	Poly(Lactic Acid)
PLGA	Poly(Lactide-co-Glycolide)
PP	Peyer's Patches
PPI	Prepulse Inhibition
PVA	Polyvinyl Alcohol
RES	Reticuloendothelial System

RME	Receptor Mediated Endocytosis
ROS	Reactive Oxygen Species
SD	Sprague-Dawley
SGF	Simulated Gastric Fluid
SHBG	Sex Hormone Binding Globulin
SIF	Simulated Intestinal Fluid
T-80	Tween 80
TBA	Thiobarbituric Acid
TBARS	Thiobarbituric Acid Reacting Substances
TC	Total Cholesterol
TG	Triglycerides
VLCL-C	Very Low-Density Lipoprotein Cholesterol
WHI	Women's Health Initiative
ZP	Zeta Potential

Chapter-1
General Introduction

1.1 Oestrogens

Oestrogens are endogenous hormones with several physiological actions (Table 1.1) (Birkhauser *et al*., 1996; Ruggiero and Likis, 2002). There are three principal forms of oestrogens found in the human body: oestrone (E1), oestradiol (E2) and oestriol (E3). Among these naturally occurring oestrogens, oestradiol has the highest affinity for oestrogen receptors and therefore is most potent followed by the oestrone and oestriol. It is also the predominant circulatory oestrogen during the pre-menopausal period, and is mainly secreted by the ovaries. In post-menopausal women, the principal form of circulating oestrogen is oestrone, which is synthesized in the adipose tissue by peripheral conversion of adrenal androstenedione. However, during pregnancy, oestriol is the main oestrogen produced by placenta (Loose-Mitchell and Stancel, 2001; Bennink, 2004).

1.1.1 Biosynthesis

In humans, the biosynthesis of oestrogens takes place at a number of different sites. The major sites are the ovarian follicles in pre-menopausal women, the adipose tissue in post-menopausal women, and the placenta in pregnant women (Nelson and Bulun, 2001; Ackerman and Carr, 2002). The ovarian follicles are composed of an outer layer of thecal cells and an inner layer of granulosa cells surrounding the oocyte. Thecal cells have the luteinizing hormone (LH) receptors situated on them. LH stimulates the activity of adenylate cyclase, which produces cyclic adenosine monophosphate (cAMP). cAMP serves as a second messenger to increase the messenger RNA (mRNA) for the low-density lipoprotein (LDL) receptor and thereby, increasing the binding and uptake of LDL cholesterol. Cholesterol is then transported to the inner mitochondrial membrane by cAMP-activated steroidogenic acute regulatory (StAR) protein, a 30-kDa mitochondrial

Table 1.1

Key physiological actions of oestrogens

	Action	Significance
Genital tract	Development and maintenance of the female sex organs and secondary sex characteristics. Proliferation of endometrium, regulation of gonadotrophins secretion for ovulation and preparation of tissue for progesterone response	Regulation of menstrual cycle in pre-menopausal women
Breast	Stimulate proliferation of glandular and ductal tissue in breast (trophic effect) and alveolar growth	Develop breast tissue in puberty secondary to onset of ovulation and ovarian production of oestriol
Skin and muscle	Increase water and hyaluronic acid concentrations; alters collagen metabolism and decreases epithelial proliferation	Decreased oestrogen induces wrinkles and vaginal atrophy in post-menopausal women
Bone	Maintenance of bone mass by increasing the production of transforming growth factor-β by osteoclasts which may induce osteoclasts cell death and thus inhibit bone resorption and thereby, increase the bone mineral density (BMD)	Increased risk of fracture in post-menopausal women
Liver	Increase the synthesis of high-density lipoproteins (HDL), and clearance of low-density lipoproteins (LDL)	Improve lipid profile with decreased risk for atherosclerosis and/or cardiovascular disorders
Brain	Neuroprotective action	Increased risk of neurodegenerative disorders in post-menopausal women

(Adapted with modifications from Ruggiero and Likis, 2002)

protein which is believed to be the key moderator in the induction of steroidogenesis. Thecal cells produce the androgens (androstenedione and testosterone) in response to LH. The androgens cross the basement membrane to reach granulosa cells where aromatase transforms them into oestrogens (oestrone and oestradiol respectively). Aromatase is a follicle-stimulating hormone (FSH) dependent enzyme and the FSH receptors are located on granulosa cells (Simoni *et al*., 1997; Findlay and Drummond, 1999). Oestrone is also subsequently converted to oestradiol by the enzyme 17β-hydroxysteroid dehydrogenase. In humans, oestrogens are produced by pregnenolone pathway and steroidogenesis starts with the conversion of cholesterol to pregnenolone. The biosynthetic pathway involves 3 cytochrome P450 isoforms: cholesterol side-chain cleavage (CYP11A1), 17α-hydroxylase (CYP17) and aromatase (CYP19). In addition, it also involves two hydrogenases: 3β-hydroxysteroid dehydrogenase and 17β-hydroxysteroid dehydrogenase (McAllister *et al*., 1989). The entire pathway of oestrogens biosynthesis in the human ovary is presented in Fig. 1.1.

1.2 Menstrual cycle

The menstrual cycle can be described as a recurring event of physiological changes that take place in females of reproductive age. In humans, there is an overt menstruation (where there is blood flow from the vagina) while females of other species of placental mammal have oestrous cycle, which is characterized by complete reabsorption of endometrium at the end of reproductive cycle (also known as covert menstruation). The menstrual cycle is essential for reproduction and is controlled by the endocrine system of the body. It can be divided into 3 phases: follicular phase, ovulatory phase, and luteal phase. The length of each menstrual phase can vary from woman to woman and cycle to cycle and the average menstrual cycle length is

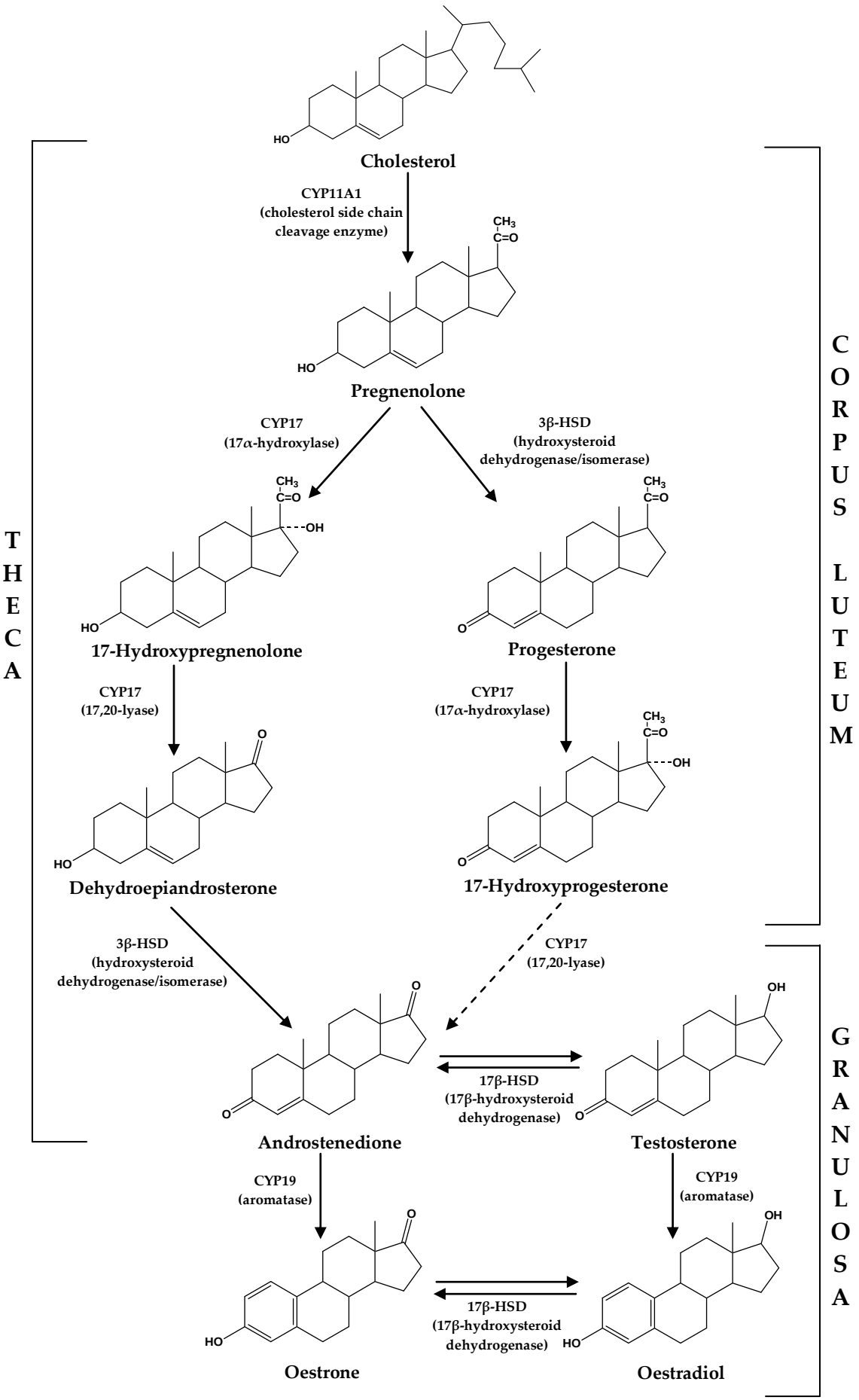

Fig. 1.1 Pathway of oestrogen biosynthesis in the human ovary.
(Adapted from Ackerman and Carr, 2002).

considered as 28 days. Serum oestrogen levels are not constant in the pre-menopausal women and depend on the phase of menstrual cycle (Owen, 1975; Chabbert-Buffet and Bouchard, 2002).

Follicular phase (also called proliferative phase): The menstrual cycle begins with menstruation (also called menstrual bleeding, menses, or a period). Menstruation is the breakdown and shedding of top layers of thickened lining of the uterus (endometrium) accompanied by bleeding. Menstruation occurs as a result of fall in oestrogen and progesterone levels at the end of previous menstrual cycle. Typical menstruation lasts for 3-5 days, but anywhere from 2-7 days is considered normal. During the follicular phase, gonadotrophin releasing hormone (GnRH) from the hypothalamus increases the production of FSH from the anterior pituitary gland (Knobil and Hotchkis, 1988; le Nestour *et al*., 1993). FSH then recruits a group of ovarian follicles, of which only one (called dominant follicle) grows to maturity and produces the highest concentration of oestrogen (McGee and Hsueh, 2000). Oestrogen initiates the proliferation of epithelial cells of new layer of endometrium in the uterus. The follicular phase often varies in length from one menstrual cycle to another in an individual woman and the average duration is about 13-14 days. (Ferenczy and Bergeron, 1991).

Ovulatory phase (also termed as transition phase): This phase starts with a surge in the levels of LH from the anterior pituitary gland under the influence of increased levels of oestrogen (a positive feed-back mechanism) (Clarke, 1995). LH stimulates the mature dominant ovarian follicle to rupture and release the egg. The ovulatory phase usually lasts 16 to 32 h and ends with the ovulation (Filicori, 1999; Filicori and Cognigni, 2001).

Luteal phase (also known as secretory phase): The luteal phase lasts about 14 days and ends just before the start of a new menstrual cycle. After the ovulation,

LH causes the transformation of ruptured follicle into a new structure called the corpus luteum (a process also known as luteinization) and induces the secretion of progesterone from the remaining granulosa cells. The oestrogen levels are also high during this time of the luteal phase. The high oestrogen and progesterone level induces a negative feed-back on pituitary gonadotrophins, FSH and LH which decrease in the circulation. Progesterone and oestrogen prepares the uterus for a possible fertilization and implantation of the embryo. If fertilization does not take place, human chorionic gonadotrophin (hCG) (a hormone produced by the embryo) is not present, and the corpus luteum degenerates causing a decline in oestrogen and progesterone levels. This decline leads to shedding of the endometrium and beginning of a new menstrual cycle (de Ziegler *et al*., 1992).

1.3 Mechanism of action

Oestrogens, like other steroid hormones, act primarily by regulating gene expression (Beato, 1989). They exert their effects by interaction with oestrogen receptors (ERs), which are members of the nuclear receptor superfamily (Evans, 1988; Katzenellenbogen and Katzenellenbogen, 1996; Mangelsdorf et al., 1998). There are 2 distinct nuclear ERs termed oestrogen receptor alpha (ERα) and beta (ERβ). These ERs are ligand-activated transcription factors that increase or decrease the synthesis of mRNA from target genes. Both ERs (ERα & ERβ) are composed of three functional domains: the NH_2-terminal or A/B domain, the C or DNA-binding domain (DBD), and the E/F or ligand-binding domain (LBD). ERα and ERβ share similar DBDs (96% homology) and similar LBDs (56% homology) and bind to the same hormone response element on DNA (Warner *et al*., 1999; Nilsson *et al*., 2001; Weiser *et al*., 2008). The N-terminal domain of nuclear receptors encodes a ligand-independent activation function (AF-1), a region of the

receptor involved in protein-protein interactions, and transcriptional activation of target-gene expression (Mcinerney and Katzenellenbogen, 1996). The DBD contains a two zinc finger structure, which plays an important role in receptor dimerization and in binding of receptors to specific DNA sequences (Umesono and Evans, 1989; Schwabe *et al*., 1993). The COOH-terminal, E/F, or LBD mediates ligand binding, heat-shock protein association, receptor dimerization, nuclear translocation, and hormone-dependent transactivation (AF-2) (Berry *et al*., 1990; Kraus *et al*., 1995). At the target cell, oestrogens diffuse freely across the plasma and nuclear membranes. The ER, in the absence of its ligand, is present in the nucleus inactively as a complex with heat shock proteins. The formation of ligand-receptor complex activates the ER by mediating the dissociation of heat shock proteins and allowing dimerization of receptors. The dimerized ER then binds to specific regulatory sequences in DNA called oestrogen-response-elements (EREs) and this results in subsequent genomic effects i.e. either gene transcription (i.e. mRNA synthesis) and translation (protein synthesis) or gene repression (inhibition of transcription) (Tsai and O'Malley, 1994; Hall *et al*., 2001; Nilsson *et al*., 2001; Kuhl, 2004).

1.4 Menopause and hormone replacement therapy (HRT)

Menopause is a natural physiological event in the life span of females. It is defined as the permanent termination of menstruation resulting from the loss of ovarian follicular activity, and it marks the end of a woman's reproductive capacity (Tanna, 2003a; Bruce and Rymer, 2009). Most women go through the menopause at about the average age of 50 years, although racial, genetic and socio-economic variations influence this average age. In the UK, the mean age for the menopause is 50 years and 9 months (Rymer and Morris, 2000). Symptoms usually start appearing in the peri-menopausal years. This refers

to the time prior to last menstrual period, and is considered to be a transition phase from fertile ovulatory cycles with well-defined hormonal profiles to the post-menopause with low oestrogen and progesterone and high gonadotrophin (FSH and LH) levels. The median onset of the peri-menopause is between 45.5 and 47.5 years, and it lasts for an average of 4 years (Rymer and Morris, 2000). Menopause is manifested by signs and symptoms of hormonal deficiency. Many symptoms are associated with the menopause, but hot flushes are the most common menopausal symptom and experienced by almost 75% of (post)menopausal women (Freedman, 2001; Bachmann, 2005). They normally last for 0.5-5 years after the natural menopause, but may continue for as long as 15 years in a small percentage of women (Bachmann, 1999). Other menopausal symptoms include insomnia, night sweats, palpitations, headaches, bone and joint pain, tiredness, vaginal atrophy, breast tenderness, and depression (Bruce and Rymer, 2009). HRT is the treatment of choice in the case of menopausal symptoms (Keep, 1990; Sitruk-Ware, 1990; Deady, 2004). HRT uses both natural (oestradiol, conjugated oestrogens) as well as synthetic (ethinyl oestradiol, diethylstilbestrol) oestrogens. In HRT, oestrogens can be given alone (called unopposed oestrogen) or in combination with another female hormone, progestin (Tanna, 2003a). However, when only oestrogens are prescribed, then the treatment is sometimes specifically called as oestrogen replacement therapy (ERT) in place of HRT. The pharmacological rationale behind HRT is to increase the circulating levels of oestrogens. If the main aim of treatment is to improve the menopausal symptoms, then HRT is given for two to three years. With short-term use for symptoms relief, potential benefits (improvement of vasomotor changes such as hot flushes and night sweats) are considered to outweigh the risks (eg. breast cancer) for most women.

However, therapy needs to last for at least five years to prevent the long term consequences (eg. osteoporosis) of menopause (Tanna, 2003a). In these cases, patients should be aware of increased risk of some diseases (eg. breast cancer) and need to decide (based on individualized risk-benefit evaluation) if HRT is a good treatment option. However, in both cases (short term or long term treatment) the patient's risks and benefits should be re-evaluated each year with continued HRT use.

1.5 Oestradiol: the most potent oestrogen

Oestradiol (E2) is substantially more potent than other oestrogens (oestrone and oestriol) at ERs. It is the principal systemic oestrogen in pre-menopausal women and is mainly secreted by the ovaries. However, with the onset of menopause, the ovaries cease to produce mature follicles, which causes a decrease in the oestradiol level from 40-400 pg/ml to ~5-20 pg/ml (Ruggiero and Likis, 2002; Bennink, 2004).

1.5.1 Physicochemical properties

Oestradiol is a steroidal compound having the molecular formula $C_{18}H_{24}O_2$ and molecular weight of 272.4 Da. The chemical name is Estra-1,3,5(10)-triene-3,17β-diol. It is a creamy-white odourless and tasteless crystalline powder. Oestradiol is a highly lipophilic compound (high octanol/water partition coefficient) with poor aqueous solubility of 3.6 mg/L at 25 °C (Hakk *et al*., 2005). It is soluble in ethyl acetate, acetone, and in the solutions of alkali hydroxides. It is sparingly soluble in vegetable oils (Dollery, 1991; Loose-Mitchell and Stancel, 2001).

1.5.2 Pharmacokinetics

1.5.2.1 Absorption and Distribution

After oral administration, oestradiol is absorbed readily from the gastrointestinal (GI) tract, but undergoes extensive presystemic metabolism in gut wall and liver resulting in low (~10 %) bioavailability (Lokind and Lorenzen, 1996). Oral doses of 2-4 mg daily produce plasma drug concentrations between 300-800 pmol/L with maximum concentration occurring within 0.5-5 h (Yen *et al*., 1975; Lyrenas *et al*., 1981). After intravenous administration, oestradiol has a half-life of ~20-70 min (Dollery, 1991). Being highly lipophilic, it is distributed throughout the body but the apparent volume of distribution is only 9-15 litres because of extensive plasma protein binding (~97-99%). Out of this about 60% is bound to albumin, 38% to sex hormone binding globulin (SHBG), and 2-3% is unbound. Only the free unbound fraction is biologically active and capable of equilibrating with the tissues (Dollery, 1991; Loose-Mitchell and Stancel, 2001; Ruggiero and Likis, 2002).

1.5.2.2 Metabolism and Elimination

Oestradiol is extensively metabolized in the liver into biologically less active oestrone (~10 times less potent than oestradiol) or inactive metabolites. The metabolism of oestradiol follows the same oxidative pathway in males and females (Fishman *et al*., 1960; Mueck *et al*., 2002). The first step is the conversion of oestradiol to oestrone by oxidation in the C-17 position (a reversible process) with the help of the enzyme 17β-hydroxy dehydrogenase. From oestrone onwards, irreversible metabolic conversions continue by two different pathways, namely by hydroxylation of the A-ring on the one hand and the D-ring on the other. The products of the two metabolic pathways are

formed by cytochrome 450 enzymes namely CYP 17, CYP 3As, CYP 1A1, CYP 1A2 and CYP 1B1 (Martucci and Fishman, 1993). The main metabolites formed by A-ring metabolism are 2-hydroxyestrone and 4-hydroxyestrone, and by D-ring metabolism 16α-hydroxyestrone and oestriol (Fig. 1.2). Oestradiol, oestrone and their metabolites are conjugated in the liver into water soluble form and excreted in the urine as glucuronide, sulfate or methyl conjugates (Dollery, 1991).

1.5.3 Therapeutic indications

Oestradiol is therapeutically indicated in (post)menopausal symptoms as a part of HRT (Lobo, 1995; Tanna, 2003b; Bennink, 2004; Yoo and Lee, 2006). Many short and long term effects of decreased oestradiol levels in post-menopausal women are discussed below:

1.5.3.1 Climacteric complaints

Vasomotor changes such as hot flushes and night sweats are one of the earliest menopausal symptoms and are the most likely reason for starting HRT. Oestrogen treatment has been found effective for the improvement of menopausal vasomotor symptoms if given for at least 2-3 years (Bennink, 2004; Yoo and Lee, 2006). Urogenital atrophy also responds favourably to HRT and many vaginal oestrogen preparations for a local relief are available for women who do not wish to take systemic HRT (Tanna, 2003b).

1.5.3.2 Osteoporosis

Osteoporosis is characterized by reduced bone mineral density (BMD) leading to increased bone porosity, and consequently, an increased risk of fracture. The bone loss starts in the first year of menopause and continues till 6 years. The overall bone loss during this phase is estimated to be ~15% (Mazzuoli *et al*., 2000). HRT has been established effective for the prevention

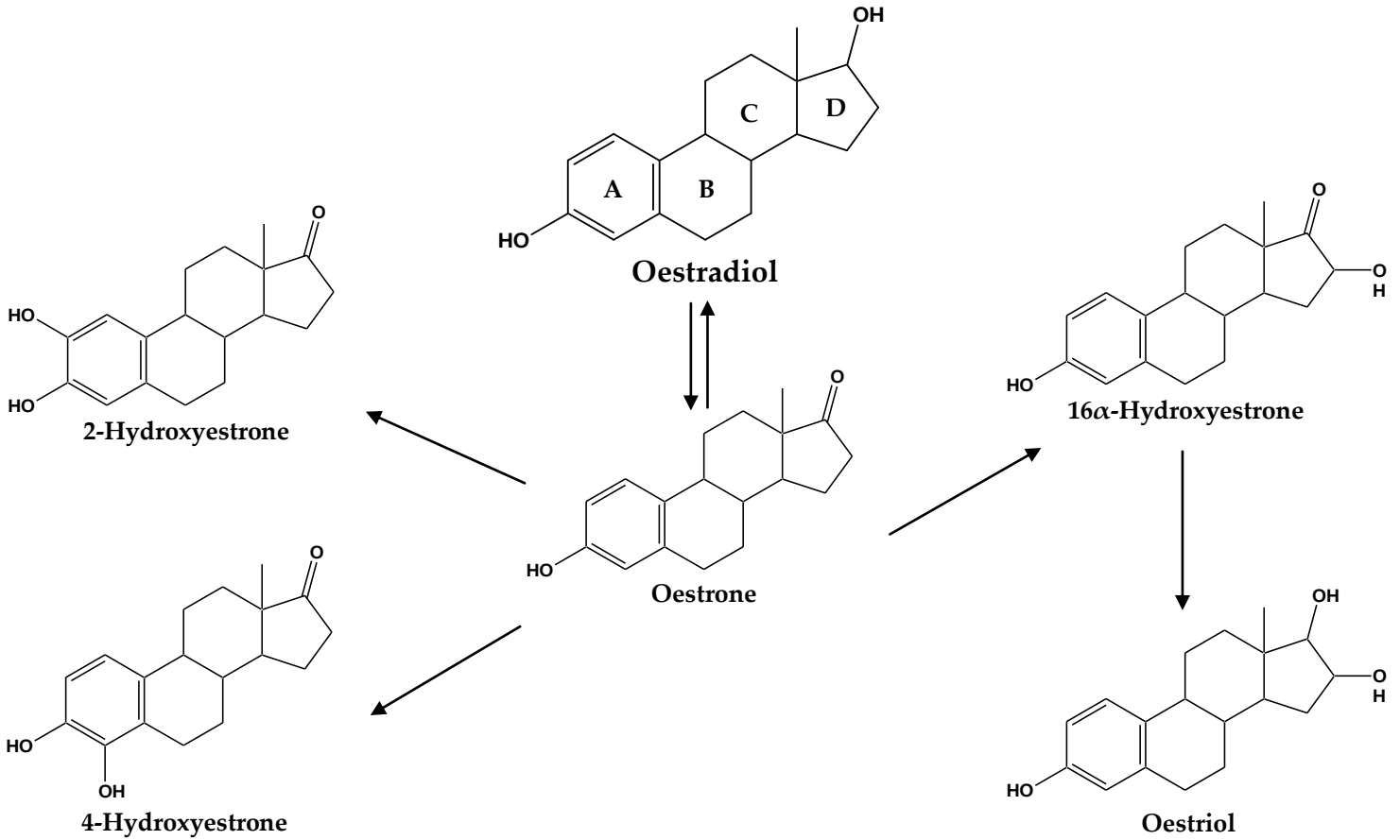

Fig. 1.2 Metabolic pathways of oestradiol showing its main A- and D-ring metabolites. The cited oestrogen metabolites undergo an additional degradation step by conjugation, either by glucuronidation, sulfation, or methylation. (Adapted from Mueck *et al*., 2002)

of post-menopausal osteoporosis (Stevenson, 1990; Stevenson, 2005). Oestrogens prevent bone loss by inhibition of bone resorption and thereby, increasing the BMD (Quigley, 1987; Ettinger *et al*., 1992). Oestrogen use is also associated with a decrease in the risk of osteoporotic fractures (e.g. fractures of the hip and vertebrae). The WHI (Women's Health Initiative) study has demonstrated that HRT is effective in end-point fracture prevention (Rossouw *et al*., 2002).

1.5.3.3 Cardiovascular disease (CVD)

CVD is the leading cause of death in post-menopausal women (Stevenson, 2000; Pines, 2002). Numerous epidemiological studies have suggested that post-menopausal HRT reduces the cardiovascular disease risk by up to 50% (Stampfer and Colditz, 1991; Grodstein and Stampfer, 1995; Grodstein *et al*., 1996). Various mechanisms have been put forward to understand the cardiovascular benefits offered by oestrogens. This includes reduction in LDL and increase in HDL level (Stevenson, 1998; Abbey *et al*., 1999; Tolbert and Oparil, 2001).

1.5.3.4 Colorectal cancer

Colorectal cancer is the second most common cancer in women after breast cancer in many countries, such as USA, UK and Australia. HRT use is evidently associated with a reduced risk of colon cancer, as confirmed by various epidemiological studies (Newcomb and Storer, 1995; Grodstein *et al*., 1999; Nanda *et al*., 1999) as well as clinical trials like WHI study (Rossouw *et al*., 2002) and HERS II (Heart and Estrogen/Progestin Replacement Study) (Hulley *et al*., 2002).

1.5.3.5 Alzheimer's disease (AD)

The risk of AD is more in women as compared to men and deprivation of endogenous oestrogen after menopause seems to play an important role in the pathological development of AD in post-menopausal women (Henderson, 1997; Casadesus *et al*., 2008; Craig and Murphy, 2009). Oestrogen induced neuroprotective actions on the brain has been very well established (Brinton, 2001; Behl, 2003; Nilsen, 2008; Simpkins and Singh, 2008; Vasudevan and Pfaff, 2008) and many clinical studies demonstrate that HRT may protect the post-menopausal women from AD and improve their cognitive function (Ohkura *et al*., 1995; Yaffe *et al*., 1998; Sherwin, 1999; Dykens *et al*., 2005).

1.5.3.6 Stroke

The cerebrovascular stroke occur more frequently in post-menopausal women than in age-matched or young pre-menopausal women, suggesting that oestrogens exert neuroprotective actions in the brain (Beyer, 1999; Wise *et al*., 2001; McCullough and Hurn, 2003). Though findings from the WHI study suggest that HRT increases the risk of stroke in post-menopausal women (Rossouw *et al*., 2002), the results of the WHI can not be generalized as those could be due to the doses, specific hormones used, when they were administered relative to the peri-menopausal transition, or the subpopulation of women who were included in the study. Many other animal and epidemiological studies have demonstrated beneficial effects of HRT in reducing the risk of stroke in post-menopausal condition and one mechanism of protection suggested is that oestrogens may act as direct vasodilators or through vasodilatory mediators during cerebral ischaemia (Paganini-Hill, 1995; Sherwin, 1997; Wise and Dubal, 2000; Wise, 2006).

1.5.4 Risks associated with HRT

The most common side effects of oestrogen use are nausea, breast pain, vaginal bleeding, and headache, but these are usually mild and temporary. However, other serious health risks include breast cancer, endometrial cancer, venous thromboembolism, and ovarian cancer (Lobo, 1995; Tanna, 2003b; Bennink, 2004; Yoo and Lee, 2006). In general, the risk of breast cancer is considered to be largest among HRT users. The Million Women Study reported that there was an increased breast cancer incidence and mortality among women taking HRT (Beral, 2003). A large meta-analysis study showed that no significant increase in breast cancer risk was observed for women using HRT for less than five years, but for women who used oestrogen with or without a progestin more than five years, a relative risk of 1.35 was reported, confirming that the risk of breast cancer caused by oestrogen is treatment duration dependent. The WHI study also confirmed that the combined HRT posed a serious breast cancer risk even after four years of treatment (Rossouw *et al*., 2002). However, the study with oestrogen treatment alone did not show any major risks, suggesting that the simultaneous use of a progestin may present an appreciably greater risk of breast cancer (Anderson *et al*., 2004). All the risks associated with the use of HRT appear to depend on the dose and duration of treatment. Therefore, whenever chronic HRT is indicated, the lowest effective dose should be used (Deady, 2004).

1.5.5 Delivery systems for HRT

Various types of formulations and delivery systems (Stevenson, 1999; Tanna, 2003a; Yoo and Lee, 2006) have been developed for HRT (Fig. 1.3). Every formulation has its own advantages and disadvantages as shown in Table 1.2. The most common formulations of HRT that are being currently used are

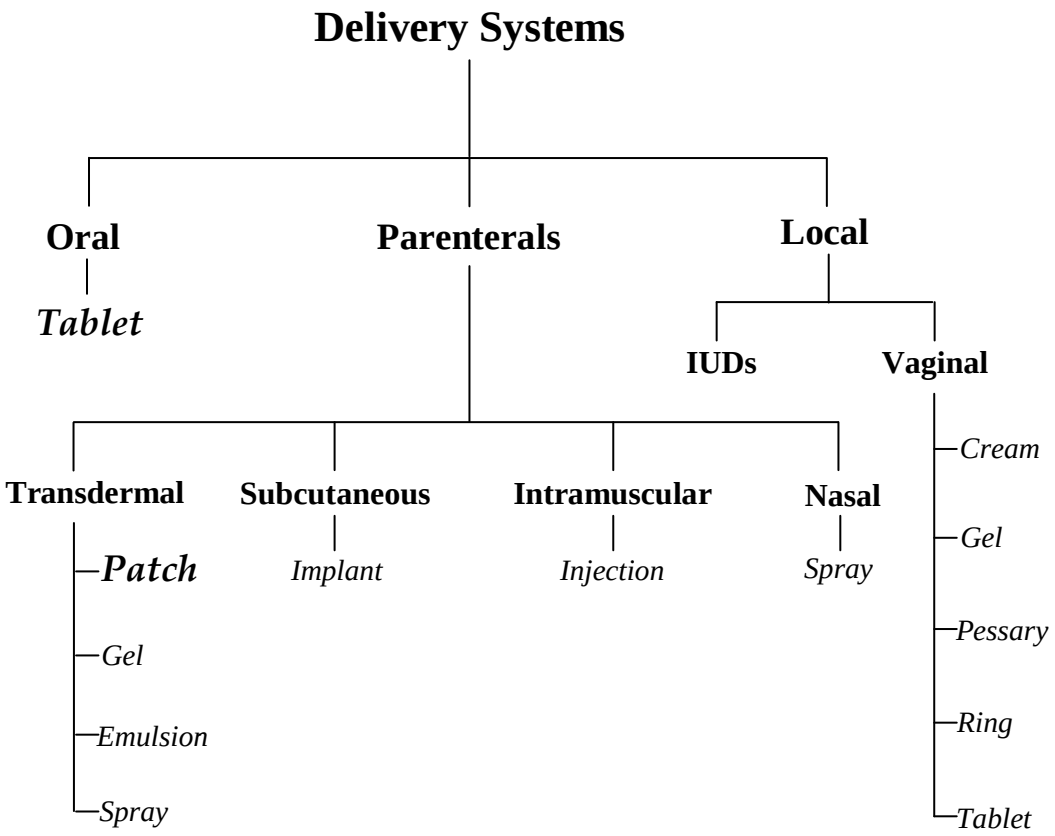

Fig. 1.3 Various delivery systems currently available for HRT.

Table 1.2
Advantages and disadvantages of formulations used for HRT

Formulation	Advantages	Disadvantages
Tablets	Easy to take	Adverse effects due to high dose
	Easily reversible	
	Cost effective	
	HDL-Cholesterol benefit	
Patch	Convenient to use	Can be easily detached
	Easily reversible	Skin irritation
	First choice for patients with high triglycerides or gut problems	Expensive
		Variability in absorption
		Frequent change (once or twice a week)
Implants	High compliance	Surgical procedure required
	Prolonged effect (4-8 months)	Not easily reversible
		Tachyphylaxis
		Progestogens need to be continued several months after last implant
Intrauterine devices (IUDs)	Direct effect to the uterine mucosa	Only for progesterone delivery
Vaginal preparations	High efficiency for vaginal symptoms	Risk of endometrial proliferation on long term use
	Easily reversible	
Nasal spray	Easy to use	Nasal irritation possible
	Easily reversible	
Injections	Prolonged effect (1-4 months)	Not continuously released
		Painful procedure

(Adapted with modifications from Yoo and Lee, 2006)

oral tablets and transdermal patches. But, these are also associated with some serious problems, for example the oral method of administration uses high doses of oestrogens to attain the desired therapeutic levels as they are subject to presystemic metabolism in the intestinal wall and liver. This exposes the liver to high concentrations of oestrogens resulting in increased hepatic synthesis of many proteins which can lead to adverse effects. In the case of transdermal patches, low doses of oestrogens are sufficient to achieve the same therapeutic effect as by the oral method, because GI interferences and hepatic first pass metabolism are avoided through this route. However, problems of adhesion and skin tolerability can lead to poor patient compliance (Yoo and Lee, 2006).

Therefore, optimum delivery of oestrogens still remains as a challenge and hence, it is worth investigating a new formulation approach for oestradiol that could offer maximum drug efficacy along with the patient's compliance.

1.6 Polymeric nanoparticles for oral delivery

Oral drug delivery, being non-invasive in nature is by far the most convenient and preferred route of administration. However, many drug molecules have low bioavailability problems when given orally because of their poor biopharmaceutical properties such as low aqueous solubility, low intestinal permeability, or lack of stability (chemical and/or enzymatic degradation) in the GI environment. In addition to this, extensive pre-systemic metabolism in intestinal wall and liver also reduces the oral bioavailability in many cases (like oestradiol in the present study). Over the years, various strategies have been investigated to address the above-mentioned problems of oral drug delivery and incorporation of the drug into particulate carriers, such as polymeric nanoparticles, is one such approach that has been explored to improve the oral bioavailability (Allémann *et al*.,

1998; Delie and Blanco-Prieto, 2005; Galindo-Rodriguez *et al*., 2005). Polymeric nanoparticles can be defined as colloidal carriers with a size range of 10-1000 nm (Speiser and Kreuter, 1976). The drug can be dissolved, entrapped, encapsulated, adsorbed, or attached to a nanoparticle matrix. Depending upon the method of nanoparticle preparation, nanocapsules or nanospheres can be produced. Nanocapsules are the reservoir system with a polymeric shell and an inner drug core, while nanospheres are matrix system in which the drug is physically and uniformly dispersed (Singh and Lillard, 2009). In recent years, significant attention has been given in fabricating polymeric nanoparticles as oral drug delivery vehicles due to numerous advantages offered by them from the pharmaceutical perspective. After oral administration, polymeric nanoparticles can protect the incorporated drug molecules from GI degradation as well as gut wall metabolism, thereby ensuring the stability of the drug in GI tract before absorption. Also, these colloidal nano-carriers have the ability to increase the oral bioavailability by preventing the first pass metabolism of the drug through their specialized lymphatic uptake mechanism (Florence, 1997; Chen and Langer, 1998; Delie, 1998; Norris *et al*., 1998; Bhardwaj *et al*., 2005).

1.6.1 Transport of nanoparticles across the GI tract

1.6.1.1 GI tract physiology

The GI tract surface is lined with an epithelium, comprised mainly of enterocytes and goblet cells. Enterocytes constitute the largest number of cells in the intestinal mucosa (~90%) and function as an efficient barrier to check the uptake of foreign particulate matter (potentially harmful materials and pathogens) from the environment. At the same time, they also control the absorption of dietary nutrients, electrolytes and fluids. Goblet cells

secrete a translucent visco-elastic fluid, known as mucus, composed mainly of water insoluble glycoproteins (mucins). The mucus also acts as a barrier by forming a protective layer over enterocytes in the intestine. However, apart from the various non-immunologic (pH, proteolytic enzymes, mucus, epithelial lining, gut-associated microflora) barriers, the mucosa is also protected by highly specialized immunologic mechanisms. Lymphoid follicles, part of the gut associated lymphoid tissue (GALT) are dispersed through the intestinal mucosa. These follicles may be isolated or aggregated into Peyer's patches (PP) and overlaid by a layer of specialized epithelium, follicle-associated epithelium (FAE), which comprises of absorptive enterocytes, M cells and few goblet cells. M cells differ from neighbouring enterocytes by underdeveloped microvilli and thinner glycocalyx on their apical surface, absence of mucus layer and high endocytotic/transcytotic capacity. M cells are specialized for endocytosis of antigens and their main function is to transport the foreign particulate material from the GI lumen to the underlying organized mucosal lymphoid tissue in order to induce the immune response. This physiological transport mechanism through M cells has been widely explored for oral delivery of colloidal carriers, such as polymeric nanoparticles (Yeh *et al*., 1998; Jung *et al*., 2000; des Rieux *et al*., 2006).

1.6.1.2 Mechanisms of particulate uptake

For the transport of particulate carriers across the intestinal epithelial barrier, two different pathways have been suggested, the paracellular route (between adjacent cells) and the transcellular route.

1.6.1.2.1 Paracellular transport

The paracellular route for nanoparticle translocation is very limited because of the very small surface area of the intercellular spaces, contributing less than 1% of the total mucosal surface area and also, tightness of the intercellular junctions (pore diameter < 10 Å) (Jung *et al*., 2000). However, paracellular transport of drugs can be enhanced using various polymers such as chitosan (Schipper *et al*., 1997), poly(acrylate) (Lehr *et al*., 1990; Kriwet and Kissel, 1996) or starch (Bjork *et al*., 1995). These polymers have been shown to facilitate paracellular transport either through charge mediated interactions between polymer and cell membrane (chitosan) or by reducing free extracellular Ca^{2+} concentration (polyacrylates), finally resulting in opening of tight junctions.

1.6.1.2.2 Transcellular transport

Transcellular transport of nanoparticles takes place through the process of transcytosis, by which particles are first internalized (endocytosis) at the cell apical plasma membrane, followed by transportation through the cell and finally, released (exocytosis) across the basolateral membrane (Okamoto, 1998). Endocytotic processes can be divided into (1) Receptor mediated endocytosis (RME) and (2) adsorptive endocytosis. RME requires binding of specific ligands to apical cell membrane receptors in order to initiate the endocytotic process (Mellman, 1996; Swaan, 1998). On the other hand, adsorptive endocytosis does not require any specific ligand-receptor interactions at the cells surface and can be initiated by physical adsorption of particulate carriers to cell surface through electrostatic forces (H-bonding or hydrophobic interactions) (Jung *et al*., 2000). Since adsorptive endocytosis does not involve the requirement of specific ligands, uptake depends largely on the particle size and surface properties of the material. Both types of

endocytotic processes are saturable and energy dependent. Transcellular uptake of nanoparticles has been shown to occur through two types of intestinal cells (1) enterocytes, and (2) M cells of PP. Enterocytes are the largest numbers of cells in the intestinal epithelium, whereas M cells, primarily located in PP, constitute a very small proportion (~1%) of total intestinal surface (des Rieux *et al*., 2006). However, studies have reported that majority of particle uptake occurs via M cells of PP because of their high transcytotic capability (Jani *et al*., 1990; O'Hagan, 1990; Lavelle *et al*., 1995; Mestecky *et al*., 1997). Although, there is evidence that some degree of particle translocation also occur through normal absorptive enterocytes, present mostly in the villous part and to some extent in the FAE of the intestine (Jani *et al*., 1992a; Desai *et al*., 1996).

Particle size and surface properties (surface charge and hydrophobic/lipophilic balance) have been found to play a crucial role in transcellular uptake and translocation of nanoparticles after oral administration. Many studies have confirmed that the mechanism of particle uptake is size dependent and nanoparticle transcytosis, via both PP and absorptive enterocytes, increases with decrease in particle size/diameter (Jani *et al*., 1992a; Jani *et al*., 1992b; Desai *et al*., 1996; Desai *et al*., 1997). It was also observed that maximum uptake occurred with particles ranging from 50-100 nm in size while particles above 1 μm remained in the PP (Jani *et al*., 1989; Jani *et al*., 1990). Similarly, it has been reported that nanoparticles prepared from hydrophobic polymers exhibited higher uptake than those with more hydrophilic surfaces (Hillery and Florence, 1996). Also, various surface modifications such as coating the surface with bioadhesive hydrophilic polymers (eg. polyethylene glycol) (Yoncheva *et al*., 2005) or by attaching specific ligands to particle surface (eg. lectins) (Clark *et al*., 2000; Yin *et al*.,

2007) have been carried out to increase the interaction between nanoparticles and intestinal epithelium and thereby, facilitate their transport across the intestinal mucosa.

1.6.2 Nanoparticle preparation and formulation principles

1.6.2.1 Preparation of nanoparticles

Polymeric nanoparticles can be prepared by two techniques: (a) dispersion of preformed polymers or (b) *in situ* polymerization of monomers. However, dispersion of preformed polymers (natural and synthetic) is the most common technique for the preparation of polymeric nanoparticles. Several methods for the preparation of nanoparticles using preformed polymers have been reported (Allémann *et al*., 1993a; Quintanar-Guerrero *et al*., 1998; Vauthier and Bouchemal, 2009). A brief outline of some commonly used methods is given below.

1.6.2.1.1 Emulsion-evaporation method

In this method, first polymer and drug is dissolved in a water immiscible organic solvent like dichloromethane, or chloroform and thereafter, this solution is emulsified in an aqueous solution containing the stabilizer to make oil-in-water (o/w) emulsion. After reducing the droplet size with high-speed homogenization or sonication, organic solvent is evaporated under reduced pressure or by continuous stirring, which results in the formation of aqueous dispersions of nanoparticles. However, this method suffers from limitation of poor loading efficiency of hydrophilic drugs due to their partitioning from the organic phase into the aqueous phase. Therefore, this method is mainly used to encapsulate the lipophilic drugs (Gurny *et al*., 1981; Song *et al*., 1997; Jaiswal *et al*., 2004).

1.6.2.1.2 Double emulsion-evaporation method

This method is best suited for the incorporation of hydrophilic drugs like peptides, proteins and vaccines (Zambaux *et al*., 1998). In this method, aqueous drug solution is added to the organic polymer solution under stirring, resulting in the formation of water-in-oil (w/o) emulsion. This w/o emulsion is then added with stirring into another aqueous phase containing stabilizer to form the water-in-oil-in-water (w/o/w) double emulsion. Organic solvent is finally removed by evaporation under reduced pressure or by continuous stirring.

1.6.2.1.3 Salting-out method

The salting-out process (Allémann *et al*., 1992; Allémann *et al*., 1993b) is based on the non-miscibility of an otherwise water-miscible solvent in saturated aqueous solution. It involves the formation of o/w emulsion after addition of drug and polymer solution in water-miscible solvent, such as acetone, to an aqueous solution containing the salting-out agent (electrolytes, such as magnesium chloride, calcium chloride, and magnesium acetate, or non-electrolytes such as sucrose) and a stabilizer. A further dilution of this emulsion with sufficient volume of water facilitates the complete diffusion of organic solvent into aqueous phase, resulting in polymer precipitation and formation of nanoparticles. The solvent and salting-out agent is separated by cross-flow filtration.

1.6.2.1.4 Solvent-displacement/nanoprecipitation method

Polymer, drug and surfactant solution in a water-miscible solvent (such as acetone or ethanol) is poured or injected into an aqueous solution containing a stabilizer under magnetic stirring. Nanoparticles are formed instantaneously by interfacial polymer deposition following rapid solvent

displacement and the solvent is then removed from the suspension under reduced pressure (Fessi *et al*., 1989; Govender *et al*., 1999).

1.6.2.1.5 Emulsion-diffusion

In this method, drug and polymer solution in partially water-miscible solvent, such as ethyl acetate, benzyl alcohol, or propylene carbonate, is added to an aqueous solution containing the stabilizer. After the mutual saturation of two phases, both liquids come in the state of thermodynamic equilibrium and stirring then causes the formation of o/w emulsion with the dispersion of the solvent solution as globules in equilibrium with the continuous aqueous phase. The addition of sufficient volume of water to the emulsion disturbs the equilibrium between the two phases and causes the diffusion of the solvent into the external phase and subsequently, precipitation of the polymer as nanoparticles. Finally, solvent is eliminated by cross-filtration or dialysis (Leroux *et al*., 1995; Quintanar-Guerrero *et al*., 1996; Kwon *et al*., 2001).

1.6.2.1.6 Emulsion–diffusion–evaporation

This is a modification of the emulsion–diffusion method described above where both diffusion as well as evaporation of organic solvent takes place at the same time. The method was first used by Kumar *et al*., (2004) to prepare the cationic PLGA nanoparticles with a PVA-chitosan blend as stabilizer and was found to be robust in terms of both, size and shape of nanoparticles. Also, the method exhibited reproducibility even when polymer amount was increased from 50 mg to 500 mg, demonstrating its potential in the scale-up of nano-formulations.

Apart from the above described methods, some more techniques of nanoparticle preparation like the spray-drying method, supercritical fluid

technology and the coacervation/ionic gelation method have also been reported in the literature.

1.6.2.2 Formulation principles

1.6.2.2.1 Polymers

Nanoparticles have been prepared from both natural (e.g., chitosan, albumin, alginates, and gelatin etc.) as well as synthetic (e.g., polyesters, polyacrylates and phthalates etc.) polymers. An appropriate selection of the polymeric matrix is crucial in fabricating a successful drug delivery vehicle. The choice of the proper matrix depends on several factors such as particle characteristics (particle size and surface properties) required, physicochemical properties of the drug to be incorporated, degree of biocompatibility, biodegradability, and toxicity of the polymer, and finally, drug release profile desired. Until now, a number of polymers have been investigated for designing these nano-carriers, of which poly(lactide-co-glycolide) (PLGA), a copolymer of poly(lactic acid) (PLA) and poly(glycolic acid) (PGA) (Fig. 1.4), has been most comprehensively explored because of its biocompatibility, biodegradability, non-toxicity, ease of production and most importantly, versatile degradation kinetics (Shive and Anderson, 1997; Jain, 2000; Bala *et al*., 2004). PLGA undergoes degradation through the hydrolytic cleavage of its backbone ester linkage. The degradation rate of PLGA largely depends on its copolymer composition (molar ratio of the lactic and glycolic acids in the polymer chain) and molecular weight. Therefore, by varying the molecular weight and lactide/glycolide ratio, the degradation rate of PLGA and subsequently, the release kinetics of active agent can be tailored accordingly. In general, the degradation rate will be faster for more hydrophilic low molecular weight polymers, and copolymers

(a)

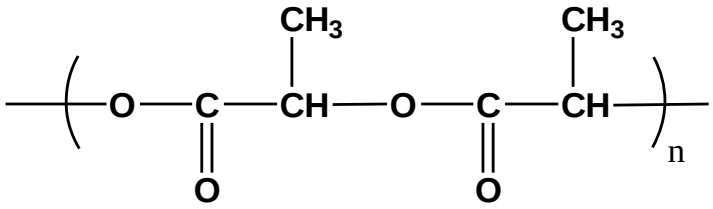

(b)

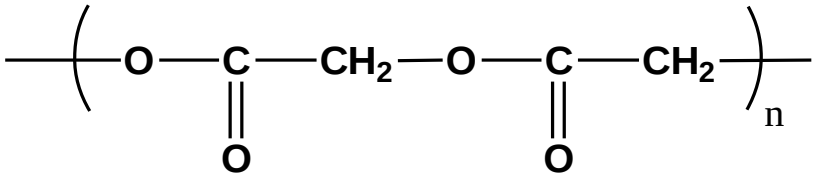

(c)

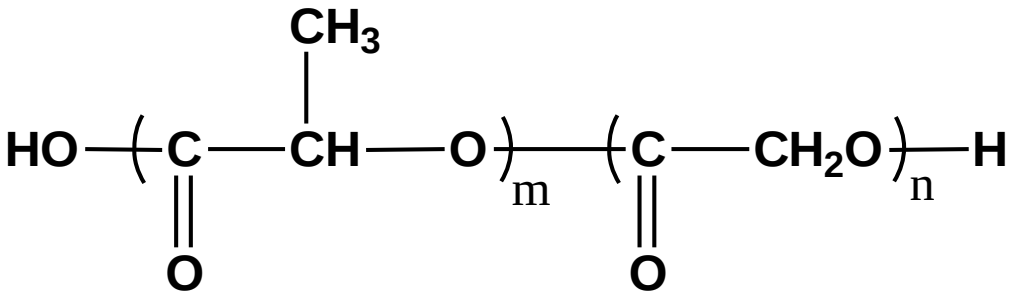

(m represents lactide and n represents glycolide monomeric units)

Fig. 1.4 Structures of (a) Poly(lactic acid) (PLA), (b) Poly(glycolic acid) (PGA), and (c) Poly(lactide-co-glycolide) (PLGA).

with higher content of glycolide as lactic acid is more hydrophobic than glycolic acid (Jalil and Nixon, 1990; Lewis, 1990; Cohen *et al*., 1994; Panyam *et al*., 2003). Glass transition temperature, Tg, is another key factor determining the physical strength of the delivery system. The Tg of PLGA is 45-55°C, which is above physiological temperature of 37°C, thereby imparting them significant mechanical strength to be formulated as drug carriers. The degradation products of PLGA are also completely safe as it degrades first into its monomers, lactic and glycolic acid, which enter the tricarboxylic acid cycle (Krebs' cycle), are metabolized and subsequently, eliminated from the body as carbon dioxide (CO_2) and water (H_2O) (Marcus and Kaeding, 2004). On the whole, the physical properties and the United States Food & Drug Administrations (US FDA) approval of the various drug delivery products containing these biodegradable polymers have made them the most extensively used polymers in the field of colloidal drug delivery.

1.6.2.2.2 Stabilizers

A stabilizer is used to prevent the coalescence of small oil droplets and formation of aggregates during and after the emulsification process of nanoparticle preparation. The high interfacial tension, because of the large surface area of small oil globules formed during emulsification, always keeps the system at risk of coalescence. Stabilizer molecules get adsorbed at the interface between the aqueous and oil phase and prevent the coalescence by lowering the interfacial tension and energy of the system. The type and concentration of stabilizer used may influence the particle properties such as particle size and zeta potential (Vandervoort and Ludwig, 2002). Particle size is an important parameter as it can directly affect the physical stability, cellular uptake, biodistribution and the drug release, and in general, smaller is better (Panyam and Labhasetwar, 2003). Zeta potential is a measure of

surface charge and determines the stability of the particles. Nanoparticles with a zeta potential value of above ± 30 mV have been reported to be stable in suspension, as the electrostatic repulsion between particles with the same surface charge prevents their aggregation (Singh and Lillard, 2009). Polyvinyl alcohol (PVA) (Fig. 1.5 a) has been the most widely used stabilizer for the preparation of PLGA nanoparticles (Murakami *et al*., 1997; Lamprecht *et al*., 1999; Sahoo *et al*., 2002; Vandervoort and Ludwig, 2002). However, a study by Kwon *et al*., (2001) showed that the use of quaternary ammonium salt, didodecyl dimethyl ammonium bromide (DMAB) (Fig. 1.5 b), as a stabilizer resulted in much smaller particle size (<100 nm) as compared to PVA. Our group also, through comprehensive studies using a wide range of drug molecules, has demonstrated the capability of DMAB in producing nanoparticles of small particle size with narrow size distribution (Hariharan *et al*., 2006; Ankola *et al*., 2007; Mittal *et al*., 2007; Ratnam *et al*., 2008; Sahana *et al*., 2008). Also, the surfactant itself and particles made from it were found to be safe to cells *in vitro*, even with the highest concentration of surfactant (1% w/v) used (Bhardwaj *et al*., 2009). Moreover, Peetla and Labhasetwar, (2009) have recently reported that this dichained cationic surfactant (DMAB) facilitated the interaction of the nanoparticles with a model cell membrane, and the interaction was found to be proportional to their cellular uptake *in vitro,* signifying the role of surface charge and molecular structure of surfactant in transport of nanoparticles across the cell membrane.

1.6.2.2.3 Solvents

The proper selection of an organic solvent is critical in the preparation of particulate formulations. The parameters which should be considered when deciding an organic solvent for nanoparticle preparation include: physical properties of the solvent (Table 1.3) and its ability to dissolve the polymer

(a)

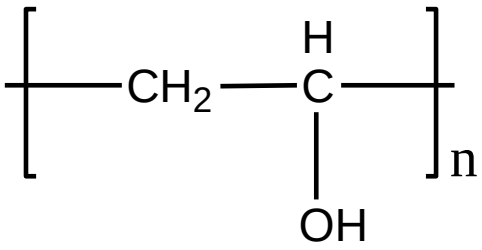

(b)

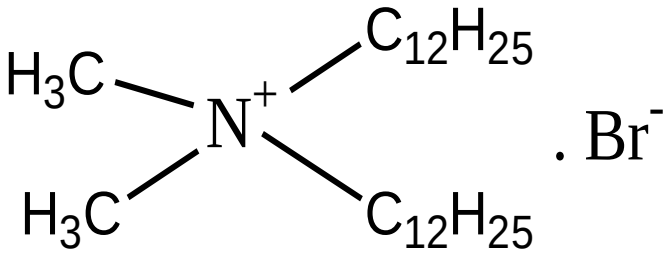

Fig. 1.5 Structures of (a) Polyvinyl alcohol (PVA), and (b) didodecyldimethyl ammonium bromide (DMAB).

Table 1.3
Physical properties of some solvents.

Solvent	b.p. (°C)	m.p. (°C)	Solubility in H_2O at 25°C	Interfacial tension* (dyne/cm)	Vapour pressure* (mmHg)	Viscosity* (Cp)
Acetone	56.5	-94	Miscible	6.8	185.23	0.32
Chloroform	61-62	-63.5	1 in 200	32.8	159.62	0.57
Dichloromethane	39.75	-95	1 in 50	28.3	348.75	0.44
Ethyl acetate	77	-83	1 in 10	1.7	76	0.46-0.47

*all values are at 20°C
(Adapted from Sahana *et al.,* 2008)

and drug. Based on these properties, an organic solvent can directly affect the particle characteristics such as particle size and entrapment efficacy, which in turn could influence the overall performance of the formulation (Sah, 1997; Birnbaum *et al*., 2000; Sahana *et al*., 2008). The selection of solvents also depends on the method of preparation of nanoparticles. The emulsion-diffusion-evaporation method requires a partially water soluble solvent such as ethyl acetate, while the solvent displacement/nanoprecipitation technique uses a water miscible solvent like acetone. Another most important aspect which must be considered during solvent selection is its toxicity due to presence of residual solvent in final preparation, irrespective of the purification method used. International Conference on Harmonization (ICH) guidelines (Q3C) for limiting residual solvent levels in active substances, excipients and medicinal products has categorized the solvents into three classes. The Class 1 solvents should not be used in pharmaceutical manufacture because of toxicity or environmental impact, while use of Class 2 solvents should be limited due to their potential toxicity. However, Class 3 solvents present a lower risk to human health and are regarded as safe in the range generally used. Therefore, use of the halogenated alkanes, such as methylene chloride and chloroform (Class 2 solvents) is not recommended while solvents such as ethyl acetate and acetone are much safer to use as they fall under the category of Class 3 solvents.

Overall, polymeric nanoparticles represent a potential approach in oral drug delivery. Since our interest lies in improving the oral delivery of oestradiol, we developed and optimized PLGA nanoparticles carrying oestradiol for oral administration (Hariharan *et al*., 2006; Mittal *et al*., 2007; Sahana *et al*., 2008).

1.7 Objective and specific aims

The objective of the dissertation was to be able to deliver oestradiol orally at lowest effective dose to maximize its utility and minimize the risks associated. The objective was accomplished by the following specific aims:

(a) Understand the pharmacokinetics of oestradiol as a function of nanoparticle characteristics and dose for optimal dosage regimen.

(b) Development and optimization of nanoparticles that are able to improve brain levels of oestradiol on oral administration.

(c) Understand the tissue distribution profile as a function of surface characteristics of nanoparticles.

(d) Pharmacodynamic evaluations of oral oestradiol nanoparticles in rat models of hyperlipidaemia and AD.

Chapter-2

A dose-dependent pharmacokinetic study of oral oestradiol nanoparticles*

*This part of study was conducted in National Institute of Pharmaceutical Education and Research (NIPER), India and has been published in Journal of Pharmaceutical Sciences, 98, 3730-3734 (2009)

2.1 Introduction

Pharmacokinetic (PK) studies have always proven to be authoritative and informative implements, particularly in explaining vital facets of human pharmacology. Pharmacokinetics is the basic area of pharmacology that deals with drug administration, absorption, distribution, tissue binding, metabolism, and excretion. A fundamental concept in pharmacology is that a drug must reach specific tissues/site of action in the body in a sufficient concentration to exert its required therapeutic effects (Ciccone, 1995). Therefore, pharmacokinetic parameters of a drug must be known so that an accurate amount of the dose can be administered to reach target tissues and produce therapeutic responses in a reasonably predictable and timely fashion, without causing any adverse effects. The pharmacological response i.e. pharmacodynamics of a drug is generally believed to be directly correlated to its concentration at the site of action, which in turn is dependent on the administered dose and at the same time a number of pharmacokinetic processes involved such as absorption, distribution, biotransformation (metabolism) and excretion (Abdel-Rahman and Kauffman, 2004; Dingemanse and Appel-Dingemanse, 2007). Generally, absorption and elimination of most drugs follow linear kinetics, and pharmacokinetic parameters describing these processes do not change over the therapeutic dose range. However, other processes, such as drug metabolism and protein binding, involve carriers (enzymes or proteins) with definite capacities which on saturation leads to non-linear/saturation pharmacokinetics. The pharmacokinetic parameters of most drugs do not change when different doses are administered or when the drug is given as single or multiple doses. The kinetics of such drugs are said to be linear or dose-independent. In other words, a drug is said to follow linear kinetics if increase in dose leads to

proportionate increase in plasma concentration or area under the plasma concentration-time curve (AUC). On the other hand, dose-dependent/non-linear pharmacokinetics usually reflects to greater than or less than proportional increase in area under the drug concentration-time curve (AUC) with increase in the dose. Nonlinearity may occur at various kinetic levels of absorption, distribution, metabolism and/or elimination, but metabolism is considered to be most common source of nonlinearity (Lin, 1994; Mehvar, 2001). Often, the non-linear kinetics complicates the design of dosage regimens and prediction of efficacy and toxicity of drugs having vastly different clinical dose ranges. Thus, an understanding of the pharmacokinetics of drugs is important in the evaluation of their efficacy and toxicity. Moreover, drug delivery systems and in particular polymeric nanoparticles can appreciably modulate various pharmacokinetic parameters of the incorporated drug. The pharmacokinetics of oestradiol as a function of nanoparticle characteristics and dose is presented in this chapter.

2.2 Materials

PLGA (Resomer RG 50:50 H; molecular weight 35-40KDa) was purchased from Boehringer Ingelheim (Ingelheim, Germany) and DMAB was purchased from Aldrich (St. Louis, MO, USA). Oestradiol was a gift sample from Orion Pharma (Espoo, Finland). Enzyme-linked immunosorbent assay (ELISA) kits were procured from DRG Diagnostics (Marburg, Germany). Ethyl acetate (AR grade) and acetonitrile (HPLC grade) were purchased from Rankem Fine Chemicals (New Delhi, India).

2.3 Experimental

2.3.1 Preparation and characterization of PLGA nanoparticles

Preparation, optimization and characterization (*in vitro* and *in vivo* drug release studies) of oestradiol entrapped PLGA nanoparticles has already been reported by our group (Hariharan *et al*., 2006; Mittal *et al*., 2007; Sahana *et al*., 2008), where nanoparticles made from PLGA 50:50 (MW 35-40KDa) were found to be more effective in improving the AUC values along with sustained drug release. Moreover, histopathological examination of the liver, spleen, and the intestinal segments (duodenum, jejunum, and ileum) also showed absence of any inflammatory response after oral administration of these formulations. Therefore, oestradiol nanoparticles prepared of PLGA 50:50 were selected for our further pharmacokinetic and pharmacodynamic evaluations. In brief, 50 mg of PLGA and 5 mg of oestradiol (10% w/w of polymer) were dissolved in 2.5 ml of ethyl acetate at room temperature for 2 h. The organic phase was then added to 5 ml of an aqueous phase containing DMAB (50 mg in 5 ml; 1% w/v) as stabilizer. The resulting primary o/w emulsion was stirred at 1000 rpm for 3 h and subsequently homogenized at 15,000 rpm for 5 min using a high-speed homogenizer (Polytron PT4000;

Kinematica, Lucerne, Switzerland). To this nanoemulsion, water was added with constant stirring to facilitate diffusion and finally, evaporation of organic solvent. This resulted in polymer precipitation and formation of nanoparticles. The size and zeta potential of the nanoparticles were measured with Zetasizer (Nano ZS; Malvern Instruments Ltd, Malvern, UK). Drug entrapment efficiency was determined by centrifuging the drug loaded nanoparticles at 10,000xg for 20 min and dissolving the pellet in acetonitrile. The drug content was then calculated using a validated high-performance liquid chromatography (HPLC) method, previously reported by our group (Hariharan *et al*., 2006; Mittal *et al*., 2007; Sahana *et al*., 2008). Briefly, Waters HPLC system (Waters Corporation, MA, USA) consisting of 996 Photodiode Array (PDA) detector and Merck LiChoCART® 100 RP-18 end-capped 5 μm column (Darmstadt, Germany) was used. Acetonitrile and water (65:35) was used as the mobile phase with a flow rate of 0.5 ml/min. The injection volume was 15 μl and retention time of oestradiol was ~7.1 min. The detection wavelength (λ_{max}) for oestradiol was 281 nm.

2.3.2 Pharmacokinetic Study

The study was carried out in male Sprague-Dawley (SD) rats weighing between 180-200 g. Rats were kept on 12/12 h light/dark cycles under controlled temperature (20-22°C). The animals were provided with normal pellet diet and free access to water during the entire period of experimentation. All animal experiments were performed according to a protocol duly approved by the Institutional animal ethics committee (IAEC) of National Institute of Pharmaceutical Education and Research (NIPER), India. Animals were first divided into three groups based on the 3 different doses i.e. 100, 200 & 500 μg/kg and after that each dose group was further divided into 3 subgroups (n=5). Subgroups were administered either, a) oral

pure drug suspension, b) oral nanoparticulate formulation or c) pure drug intravenous (i.v.) solution. Different dose PLGA nanoparticles (dispersed in water) and pure drug suspensions (dispersion in 0.05% dimethyl sulfoxide) were administered by oral gavage and thereafter blood samples were collected from the retro-orbital plexus in the heparinized microcentrifuge tubes (50 units heparin/ml of blood) at predetermined time intervals for 5 days and 1 day respectively. For i.v. administration, oestradiol solution (dissolved in 40% ethanol) was given through the femoral vein and the blood levels were monitored over a time period of 0.08, 0.17, 0.25, 0.33, 0.50, 0.75, 1, 2, 4, 6, 12 and 24 h. For oral oestradiol suspension and i.v. oestradiol solution blood sampling was done for 24 h only as our previous findings (Mittal *et al*., 2007; Sahana *et al*., 2008) have shown that plasma oestradiol levels went below therapeutic levels by that time period. Volume was kept constant (0.5 ml) in all the administrations.

2.3.3 Measurement of plasma oestradiol

The physiological and pharmacological plasma levels of oestradiol are present in the concentration range of pg/ml. However, the developed HPLC method was not sensitive enough (linearity 1-10 μg/ml) to quantify such low drug levels. Therefore, plasma oestradiol levels were measured using commercially available ELISA kits (DRG Diagnostics, Marburg, Germany) having linearity range of 0-2000 pg/ml. As the kits were designed for human serum, oestradiol was extracted from rat plasma and reconstituted with steroid-free human serum (DRG Diagnostics) to avoid protein matrix effects. Briefly, plasma was separated by centrifuging the blood samples at 10,000xg for 15 min. To 200 μl of plasma, 800 μl of methanol was added for 15 min in 1.5-ml safe-lock Eppendorf caps and subsequently vortexed for 1 min. The samples were then centrifuged at 10,000xg for 5 min. Thereafter, the

supernatant was separated and vacuum-dried in Speed-Vac evaporator (SPD121P; Savant Instruments Inc., NY, USA) for 6 h. Finally, the residue was reconstituted in steroid-free human serum and ELISA measurements were performed according to the manufacturer's instructions.

2.3.4 Pharmacokinetic analysis

Plasma drug concentration data was plotted on a semi-log plot and it revealed that plasma concentration after i.v. administration can be best described by a two-compartment model, while for oral administration; it was best fit in one-compartment model.

2.3.5 Statistical analysis

One way analysis of variance (ANOVA) and subsequent Tukey test was used to determine statistically significant differences between the results and values with $p<0.05$ were considered statistically significant.

2.4 Results and Discussion

The particle size of drug loaded nanoparticles prepared with 1% w/v DMAB was found to be 110.7 ± 3.2 nm with zeta potential values of 95.2 ± 5.6 mV (pH range of the preparation was 4.03-4.11). The drug entrapment efficiency at 10% (w/w of polymer) initial drug loading was 50.1 ± 3.2 % (~50 μg of oestradiol entrapped per mg of polymer).

Oral administration of polymeric nanoparticles demonstrated a prolonged drug release profile of 5 days in comparison to only 1 day plasma profile of simple drug suspension by oral and pure drug solution i.v. (Fig. 2.1 a,b,c). The significant pharmacokinetic parameters of drug obtained after oral and i.v. administration are shown in Tables 2.1 & 2.2 respectively. From the data shown in Table 2.1, it is clear that all nanoparticulate formulations led to significant increase in the AUC ($p<0.001$) and T_{max} ($p<0.001$) values in

(a)

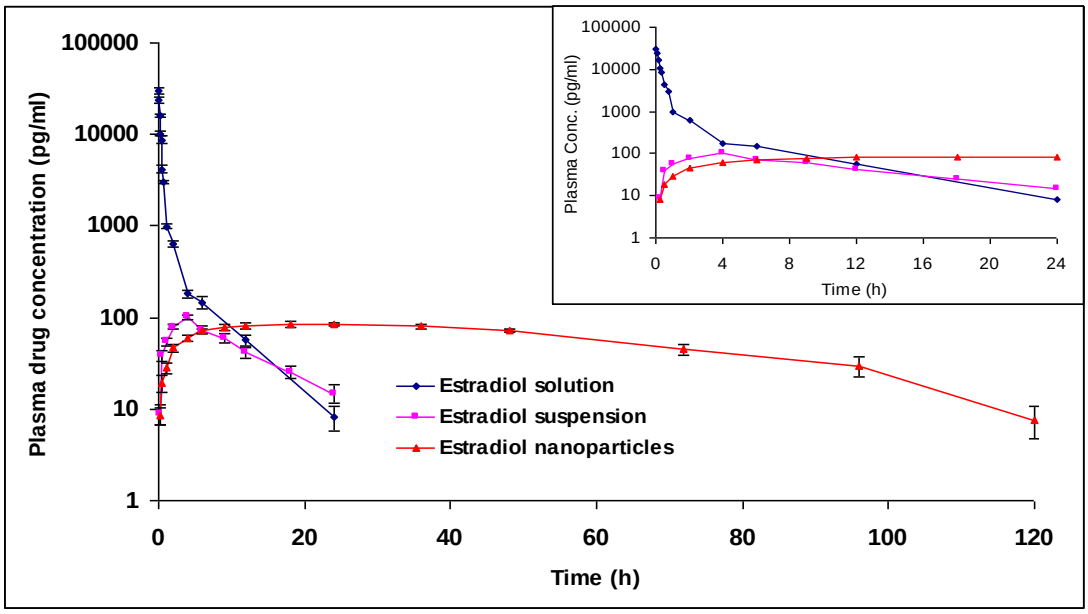

(b)

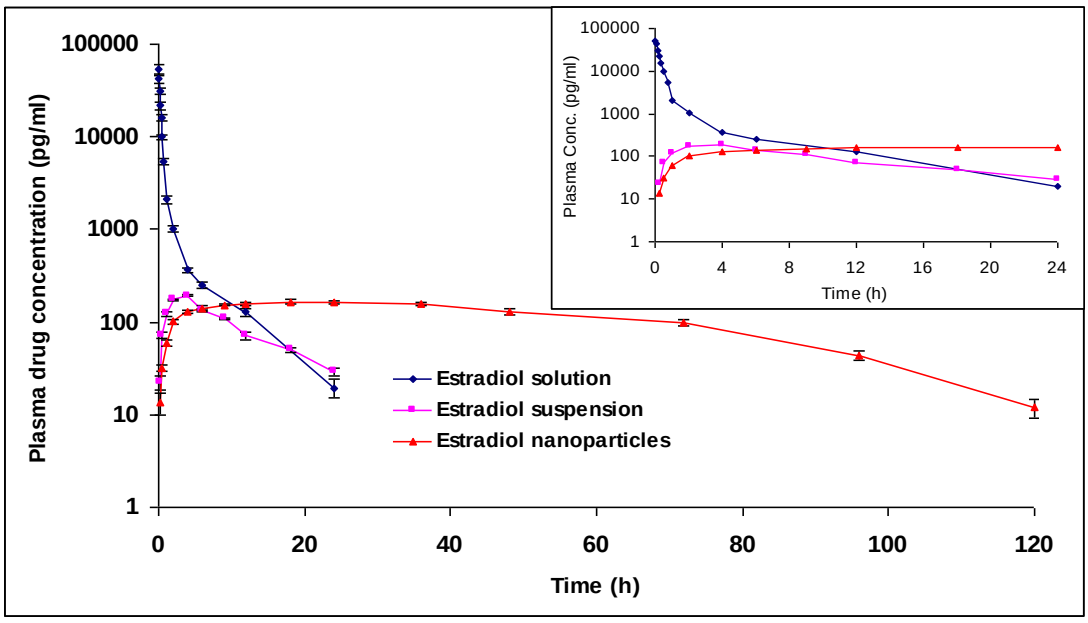

Fig. 2.1a&b Comparative plasma concentration profiles obtained after i.v. administration of drug solution and oral administration of drug suspension and drug loaded polymeric nanoparticulate formulations at doses (a) 100 μg/kg (b) 200 μg/kg. Inserts show an expanded view of first 24 h plasma profile. A plateau phase was observed in case of nanoparticles indicating its sustained release action. Data points shown are mean ± standard deviation (n=5).

(c)

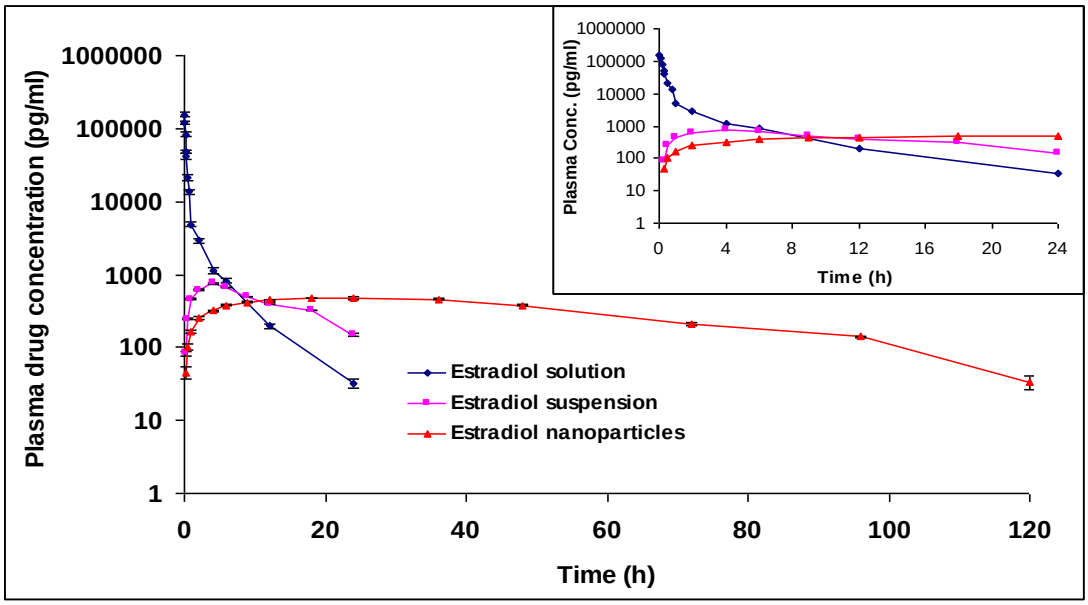

Fig. 2.1c Comparative plasma concentration profiles obtained after i.v. administration of drug solution and oral administration of drug suspension and drug loaded polymeric nanoparticulate formulations at dose 500 µg/kg. Insert show an expanded view of first 24 h plasma profile. A plateau phase was observed in case of nanoparticles indicating its sustained release action. Data points shown are mean ± standard deviation (n=5).

Table 2.1

Pharmacokinetic parameters obtained after oral administration of drug suspension and drug loaded PLGA nanoparticles at 3 different doses. (n=5; Mean ± SD)

Dose & formulation	C_{max} (pg/ml)	T_{max} (h)	$AUC_{0\text{-}inf}$ (pg.h/ml)	Absolute BA (%)	Relative BA (%)	K_a (h^{-1})	K_{el} (h^{-1})	$t_{1/2}$ (h)	MRT (h)	MAT (h)
100 µg/kg DS	101.90 ± 6.43	4	1289.50 ± 111.62	11.43 ± 0.10	-	1.099 ± 0.078	0.087 ± 0.009	7.98 ± 0.80	10.60 ± 0.59	8.69 ± 0.48
200 µg/kg DS	193.10 ± 5.76	4	2473.02 ± 87.29	11.46 ± 0.83	-	1.188 ± 0.083	0.089 ± 0.014	7.74 ± 0.56	12.35 ± 0.65	10.31 ± 0.56
500 µg/kg DS	757.03 ± 8.02	4	11339.20 ± 67.67	20.35 ± 1.42	-	0.839 ± 0.105	0.127 ± 0.007	5.46 ± 1.23	12.20 ± 0.62	10.45 ± 0.48
100 µg/kg NP	85.30 ± 2.81	24	6578.90 ± 618.81	58.32 ± 0.97	510.19 ± 3.87	0.067 ± 0.004	0.056 ± 0.006	12.32 ± 1.29	48.57 ± 2.11	46.66 ± 2.13
200 µg/kg NP	164.54 ± 5.33	24	12443.17 ± 504.29	57.67 ± 4.82	503.16 ± 9.53	0.066 ± 0.009	0.055 ± 0.008	12.71 ± 1.54	47.05 ± 3.02	45.00 ± 2.93
500 µg/kg NP	476.02 ± 8.83	18	34212.08 ± 1036.38	61.39 ± 2.96	301.72 ± 6.54	0.071 ± 0.005	0.059 ± 0.011	11.84 ± 1.67	46.47 ± 2.64	44.72 ± 2.47

C_{max}: Maximum plasma concentration, T_{max}: Time taken to attain C_{max}

DS: Drug suspension, NP: Nanoparticles, BA: Bioavailability, MRT: Mean residence time, MAT: Mean absorption time

Plasma profiles were fit in one compartment model.

Relative bioavailability (%) refers to $AUC_{0\text{-}inf}$ NP/$AUC_{0\text{-}inf}$ DS (%)

$AUC_{0\text{-}inf}$ was calculated by linear trapezoidal rule.

K_{el} was calculated by log linear regression.

K_a was calculated by back stripping of curve.

MRT was calculated by area under the first moment curve ($AUMC_{0\text{-}inf}$)/area under curve ($AUC_{0\text{-}inf}$).

MAT was calculated by MRT_{oral} - $MRT_{i.v.}$

Table 2.2

Pharmacokinetic parameters obtained after intravenous (i.v.) administration of drug solution at 3 different doses. (n=5; Mean ± SD)

Dose & formulation	AUC $_{0\text{-inf}}$ (pg.h/ml)	K_{el} (h^{-1})	$t_{1/2}$ (h)	MRT (h)
100 µg/kg i.v	11281.62 ± 874.41	0.161 ± 0.006	4.30 ± 0.33	1.91 ± 0.10
200 µg/kg i.v	21575.07 ± 1961.05	0.157 ± 0.004	4.41 ± 0.21	2.04 ± 0.09
500 µg/kg i.v	55725.67 ± 4178.00	0.151 ± 0.008	4.60 ± 0.29	1.75 ± 0.14

Plasma profiles were fit in two compartment model.

AUC $_{0\text{-inf}}$ was calculated by linear trapezoidal rule.

K_{el} was calculated by log linear regression.

MRT was calculated by area under the first moment curve ($AUMC_{0\text{-inf}}$)/area under curve ($AUC_{0\text{-inf}}$)

comparison to drug suspension, proving the potential of oral polymeric nanoparticles in preventing the first pass metabolism and extending the release of oestradiol in the present case. This is also evident from increase in absolute bioavailability and corresponding relative bioavailability of the nanoparticles. Also, apparent elimination rate constant (K_{el}) was found to be decreased ($p<0.001$) with all nanoparticulate formulations, indicating the slower rate of drug elimination from the body, also obvious from the increased apparent elimination half life ($t_{1/2}$) ($p<0.001$) and consequently prolonged drug release. The mean absorption time (MAT) of the drug suspension was significantly shorter ($p<0.001$) than that of the nanoparticles, demonstrating that absorption of drug from suspension was much more rapid than its release from the nanoparticles. In case of drug suspension, absorption rate constant (K_a) was larger than elimination rate constant ($K_a > K_{el\ i.v.}$) ($p<0.001$) showing that absorption is much faster than elimination, but K_a was found to be smaller than $K_{el\ i.v.}$ in nanoparticles ($K_a < K_{el\ i.v.}$) ($p<0.05$), which represented slow and sustained release of drug from polymer matrix and therefore, suggesting the presence of "flip-flop" pharmacokinetics (Dhanikula *et al*., 2008). (Note: in the case of oral delivery of polymeric nanoparticles, 'release' is a more appropriate term than 'absorption' as nanoparticles are taken up through the GI tract and release the encapsulated drug from the areas of disposition. However, the release at various stages after ingestion till they reach the disposition sites can not be ignored).

Moreover, linear regression analysis showed a statistically significant linear correlation between dose and AUC in nanoparticles ($F(1,13)=2876.5$ $p<0.001$) as well as drug suspension ($F(1,13)=686.8$ $p<0.001$). This indicated that drug in nanoparticles also exhibited dose-proportionality, as in the case of drug

suspension. Therefore, the data ascertains the predictable and accurate dose adjustments of nanoparticulate dosage forms, depending on the severity and type of indication.

2.5 Conclusions

The present investigation demonstrates the potential of polymeric nanoparticles for oral administration of oestradiol. The much improved AUC values along with sustained drug release with polymeric nanoparticles offers the possibility of dose reduction and reduced frequency of administration. Moreover, oestradiol nanoparticles dosed at 200 μg/kg exhibited pharmacological therapeutic plasma drug levels and therefore, the dose was selected for its further pharmacodynamic evaluation in an ovariectomized (OVX) rat model of hyperlipidaemia.

Chapter-3

Evaluating the potential of oral oestradiol nanoparticles in a rat model of hyperlipidaemia*

*This part of study was conducted in National Institute of Pharmaceutical Education and Research (NIPER), India and has been published in Pharmaceutical Research 26, 218-223 (2009).

3.1 Introduction

Cardiovascular disease (CVD) is the leading cause of morbidity and mortality in post-menopausal women, with approximately 50% developing CVD in their lifetime, 30% dying from the disease and 20% developing stroke (Stevenson, 2000; Pines, 2002). The increased incidence of CVD in post-menopausal women has been mainly attributed to menopausal metabolic syndrome manifested by obesity, dyslipidaemia (increases in total cholesterol, triglycerides, LDL cholesterol, and decreases in HDL cholesterol levels), insulin resistance and hypertension (Gorodeski, 2002; Shen *et al*., 2003; Bottner and Wuttke, 2006). Oestrogen deficiency due to loss of ovarian function at menopause is primarily responsible for the development of various metabolic abnormalities and conditions can be made reversible with ERT. Numerous epidemiological studies have suggested that post-menopausal ERT reduces the cardiovascular disease risk up to 50% (Stampfer and Colditz, 1991; Grodstein and Stampfer, 1995; Grodstein *et al*., 1996). Oestrogen cardiovascular action is mainly related to the modulation of lipids and lipoproteins. LDL are the primary means by which cholesterol is transported from liver to peripheral tissues and hepatic LDL receptors (LDLr) are responsible for maintaining the cholesterol levels in the cells by regulating the plasma LDL level. After the menopause, the clearance rate of LDL from plasma by hepatic LDLr becomes slow due to decrease in their number. This leads to elevated plasma LDL level with relatively longer circulation time, making them more susceptible to modification such as oxidation and finally, giving rise to initiation and development of atheromatous plaque. Oestrogen cholesterol lowering action is mostly achieved through up-regulation of hepatic LDLr and thereby, decreasing the plasma LDL concentration (Stevenson, 1998; Abbey *et al*., 1999; Tolbert and

Oparil, 2001). Hyperinsulinaemia and hyperglycaemia, resulting from insulin resistance are also the major post-menopausal metabolic disturbances leading to many adverse changes of the CVD. At physiological levels, oestrogens are thought to be involved in maintaining normal insulin sensitivity. However, oestrogen deficiency at menopause may promote insulin resistance. Improved glucose metabolism may contribute to the protective effect of oestrogen in CVD as ERT after menopause has been suggested to improve the insulin sensitivity and reduce the Type II diabetes risk profile (Livingstone and Collison, 2002; Liu *et al*., 2004).

Oxidative stress has also been implicated as a major factor in the pathogenesis of cardiovascular disease. Deprivation of endogenous oestradiol after menopause leads to increased oxidative stress due to an unbalanced pro-oxidant/antioxidant equilibrium and this is also thought to be a potential inducer of post-menopausal cardiovascular risk. The increased oxidative stress results in enhanced oxidative modification of LDL. Oxidized LDL are excessively taken up by the scavenger receptors on macrophages in the arterial wall, leading to cholesterol accumulation and the conversion of macrophages into foam cells, which plays a major role in the development of atherosclerotic plaque formation (Esterbauter *et al*., 1992; Berliner and Heinecke, 1996). The cardio-protective effect of oestradiol might also be partly due to its antioxidant action, resulting in protection against lipoprotein oxidation (Rifici and Khachadurian, 1992; Badeau *et al*., 2005).

The effect of oestrogens on lipids and lipoproteins depends on the type and dose of oestrogens used, and its route of administration. The oral delivery of oestrogens provides a profound beneficial effect in increasing the HDL, a change that is often considered pivotal to have cardiovascular benefit (Stevenson, 1998; Crook, 2001). However, conventional oral formulations are

required to be administered in high doses that can cause over expression of liver proteins leading to potential adverse effects (Yoo and Lee, 2006). PLGA nanoparticles have shown to be effective in improving the oral bioavailability of oestradiol (Hariharan *et al*., 2006; Mittal and Kumar, 2009). Therefore, the present study deals with the prospects of oral polymeric nanoparticulate approach in treatment of post-menopausal hyperlipidaemia. The oestradiol encapsulated PLGA nanoparticles were evaluated in oestrogen deficient (ovariectomized) high-fat diet (HFD) induced hyperlipidaemic rat model. The rationale for choosing to impose a HFD, further in the oestrogen deficient rat was to study the role of oestrogen supplementation on its protection against dyslipidaemia clinically seen in post-menopausal women. But this condition takes a long time to develop in the oestrogen deficient rat; therefore to achieve similar condition in rat we have designed a protocol involving ovariectomy followed by HFD feeding to mimic the post-menopausal dyslipidaemic state.

3.2 Materials

PLGA (Resomer RG 50:50 H; molecular weight 35-40KDa) was purchased from Boehringer Ingelheim (Ingelheim, Germany) and DMAB was purchased from Aldrich (St. Louis, MO, USA). Oestradiol was a gift sample from Orion Pharma (Espoo, Finland). ELISA kits were procured from DRG diagnostics (Marburg, Germany). Ultrapure water (SG Water Purification System, Barsbuttel, Germany) was used for all the experiments. All the other chemicals and reagents were of highest commercially available grade.

3.3 Experimental

3.3.1 Preparation and characterization of PLGA nanoparticles

Oestradiol entrapped PLGA nanoparticles were prepared and characterized as described in section 2.3.1.

3.3.2 Animals

Female SD rats (200-210 g) were procured from the central animal facility of NIPER. The animals were housed in standard polypropylene cages (three rats per cage) and maintained under controlled room temperature (21 ± 2 °C) and humidity (55 ± 5 %) with 12 h light and 12 h dark cycle. All the rats were fed with commercially available rat normal pellet diet (NPD) (Amrut Diet, New Delhi) and water ad libitum, prior to the dietary manipulation. The guidelines of the committee for the purpose of control and supervision of experiments on animals (CPCSEA), Govt. of India were followed and prior permission was sought from the institutional animal ethics committee (IAEC) for conducting the study.

3.3.3 Experimental Protocol

The animals were divided into eight groups of n=6. Ovariectomy (OVX) was done in 5 groups by bilateral incision in the lower part of the peritoneal cavity under anaesthesia and after that they were kept for one week to allow them to recover from the surgical stress. Thereafter, 4 out of 5 OVX groups and one intact ovary group were fed on HFD while the other 3 groups (Intact, Sham and OVX only) received normal pellet diet (NPD) throughout the experimental period of 6 weeks. HFD comprises of 58% fat, 25% protein and 17% carbohydrate, as a percentage of total kcal and the detailed composition of various ingredients is described in Table 3.1 (Srinivasan *et al*., 2005). Four OVX rats groups receiving HFD were again divided into one no treatment (OVX+HFD), and three treatment groups. After 4 weeks the animals were treated with oestradiol suspension (OVX+HFD+ES), oestradiol nanoparticles (OVX+HFD+ENPs), and blank nanoparticles (OVX+HFD+BNPs). Treatment was carried out for 2 weeks till the end of 6th week. Drug treatment groups (OVX+HFD+ES & OVX+HFD+ENPs) received a dose of 200 μg/kg body weight (Parini *et al*., 2000). However, same doses of nanoparticles (made freshly and dispersed in water at each dosing time) were administered once in three days as compared to daily administration of the suspension. The frequency of administration for the nanoparticle group was based on the *in vivo* pharmacokinetics of oestradiol (Mittal and Kumar, 2009).

3.3.4 Estimation of biochemical parameters

Blood sampling was done after six weeks and plasma was analyzed for total cholesterol (TC), triglycerides (TG), high-density lipoprotein cholesterol (HDL-C), low-density lipoprotein cholesterol (LDL-C), very low-density

Table 3.1
Composition of HFD

Ingredients	Diet (g/kg)
Powdered NPD	365
Lard	310
Casein	250
Cholesterol	10
Vitamin and mineral mix	60
DL-Methionine	03
Yeast powder	01
Sodium chloride	01

lipoprotein cholesterol (VLDL-C) and glucose using commercially available colorimetric diagnostic kits (Accurex Biomedical Pvt. Ltd., Mumbai, India).

3.3.5 Estimation of lipid peroxidation

Malondialdehyde (MDA), an index of lipid peroxidation and oxidative stress, was measured in the plasma. The method works on the principle of formation of thiobarbituric acid reacting substances (TBARS) upon reaction of MDA with thiobarbituric acid (TBA), a red coloured complex giving peak absorbance at 532 nm (Ohkawa *et al*., 1979). In brief, the reaction mixture consisted of 0.1 ml of 8.1% sodium dodecyl sulphate (SDS), 0.75 ml of 20% glacial acetic acid and 0.75 ml of 0.8% TBA was added to 0.1 ml of plasma. The total volume was then adjusted to 2 ml with distilled water followed by heating at 95 °C for 60 min. Thereafter, samples were cooled and the absorbance was measured at 532 nm. The amount of MDA in the plasma was calculated using a calibration curve. The MDA contents were expressed as nanomoles of MDA per ml of plasma.

3.3.6 Statistical analysis

Statistical significance between groups was determined by using one way analysis of variance (ANOVA) followed by Tukey post-hoc test for multiple comparisons and a value of $p<0.05$ was considered statistically significant.

3.4 Results and Discussion

The particle size of oestradiol loaded PLGA nanoparticles was found to be 115.3 ± 2.5 nm with zeta potential values of 92.4 ± 3.2 mV (pH range was 4.01-4.08). The entrapment efficiency at 10% (w/w of polymer) initial drug loading was 51.2 ± 3.8 %.

Ovariectomy resulted in significant reduction in circulating plasma oestradiol levels (8.4 ± 2.7 pg/ml) compared to intact and sham operated

groups (32.5 ± 5.7 pg/ml). This confirmed successful ovariectomy of the animals. After 6 weeks, body weight was slightly but not significantly increased in OVX animals, whereas HFD feeding resulted in significant increase ($p<0.05$) in body weight compared to intact animals. On the other hand, OVX+HFD group attained higher body weight than OVX or HFD groups alone, indicating that the oestrogen deficient condition further aggravated the HFD induced obesity. Treatment with oestradiol nanoparticles (ENPs) significantly ($p<0.05$) decreased the body weight, but treatment with oestradiol suspension (ES) did not show any significant difference (Fig. 3.1). The results showed that oestrogen deficiency may be related to development of obesity in post-menopausal women and effects can be attenuated by oestrogen treatment (Shinoda *et al*., 2002).

There was a little or no difference in the plasma lipids levels of both OVX and HFD fed animals. Ovary intact female animals were appeared to be protected from HFD feeding by available endogenous oestrogen, because male SD rats develop hyperlipidaemia upon HFD feeding for 4 weeks (Meena *et al*., 2008). However, a significant difference was observed in plasma lipid profile of OVX+HFD fed groups compared to intact group, closely resembling the clinical condition of post-menopausal hyperlipidaemic women having high risk of developing cardiovascular complications. Two weeks of treatment with oestradiol nanoparticles (ENPs) significantly reduced the elevated plasma levels of TC, TG, VLDL-C and LDL-C irrespective of their 3 times lower dose than suspension, indicating the potential of oral polymeric nanoparticles in improving the bioavailability as well as sustaining the drug release (Figs. 3.2-3.6). Though several mechanisms are suggested for the lipid lowering effect of oestradiol in post-menopausal hyperlipidemic condition, up-regulation of hepatic LDL

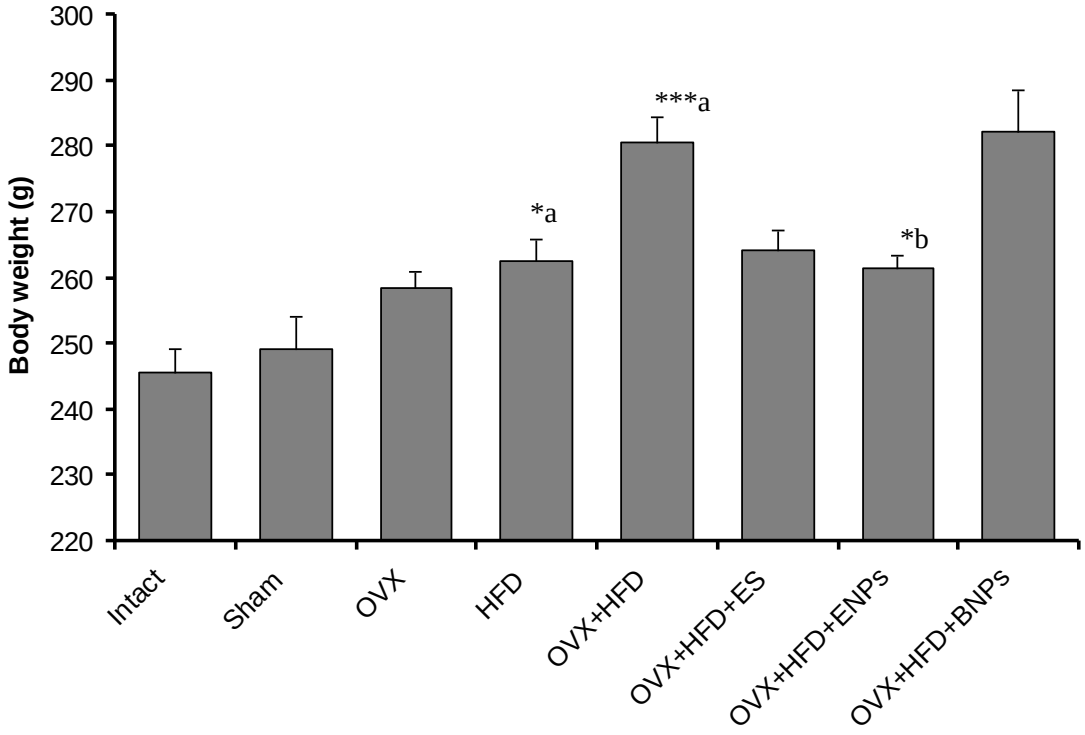

Fig. 3.1 Effect of oestradiol treatment on body weight of oestrogen deficient hyperlipidaemic rats. Each data point is represented as Mean ± SEM (n=6). ***p<0.001, ** p<0.01, *p<0.05; a vs intact and b vs OVX+HFD.

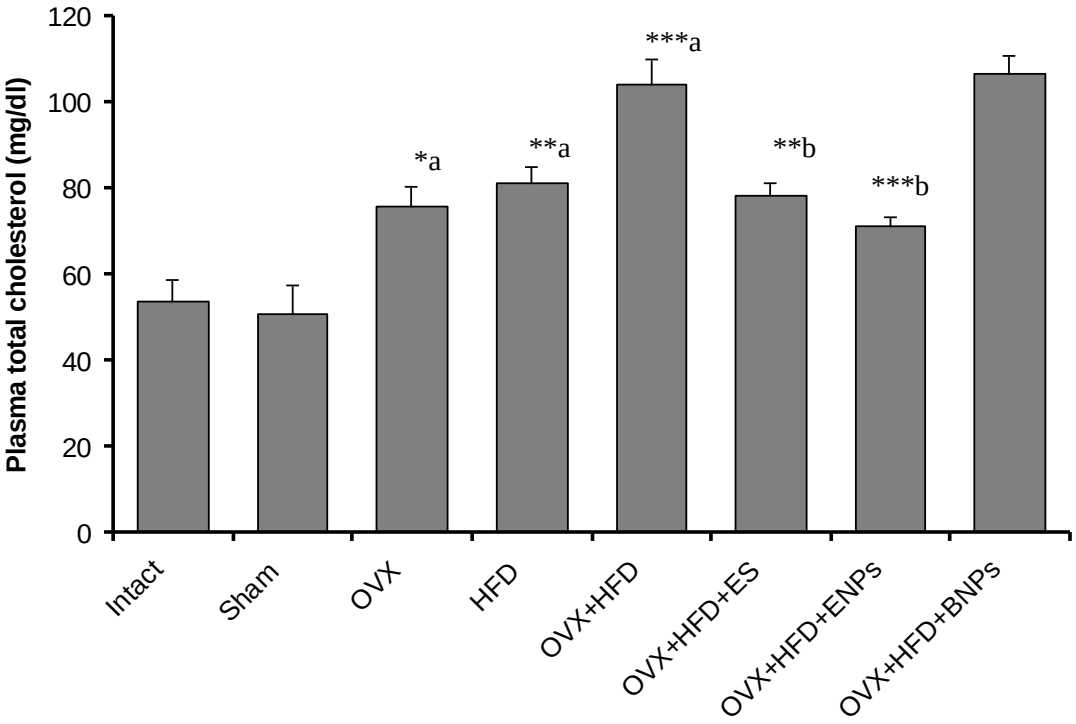

Fig. 3.2 Plasma levels of total cholesterol (TC) after 6 weeks of study. Each data point is represented as Mean ± SEM (n=6). ***p<0.001, ** p<0.01, *p<0.05; a vs intact and b vs OVX+HFD.

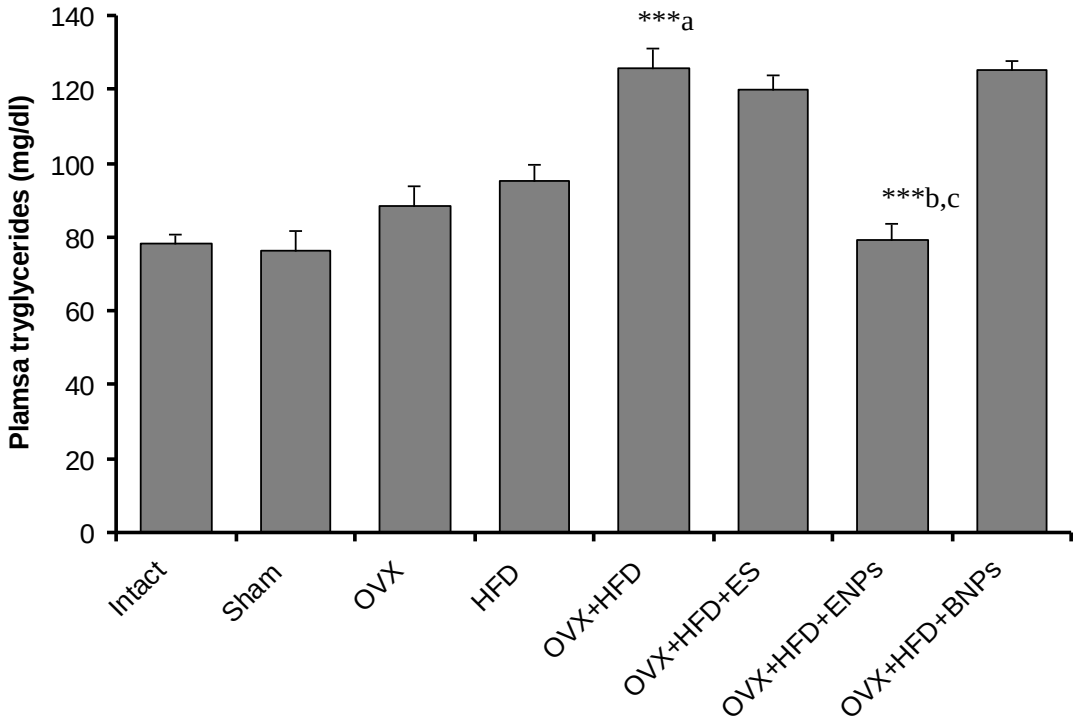

Fig. 3.3 Plasma levels of triglycerides (TG) after 6 weeks of study. Each data point is represented as Mean ± SEM (n=6). ***p<0.001, ** p<0.01, *p<0.05; a vs intact, b vs OVX+HFD and c vs OVX+HFD+ES.

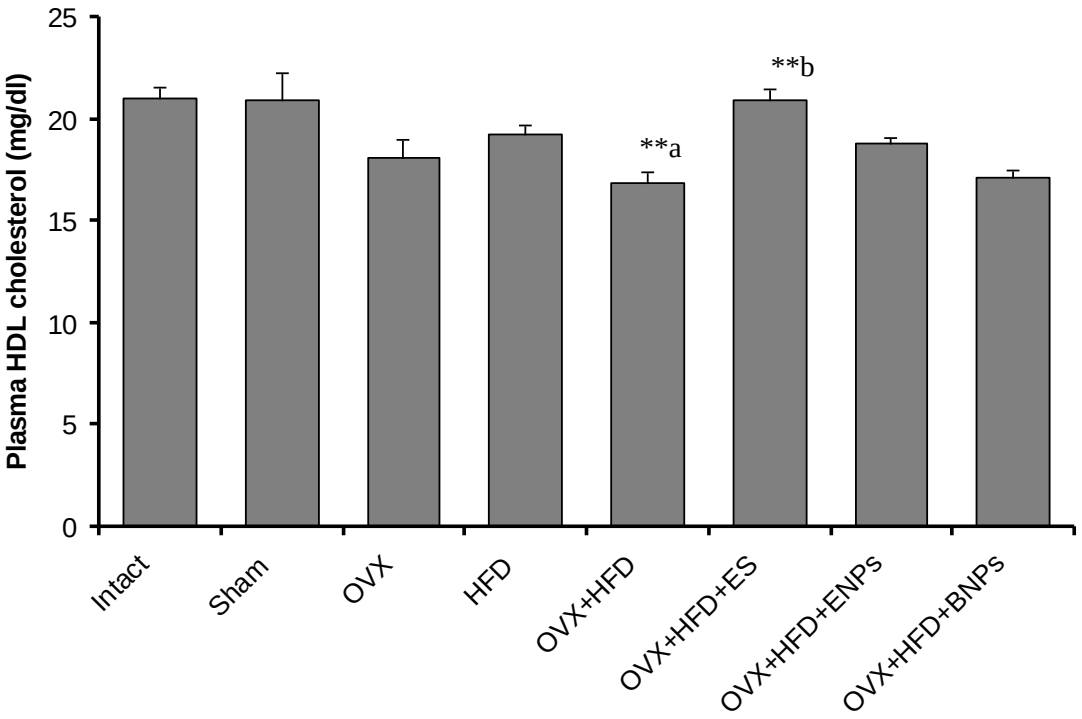

Fig. 3.4 Plasma levels of high-density lipoprotein cholesterol (HDL-C) after 6 weeks of study. Each data point is represented as Mean ± SEM (n=6). ***p<0.001, ** p<0.01, *p<0.05; a vs intact and b vs OVX+HFD.

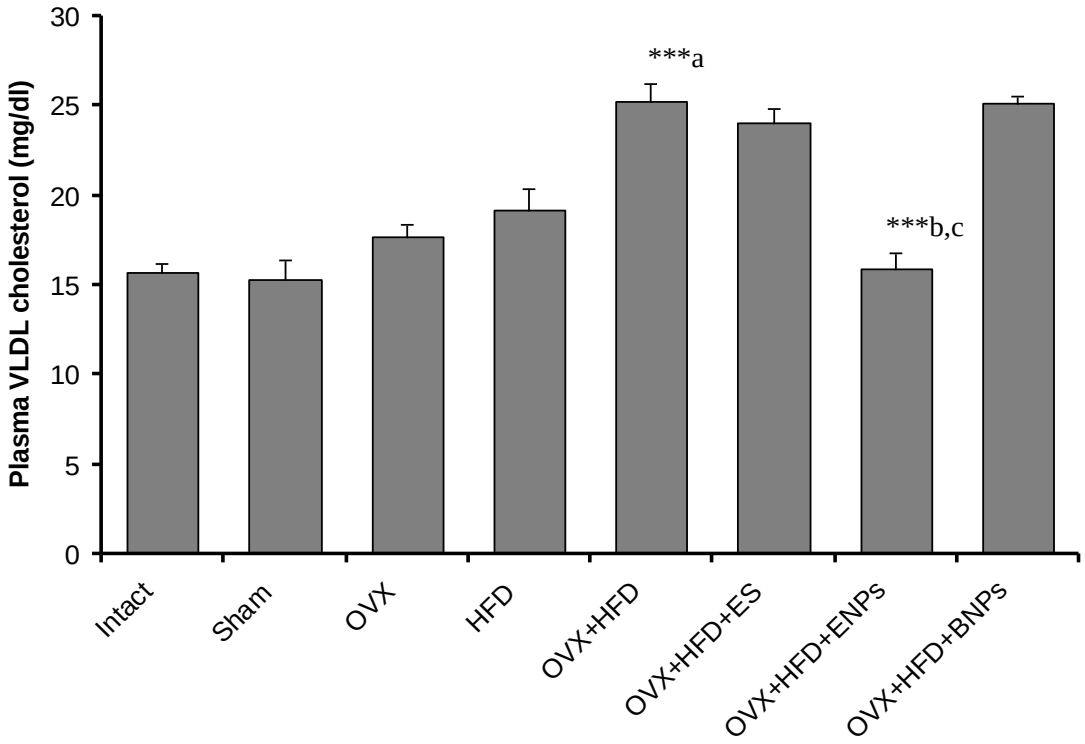

Fig. 3.5 Plasma levels of very low-density lipoprotein cholesterol (VLDL-C) after 6 weeks of study. Each data point is represented as Mean ± SEM (n=6). ***p<0.001, ** p<0.01, *p<0.05; a vs intact, b vs OVX+HFD and c vs OVX+HFD+ES.

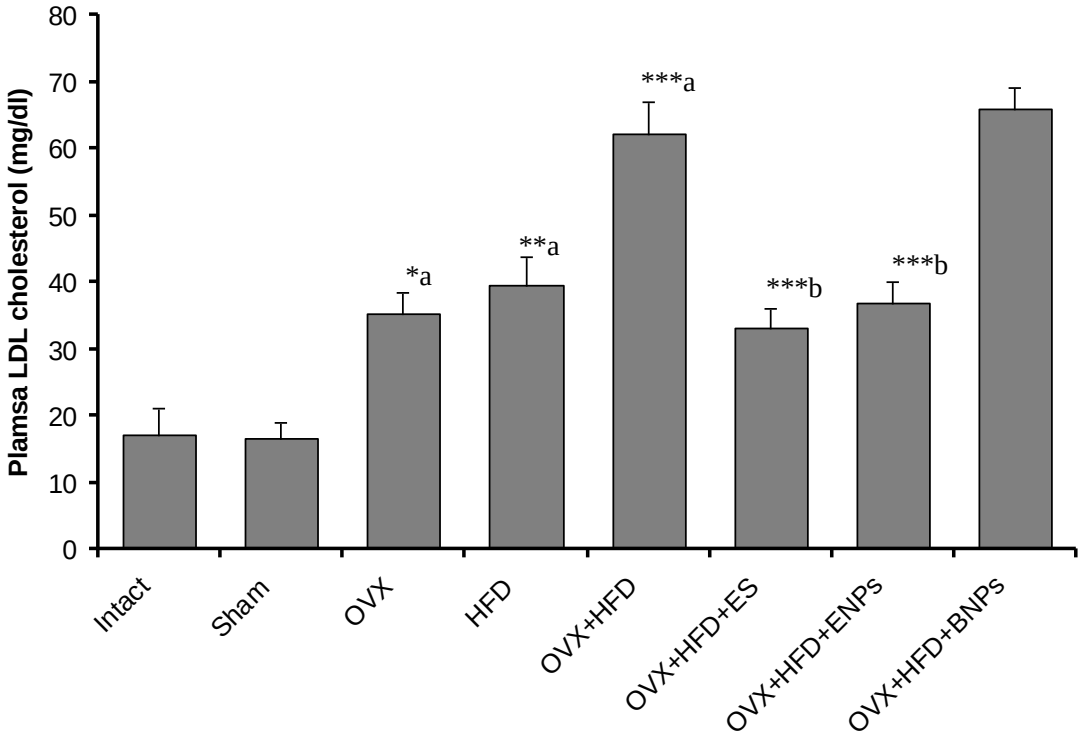

Fig. 3.6 Plasma levels of low-density lipoprotein cholesterol (LDL-C) after 6 weeks of study. Each data point is represented as Mean ± SEM (n=6). ***p<0.001, ** p<0.01, *p<0.05; a vs intact and b vs OVX+HFD.

receptors is the primary means considered to be responsible for the beneficial effect (Lundeen *et al*., 1997; Lemieux *et al*., 2006). The plasma levels of HDL-C "considered to be good cholesterol" were found to be decreased in OVX+HFD fed group. ES treated group increased the HDL-C levels after 2 weeks of treatment; whereas, ENPs were found to have no effect on plasma HDL-C levels (Fig. 3.4). This can be explained on the basis of "first pass effect" which is encountered when the formulation is given as suspension. Large doses of drug are required to overcome this first pass effect in order to attain the clinically relevant plasma drug levels. This high dose leads to increased hepatic synthesis of many proteins such as apolipoprotein A-1 (major component of HDL) and therefore, increases plasma level of HDL. However, this overdosing also leads to severe metabolic changes such as triglyceridaemia (Crook, 2001; Yoo and Lee, 2006) and this could be the reason that ES treatment did not make any difference in plasma TG level, while nanoparticulate formulation significantly ($p<0.001$) decreased them (Fig. 3.3). No significant difference was observed in the lipid profile of sham operated group as compared to intact group indicating that surgery did not alter lipid profile. Likewise, blank nanoparticles treated group (BNPs) did not improve the hyperlipidemic condition showing that blank nanoparticles did not possess any pharmacological activity. The cardiovascular risk factor was calculated by taking ratio of TC and HDL-C and the ratio is indicative of the degree of cardiovascular risk. This ratio was less than 3 (2.56) in intact animals which is considered safe, whereas OVX and HFD alone showed risk ratio of 4.19 and 4.20 respectively. These values are above the safe limit and might cause heart ailments in long term. Further, OVX+HFD animals showed 6.17 as risk ratio, where the chances of developing CVD is considered to be double. Both ES and ENPs decreased the CVD risk by bringing down the

ratio to 3.73 and 3.79 respectively (Fig. 3.7), indicating that oestradiol supplementation is effective in the post-menopausal dyslipidemic women, who are at great risk of developing CVD in later stages.

A significant elevation was observed in the blood glucose level of OVX+HFD group. This reflects the insulin resistance present in these animals, which may further lead to Type II diabetes at the advanced stages of the oestrogen deficient post-menopausal condition. E2 treatment (both suspension as well as nanoparticles) decreased the blood glucose levels (Fig. 3.8), proving that oestradiol is effective in improving insulin sensitivity in the post-menopausal condition.

MDA is an end product of lipid peroxidation and serves as oxidative stress biomarker (Dalle-Donne *et al*., 2006). MDA levels were found to be increased in OVX groups, evidencing the induction of oxidative stress due to oestrogen deficiency at menopause and this could be further related to high prevalence of cardiovascular disease in post-menopausal women. HFD feeding alone did not increase MDA levels, possibly because of the antioxidant property of oestrogen present in ovary intact HFD fed animals. However, 2 weeks of treatment with oestradiol suspension (ES) and nanoparticles (ENPs) significantly decreased the raised MDA levels (Fig. 3.9), confirming the antioxidant potential of oestradiol. Nanoparticle formulation was found to be more effective ($p<0.05$) than suspension which might be because of its controlled and sustained drug release action.

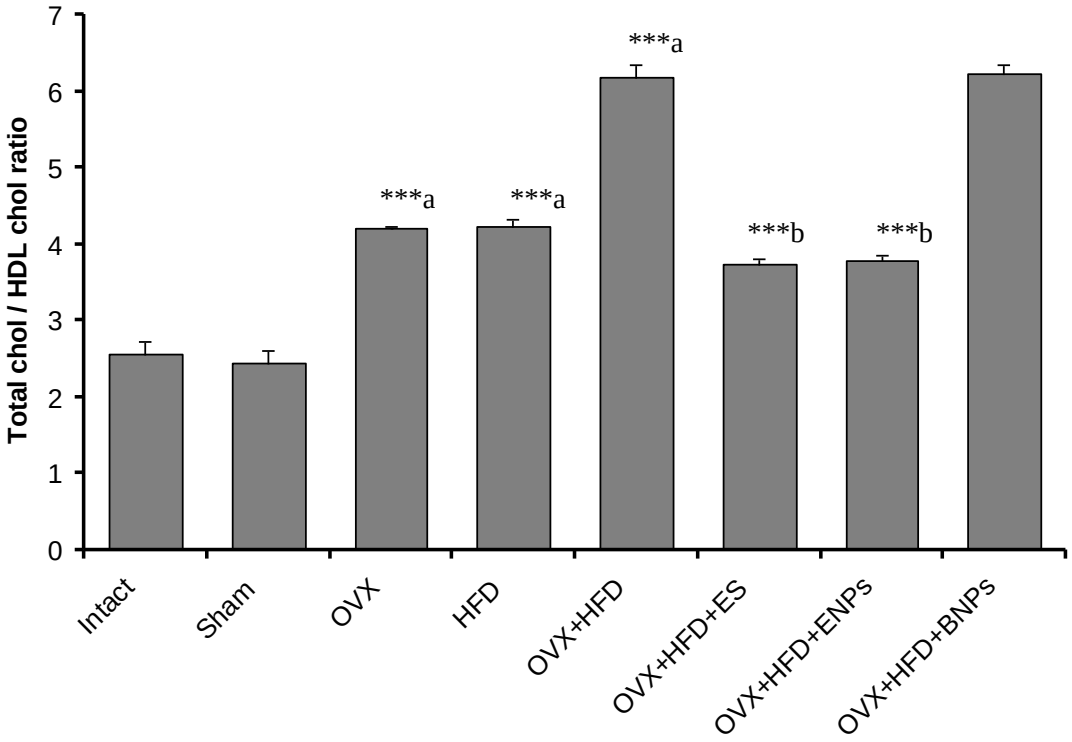

Fig. 3.7 Effect of oestradiol treatment on TC/HDL-C ratio (indicative of cardiovascular risk factor) of oestrogen deficient hyperlipidaemic rats. Each data point is represented as Mean ± SEM (n=6). ***p<0.001; a vs intact and b vs OVX+HFD.

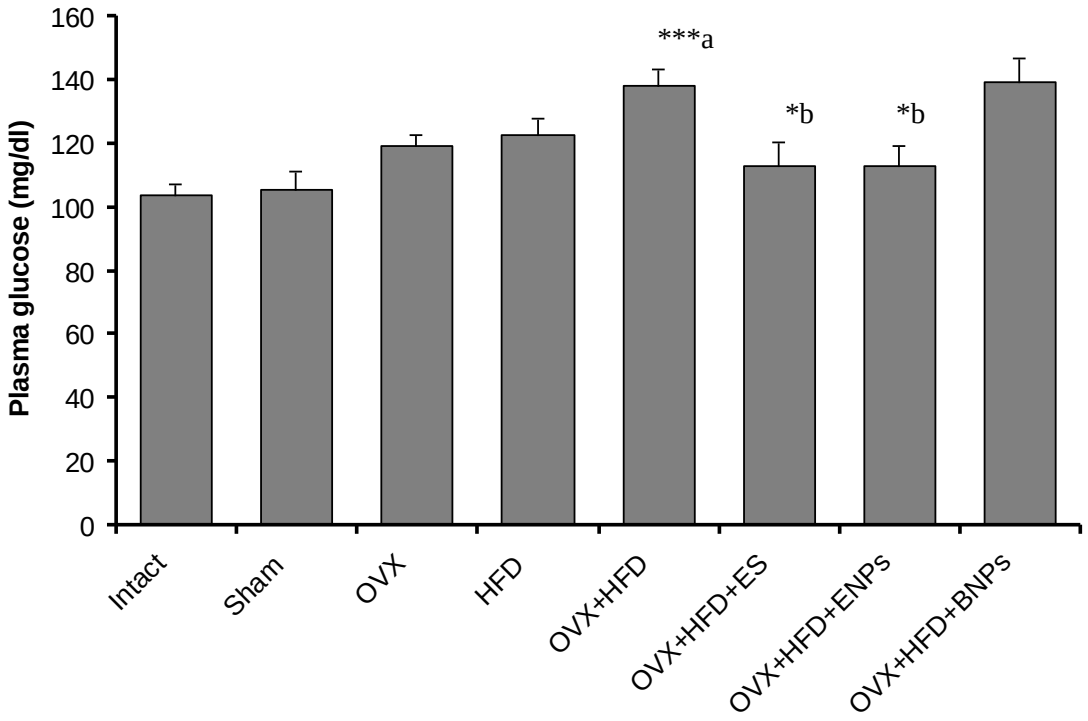

Fig. 3.8 Plasma glucose levels after 6 weeks of study. Each data point is represented as Mean ± SEM (n=6). ***p<0.001, ** p<0.01, *p<0.05; a vs intact and b vs OVX+HFD.

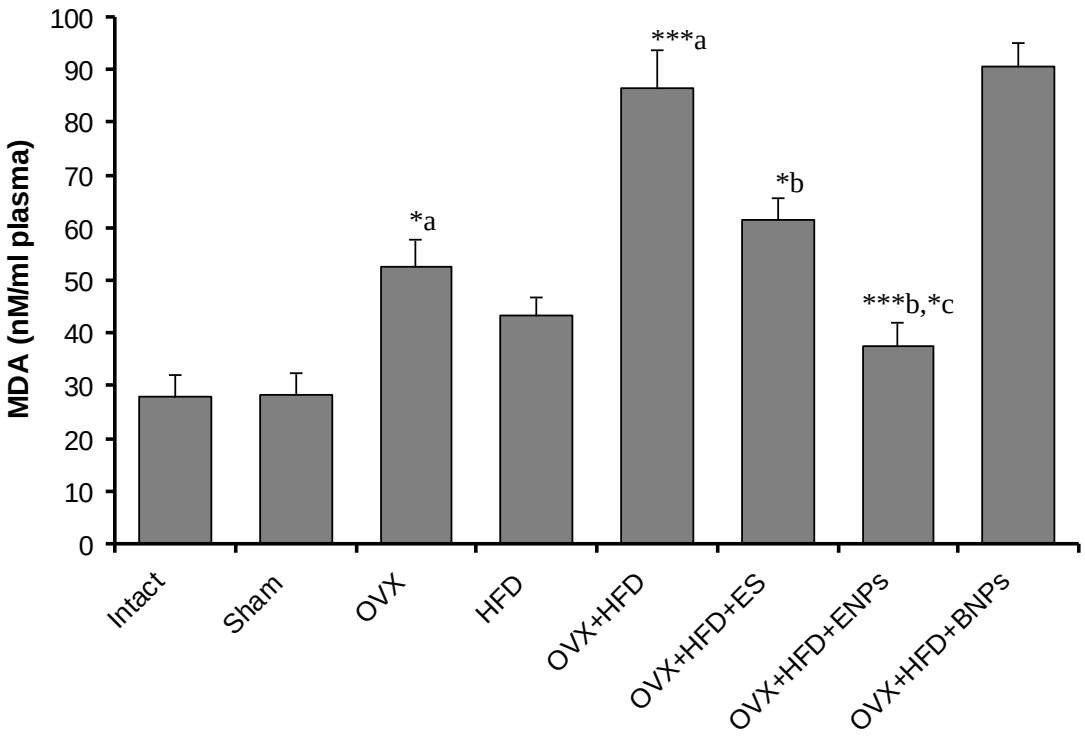

Fig. 3.9 Effect of oestradiol treatment on plasma lipid peroxidation in oestrogen deficient hyperlipidaemic rats. Each data point is represented as Mean ± SEM (n=6). ***p<0.001, ** p<0.01, *p<0.05; a vs intact, b vs OVX+HFD and c vs OVX+HFD+ES**.**

3.5 Conclusions

The study has confirmed that oestradiol therapy is efficient in treating the post-menopausal metabolic syndrome by preventing or reversing the weight gain, dyslipidaemia and insulin resistance. Furthermore, oestradiol PLGA nanoparticles were found to extend the same/better therapeutic benefits at much lower dose than suspension, indicating that they could alleviate the adverse effects of conventional oral formulations.

Chapter-4

Oral delivery of oestradiol to brain aided by biodegradable nanoparticles

4.1 Introduction

The blood–brain barrier (BBB) consists of a single layer of endothelial cells lining the brain capillaries, which are connected by much complex tighter junctions than found in the peripheral vessels (Brightman, 1977; Wolberg and Lippoldt, 2002). Therefore, drug delivery to the brain has been one of the most challenging tasks for the pharmaceutical scientists as the BBB prevents the entry of more than 98% of small molecules and approximately 100% of large molecules (Tamai and Tsuji, 1996; Misra *et al*., 2003; Pardridge, 2005). Various approaches have been explored to overcome this problem including chemical drug delivery systems (Bodor *et al*., 1992; Bodor and Buchwald, 1999; Bodor and Buchwald, 2006), magnetic drug targeting (Devineni *et al*., 1995), or carrier systems such as antibodies (Pardridge *et al*., 1991), liposomes (Huwyler *et al*., 1996) or nanoparticles (Kreuter, 2001). Nanoparticle mediated brain drug delivery by the intravenous (i.v.) route depends on the coating of the particles with tweens, especially Tween 80 (T-80)/Polysorbate 80. Several mechanisms have been proposed for the transport of T-80 coated nanoparticles across the BBB, but mechanism of endocytosis is supported by many studies. T-80 coating results in adsorption of apolipoprotein E and/or B from the blood stream onto the nanoparticle surface. Then, the coated nanoparticles mimic natural LDL particles which could interact with the LDL receptor family located in the brain capillary endothelial cells followed by their endocytotic uptake. In addition, it has been suggested that processes such as tight junction modulation or inhibition of the P-glycoprotein (Pgp) efflux system also may occur resulting in brain uptake of nanoparticles (Kreuter, 2001; Kreuter, 2005; Roney *et al*., 2005; Gao and Jiang, 2006). To date, T-80 coated nanoparticles showed best results for brain targeting in comparison to other surfactants when tested for i.v. administration (Kreuter

et al., 1997) and the specific role of T-80 coating on targeting of nanoparticles to the brain has also been categorically established (Sun *et al*., 2004). However, very few studies on oral administration of such surface-modified nanoparticles have been reported (Schroeder *et al*., 1998; Das and Lin, 2005) probably due to the degradation of the drug and/or the polymer nanoparticles in the gastrointestinal media as well as due to the limited uptake of nanoparticles across the gastrointestinal membrane. Das and Lin, (2005) reported double-coated (T-80 and PEG 20,000) poly(butylcyanoacrylate) nanoparticulate delivery systems (PBCA) for oral delivery and brain targeting of dalargin, where they observed a significant dalargin-induced analgesia with both, double-coated and only T-80 coated PBCA nanoparticles. The rationale of their second coat of PEG was to protect the drug loaded nanoparticles in the hostile GI environment, which comprises of enzymes and varying levels of pH. As many of the pharmacological effects of oestradiol are also mediated through the central nervous system (CNS), in continuation of our efforts to deliver oestradiol efficiently, we attempted to design T-80 coated PLGA nanoparticles for brain delivery of oestradiol via the oral route.

4.2 Materials

PLGA (Resomer RG 50:50 H; molecular weight 35-40KDa) was purchased from Boehringer Ingelheim (Ingelheim, Germany) and DMAB was purchased from Aldrich (St. Louis, MO, USA). Oestradiol was a gift sample from Orion Pharma (Espoo, Finland). ELISA kits were procured from DRG diagnostics (Frauenbergstr, Germany). T-80 (Fluka), cobalt nitrate hexahydrate and ammonium thiocyanate (Acros Organics) were supplied by Fisher Scientific, UK. All the other chemicals and reagents were of highest commercially available grade.

4.3 Experimental

4.3.1 Preparation of T-80 coated nanoparticles

Oestradiol loaded PLGA nanoparticles were prepared by the emulsion-diffusion-evaporation method using DMAB as stabilizer. Drug entrapment efficiency was determined by centrifuging the drug loaded nanoparticles and then calculating the drug content in the pellet using a validated HPLC method as described in section 2.3.1. The coating was carried out by the addition of 1% - 5% (v/v relative to total suspension volume) T-80 to the reconstituted nanoparticles (Table 4.1) and stirring at 400 rpm for 30 minutes. The size and zeta potential of the nanoparticles (before and after coating) were determined using Zetasizer (Nano ZS, Malvern Instruments Ltd, Malvern, UK).

4.3.2 Quantification of surfactant coating

The amount of T-80 coating on PLGA nanoparticles was determined based on a quantitative test for poly(ethylene oxide) with ammonium cobaltothiocyanate ($NH_4[Co(SCN)_3]$) (Brown and Hayes, 1955; Sun *et al*., 2004). Briefly, T-80 coated nanoparticle suspension with a known volume

Table 4.1
Concentrations and corresponding amounts of T-80 used for coating of oestradiol entrapped PLGA nanoparticles.

Formulation code	T-80 (%)*	T-80 (mg)*
E2-NP	0.0	0.0
E2-T1-NP	1.0	53.8
E2-T2-NP	2.0	107.6
E2-T3-NP	3.0	161.4
E2-T4-NP	4.0	215.2
E2-T5-NP	5.0	269.0

*v/v relative to total suspension volume

was centrifuged and then supernatant was separated to quantify the unadsorbed T-80. Supernatant containing unadsorbed T-80 was mixed with $NH_4[Co(SCN)_3]$ solution (obtained by dissolving $Co(NO_3)_2.6H_2O$ and NH_4SCN in distilled water) with vigorous shaking, resulting in a complex which was subsequently extracted into chloroform. The absorption of the chloroform solution was measured at a wavelength of 318.5 nm using UV spectrophotometer (Unicam UV1, Unicam Ltd., UK). The amount of T-80 coating on nanoparticles was determined by calculating the uncoated/unadsorbed T-80 amount in supernatant using a calibration graph.

4.3.3 Stability of T-80 surface coating in simulated gastric fluid (SGF) and simulated intestinal fluid (SIF)

The stability of T-80 coat was evaluated in SGF and SIF, prepared according to British Pharmacopoeia (BP). Briefly; SGF was prepared by dissolving 2 g of NaCl and 3.2 g of pepsin in 80 ml of 1M HCl and finally made up to 1000 ml with adjustment of final pH to 1.2. SIF was prepared by dissolving 6.8 g of monobasic potassium phosphate in 250 ml water followed by addition of 77 ml of 0.2N NaOH, 500 ml of water, and 10 g of pancreatin and then pH was adjusted to 7.4. 1 ml of T-80 coated nanoparticles was added to 9 ml of simulated fluids and the intactness of the coating was evaluated at 2 h for SGF while for SIF the time interval was 6 h. After the respective time intervals, a known volume of suspension was centrifuged and then supernatant was separated to quantify the T-80 amount and thereby, calculating the percentage of coating remaining.

4.3.4 Animal Study

The tissue distribution experiments were conducted on male SD rats weighing 230-250 g. All procedures were carried out under as Project Licence

issued by the UK Home Office under the Animals (Scientific Procedures) Act 1986. The animals were housed under conditions of controlled illumination (12:12 h light/dark cycle), humidity, and temperature (18–22°C). After one week of acclimatization, rats were randomly and equally divided into different groups: oestradiol only (E2); oestradiol in uncoated nanoparticles (E2-NP) and oestradiol in T-80 coated nanoparticles (E2-T1-NP & E2-T4-NP). Oestradiol only was given through oral, intravenous (i.v.), and intramuscular routes at a dose of 200 μg/rat (~800 μg/kg). Selection of this particular dose was based on a published study which reported the therapeutic efficacy of oestradiol (at the dose of 200 μg/rat given intramuscularly after every 48 h for 6 weeks) in an ovariectomized (OVX) rat model for AD (Hua *et al*., 2007). However, uncoated (E2-NP) and surface coated (E2-T1-NP & E2-T4-NP) nanoparticulate groups were administered through oral route at three different doses of 100, 200 and 400 μg/rat while E2-NP as well as E2-T1-NP group was also given by i.v route at dose of 100 μg/rat. In each case, after single administration, 3 animals from each treatment group were sacrificed (post-blood sampling) after 1, 2 and 3 days and target tissue of interest, the brain, as well as non-target tissues small intestine, kidney, spleen, heart, liver, and lung were removed, homogenized and analysed for drug concentration using commercially available oestradiol ELISA kits as described in section 2.3.3.

4.3.5 Statistical analysis

The results were expressed as mean ± standard deviation (SD). Statistical analysis was carried out by one way ANOVA and subsequent Tukey post-hoc test for multiple comparisons. A p-value less than 0.05 was considered as significant.

4.4 Results and Discussion

The particle size of oestradiol entrapped nanoparticles, before coating, was found to be 134.7 ± 1.4 nm with zeta potential values of 68.5 ± 2.7 mV at pH 4.1 ± 0.2, while after coating with 1% T-80 it was 138.8 ± 4.3 nm with zeta potential of 19.2 ± 2.1 mV at pH 5.6 ± 0.3 (Fig. 4.1). The coating reduced the zeta potential significantly suggesting a possible masking effect. The entrapment efficiency at 10% (w/w of polymer) initial drug loading was 50.7 ± 1.4 %. Tissue distribution profile after one day of oral administration (Fig. 4.2 a) showed significantly higher tissue (including plasma) oestradiol levels ($p<0.05$) when given as nanoparticles (both E2-NP and E2-T1-NP) as compared to drug only (E2). This showed that nanoparticulate formulation is facilitating the systemic uptake of drug (improved bioavailability) as free drug is highly susceptible for gut wall and first pass metabolism. After 2 and 3 days of dosing, plain E2 was neither detected in the tissues nor in plasma, while appreciable drug levels were still observed in target as well as non-target tissues and plasma when administered as nanoparticles, indicating the sustained release action of PLGA nanoparticles (Fig. 4.2 b & c). However, no difference was found in the brain oestradiol levels of uncoated (E2-NP) and 1% T-80 coated (E2-T1-NP) nanoparticles after 1, 2 and 3 days of oral administration. On the other hand, the results obtained after i.v. administration showed that 1% T-80 coated (E2-T1-NP) nanoparticles were able to transport the drug to the brain to produce significantly higher levels ($p<0.001$) in comparison to the E2-NP (Fig. 4.3 a,b,c). For the E2 group, after i.v. administration, no oestradiol was detected even after one day, probably due to shorter half-life and therefore, rapid clearance from the body. Also, after i.v administration, accumulation of oestradiol in the liver and spleen was found to be reduced ($p<0.05$), when nanoparticles were coated with 1%

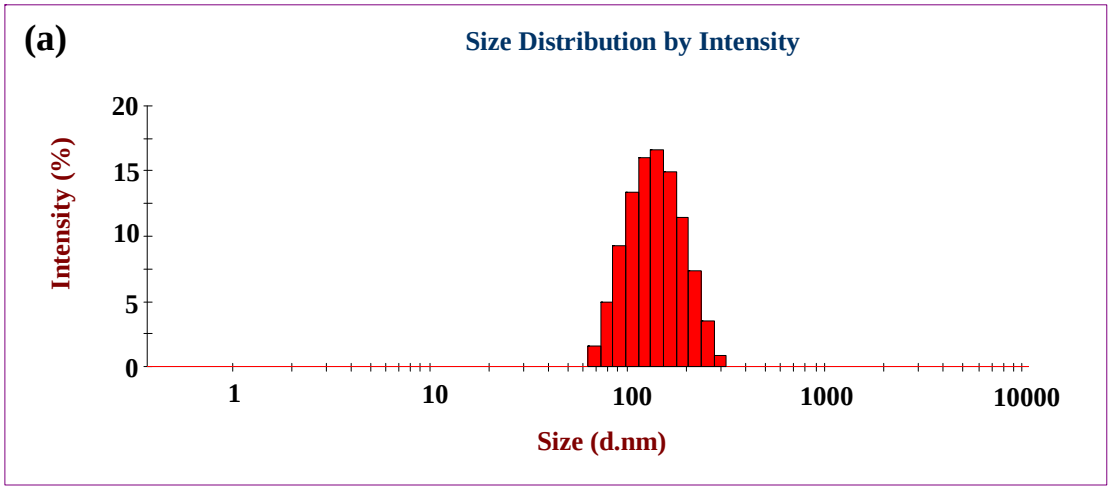

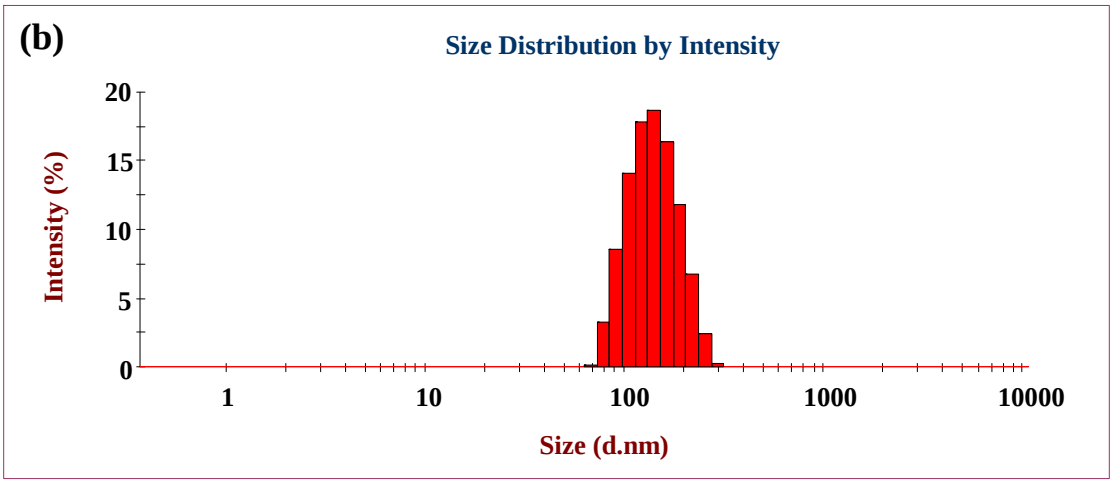

Fig. 4.1 Size distribution by intensity (%) of oestradiol entrapped PLGA nanoparticles (a) before, and (b) after coating with 1% T-80.

(a)

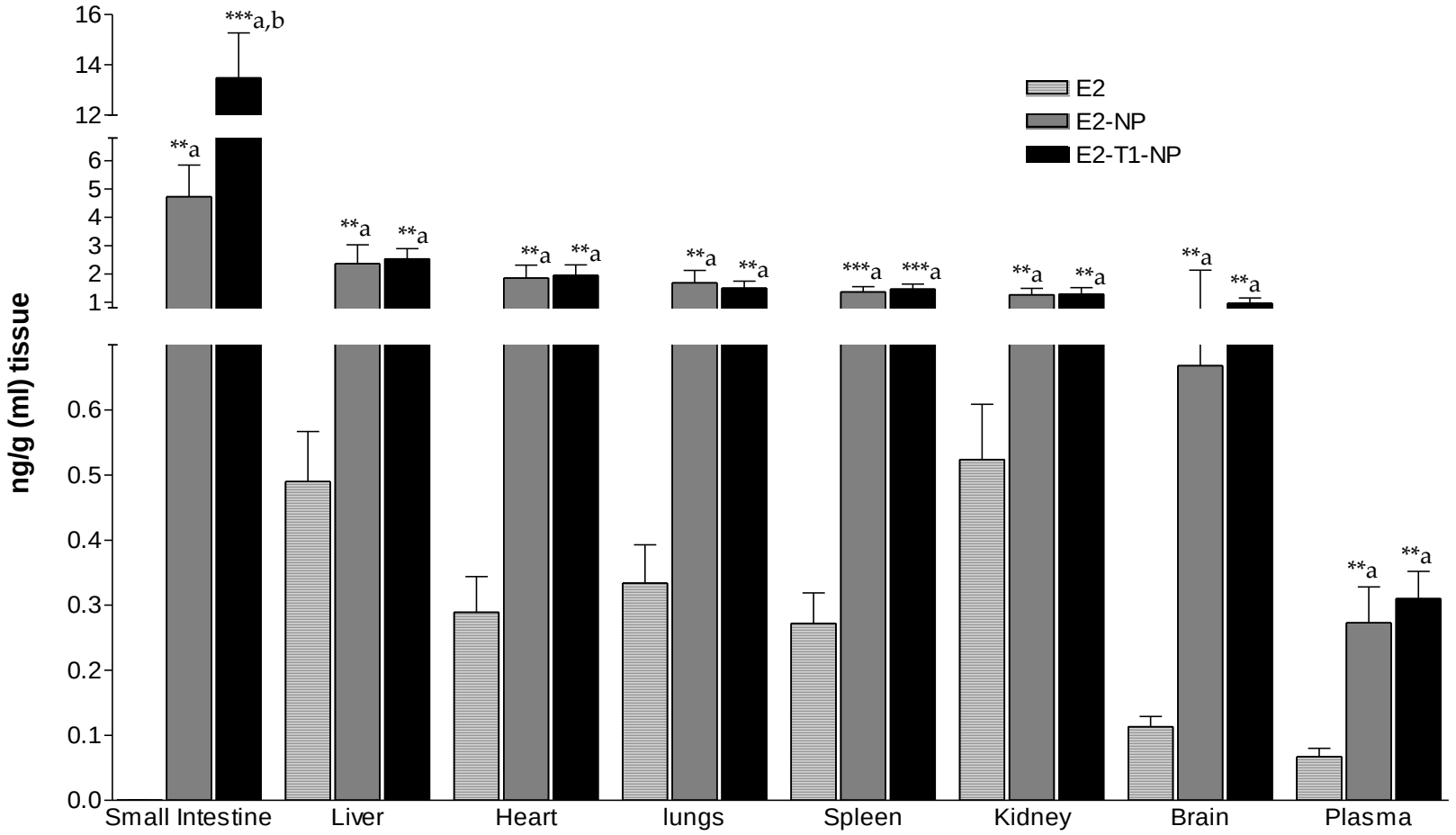

Fig. 4.2a Oestradiol levels in various organs 24 h after oral administration at a dose of 200 and 100 μg/rat for E2 and nanoparticulate groups respectively. Data represented as Mean ± SD (n=3). * $p<0.05$; ** $p<0.01$; *** $p<0.001$; a vs E2, b vs E2-NP.

(b)

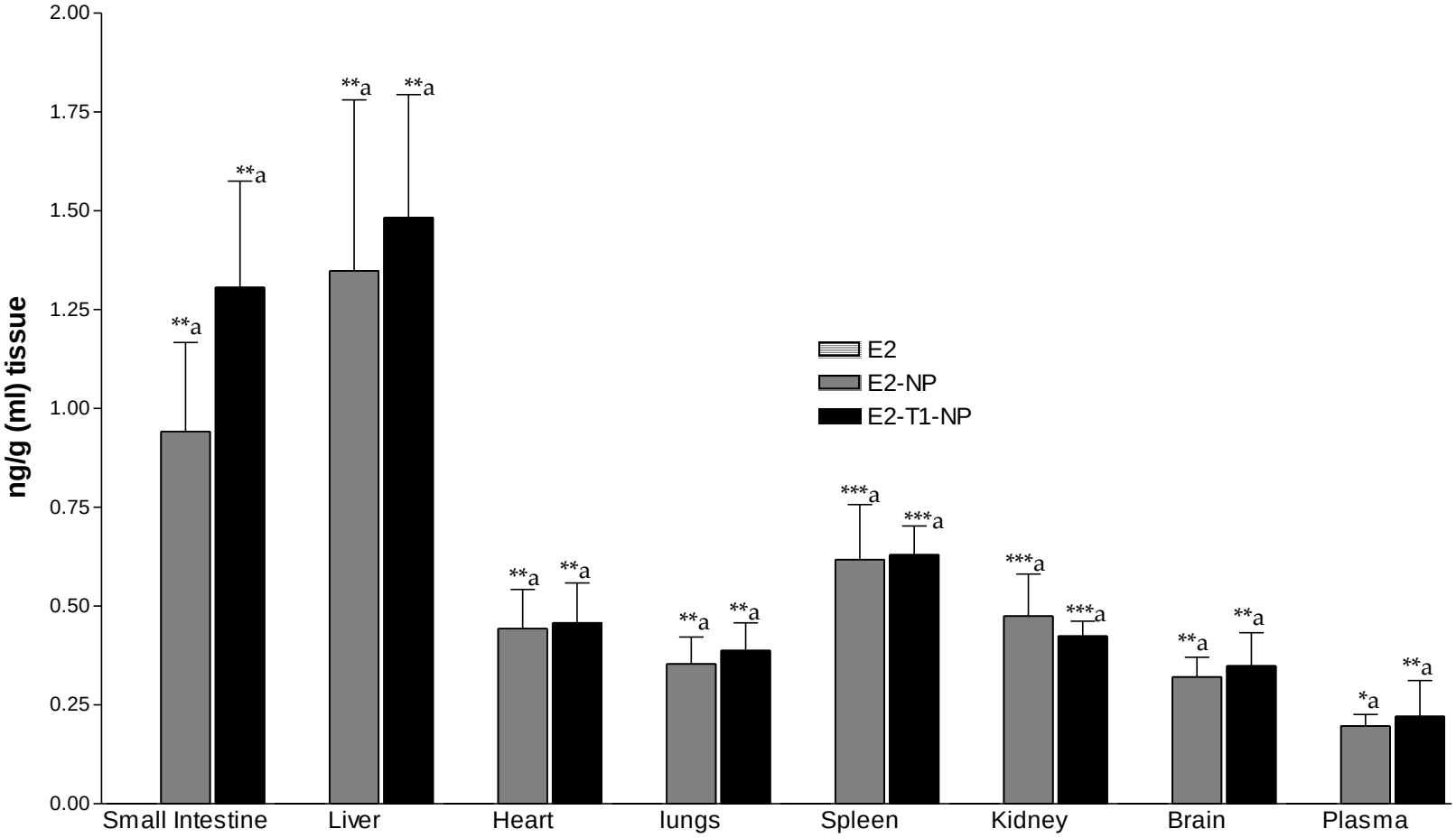

Fig. 4.2b Oestradiol levels in various organs 48 h after oral administration at a dose of 200 and 100 μg/rat for E2 and nanoparticulate groups respectively. Data represented as Mean ± SD (n=3). * p<0.05; **p<0.01; ***p<0.001; a vs E2.

(c)

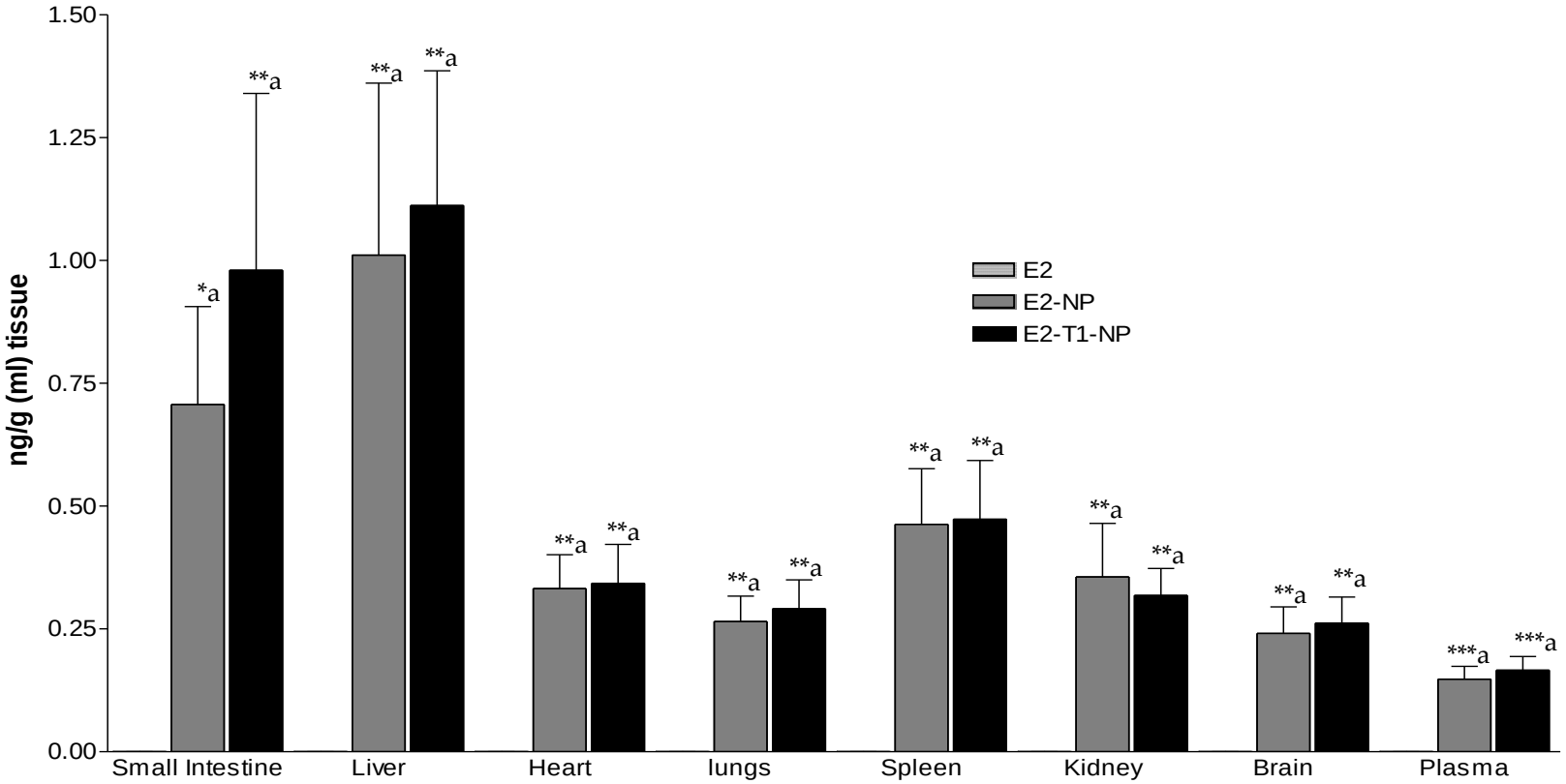

Fig. 4.2c Oestradiol levels in various organs 72 h after oral administration at a dose of 200 and 100 μg/rat for E2 and nanoparticulate groups respectively. Data represented as Mean ± SD (n=3). * $p<0.05$; ** $p<0.01$; *** $p<0.001$; a vs E2.

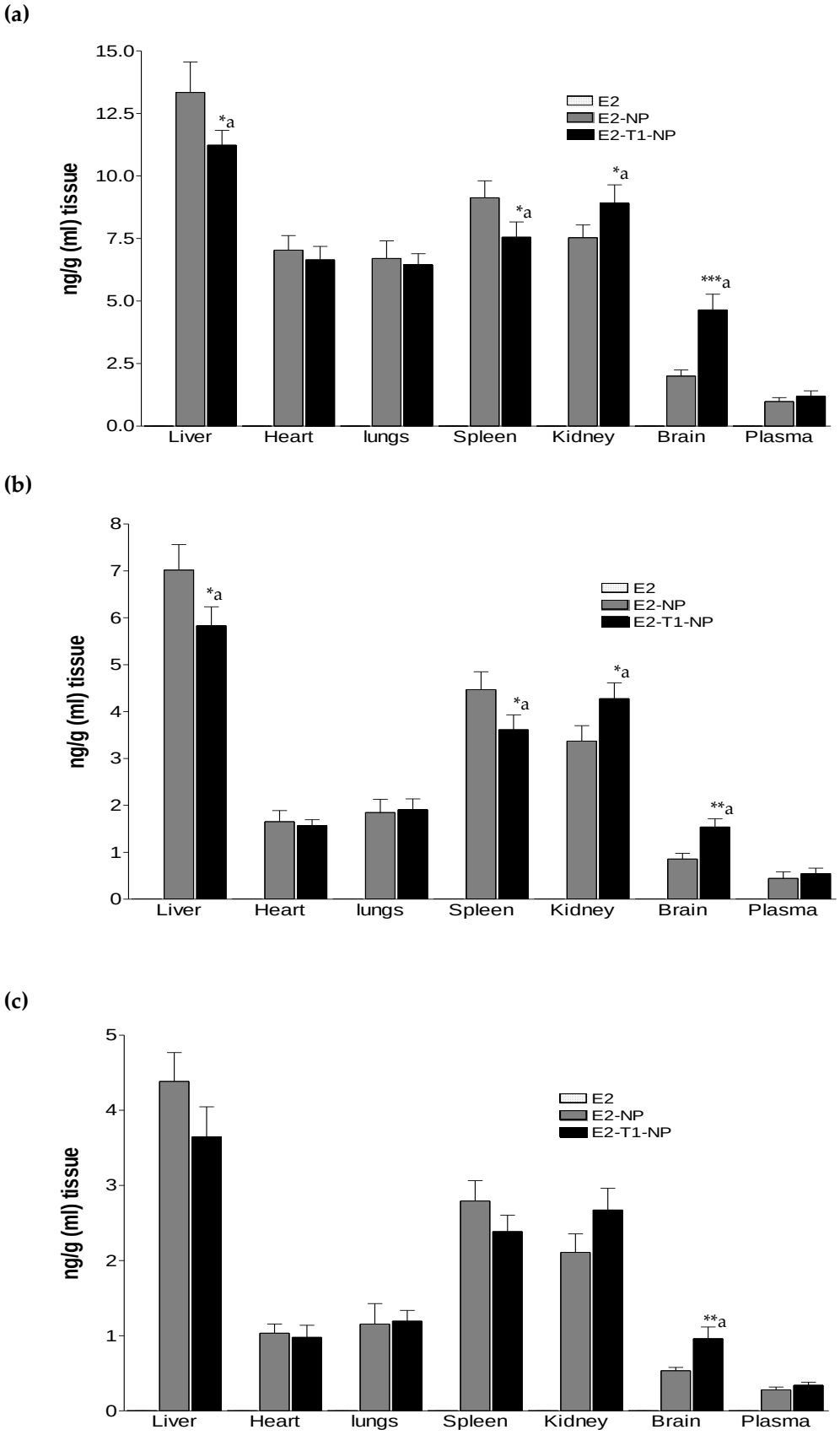

Fig. 4.3 Oestradiol levels in various organs (a) 24 h (b) 48 h and (c) 72 h after i.v. administration at a dose of 200 and 100 μg/rat for E2 and nanoparticulate groups respectively. Data represented as Mean ± SD (n=3). * $p<0.05$; ** $p<0.01$; *** $p<0.001$; a vs E2-NP.

T-80, indicating the role of surface properties in biodistribution of nanoparticles. It is known that after entering in the systemic circulation, nanoparticles are rapidly recognized and cleared of the circulation by the macrophages of mononuclear phagocytic system (MPS), also known as the reticuloendothelial system (RES). These particles then tend to sequester in the RES organs (liver and spleen) very rapidly. The macrophages, like Kupffer cells of liver, cannot directly identify the nanoparticles themselves, but rather recognize specific opsonin (such as IgG, complement factors, and fibrinogen) proteins bound to the surface of the particles. Apart from the size of nanoparticles, their surface properties (charge and hydrophobicity) also determine the amount of opsonization and this in turn finally influences the biodistribution pattern of nanoparticles. For example, neutral particles have slower opsonization rates than charged particles. Similarly, hydrophobic nanoparticles are opsonized more quickly than hydrophilic particles (Owens and Peppas, 2006; Aggarwal *et al*., 2009). In the present study also, after i.v administration, higher brain drug levels and lower liver and spleen levels of oestradiol from 1% T-80 coated nanoparticulate group (E2-T1-NP) as compared to the uncoated group (E2-NP) confirmed the role of surface properties in dictating the *in vivo* fate of nanoparticles, as without surface modification with surfactant coating, nanoparticles were supposed to be predominantly engulfed by cells of RES.

However, absence of brain targeting with 1% T-80 coated (E2-T1-NP) nanoparticles after oral administration led us to suspect the stability of the coating while crossing the gastrointestinal barrier rather than role of T-80 coating in brain targeting (which was already proved in the study after i.v administration) and therefore, nanoparticles were coated with increasing concentration of T-80 and amount coated in each formulation was quantified

(Table 4.2). Table 4.2 showed that increase in T-80 concentration from 1% to 5% led to increase in coating amount of T-80 from 9.72 ± 1.07 mg to 63.84 ± 3.59 mg (194.3 ± 21.4 to 1276.8 ± 71.7 μg/mg polymer) while zeta potentials of formulations showed a negative shift from 19.2 ± 2.1 mV at pH 5.6 ± 0.3 to -6.5 ± 0.4 mV at pH 7.2 ± 0.1 respectively with this increase in the amount of surfactant coating. Particle size was also found to increase from 138.8 ± 4.3 nm to 172.4 ± 1.0 nm with increase in the T-80 concentration from 1% to 5%. Since the intactness of the T-80 coating on the nanoparticles during the transit was a question, all the T-80 coated formulations were subjected to investigation in SGF and SIF. When different formulations were evaluated after 2 h of incubation in SGF (Fig. 4.4 a), it was observed that percentage of coating remaining was 77.3 ± 5.1 % (49.3 ± 4.7 mg) for formulation E2-T5-NP in comparison to 43.7 ± 4.3 % (4.2 ± 0.8 mg) for the E2-T1-NP formulation. A similar trend was observed after 6 h of incubation in SIF (Fig. 4.4 b), where percentage of coating remaining for formulation E2-T5-NP was 65.6 ± 4.9 % (41.8 ± 1.5 mg) in comparison to 37.8 ± 4.5 % (3.7 ± 0.8 mg) for the E2-T1-NP formulation. These findings suggest that the percentage and hence, amount of coating remaining/protected increased with increasing concentration of T-80 and therefore, a formulation coated with 4% T-80 (E2-T4-NP) was selected (because of its smaller particle size as well as large amount of protected T-80 coating) for oral administration in rats at same dose of 100 μg/rat to observe the effect of higher amount of coating, if any, on biodistribution of nanoparticles. 24 h post-dosing of oral administration, the tissue/plasma distribution profile of E2-T4-NP formulation (Fig. 4.5 a) exhibited significantly higher brain oestradiol levels as compared to both, uncoated (E2-NP) ($p<0.01$) as well as 1% T-80 coated (E2-T1-NP) ($p<0.05$) formulations

Table 4.2
Effect of increasing concentration of T-80 on particle properties and amount of surface coating.

Formulation	PS (nm)	PDI	ZP[a] (mV)	Amount of T-80 used (mg)*	Amount of T-80 coated (mg)	Amount of T-80 coated (μg/mg polymer)
E2-T1-NP	138.8 ± 4.3	0.035 ± 0.021	19.2 ± 2.1	53.8	9.72 ± 1.07	194.3 ± 21.4
E2-T2-NP	141.8 ± 1.6	0.083 ± 0.013	7.7 ± 0.4	107.6	24.46 ± 2.70	489.2 ± 54.0
E2-T3-NP	153.1 ± 2.1	0.047 ± 0.021	-1.1 ± 0.1	161.4	33.75 ± 4.37	674.9 ± 87.4
E2-T4-NP	157.0 ± 3.3	0.056 ± 0.032	-3.6 ± 0.6	215.2	49.35 ± 3.49	987.1 ± 69.8
E2-T5-NP	172.4 ± 1.0	0.062 ± 0.019	-6.5 ± 0.4	269.0	63.84 ± 3.59	1276.8 ± 71.7

PS: particle size, PDI: polydispersity index, ZP: zeta potential
[a]The zeta potentials reported are in the pH range of 5.6 ± 0.3 to 7.2 ± 0.1
*Relative to total suspension volume.

(a)

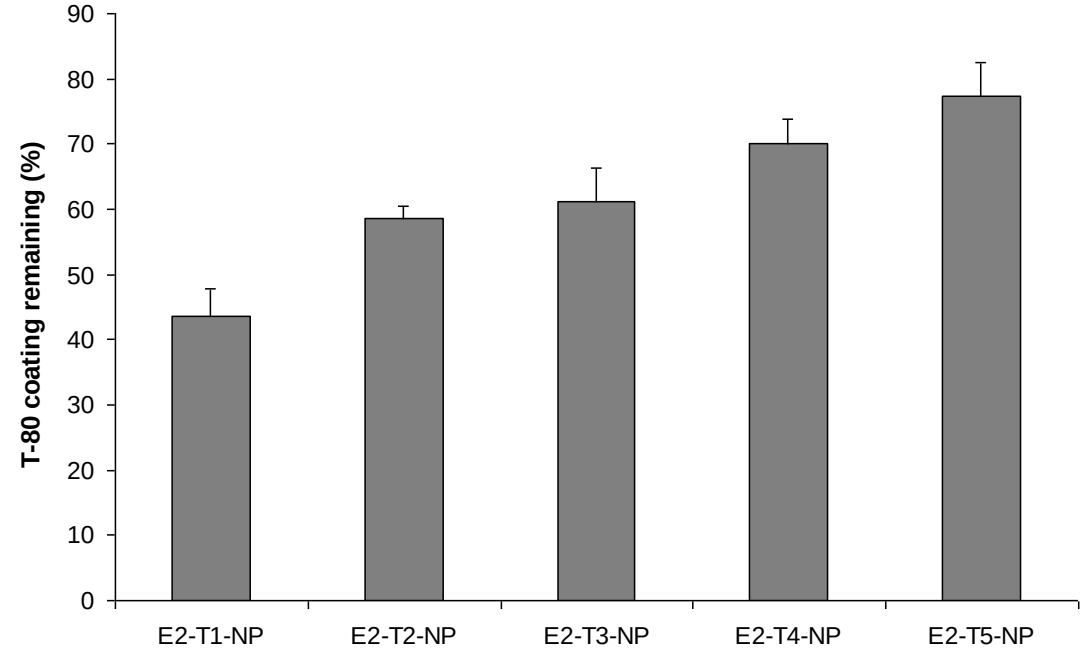

(b)

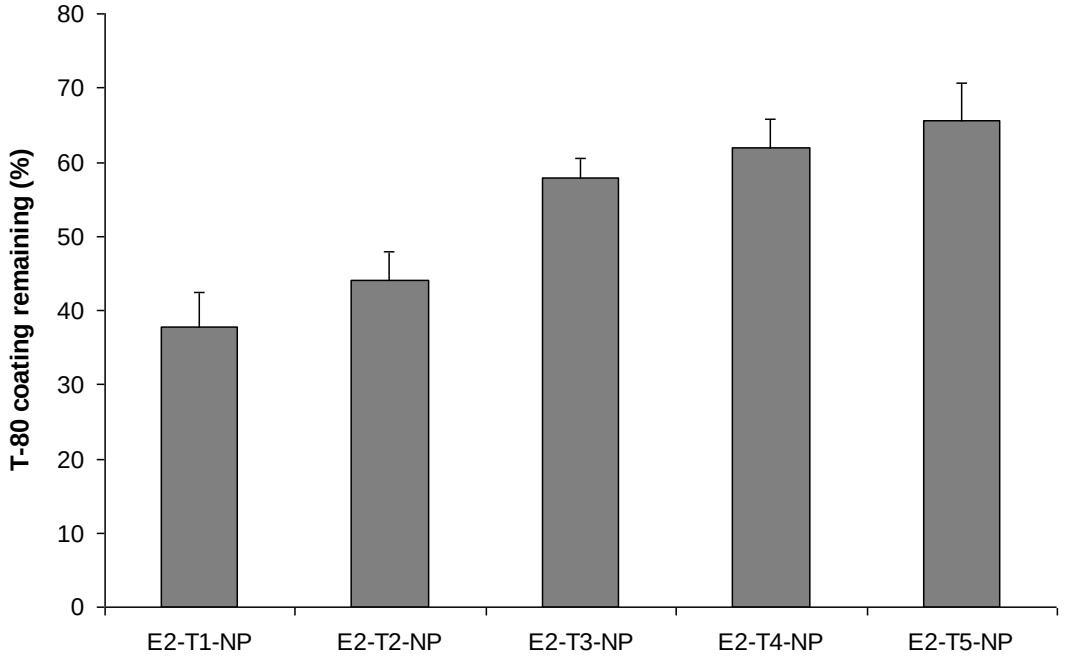

Fig. 4.4 Stability of T-80 surface coating in (a) simulated gastric fluid (SGF) and (b) simulated intestinal fluid (SIF) (n=3).

(a)

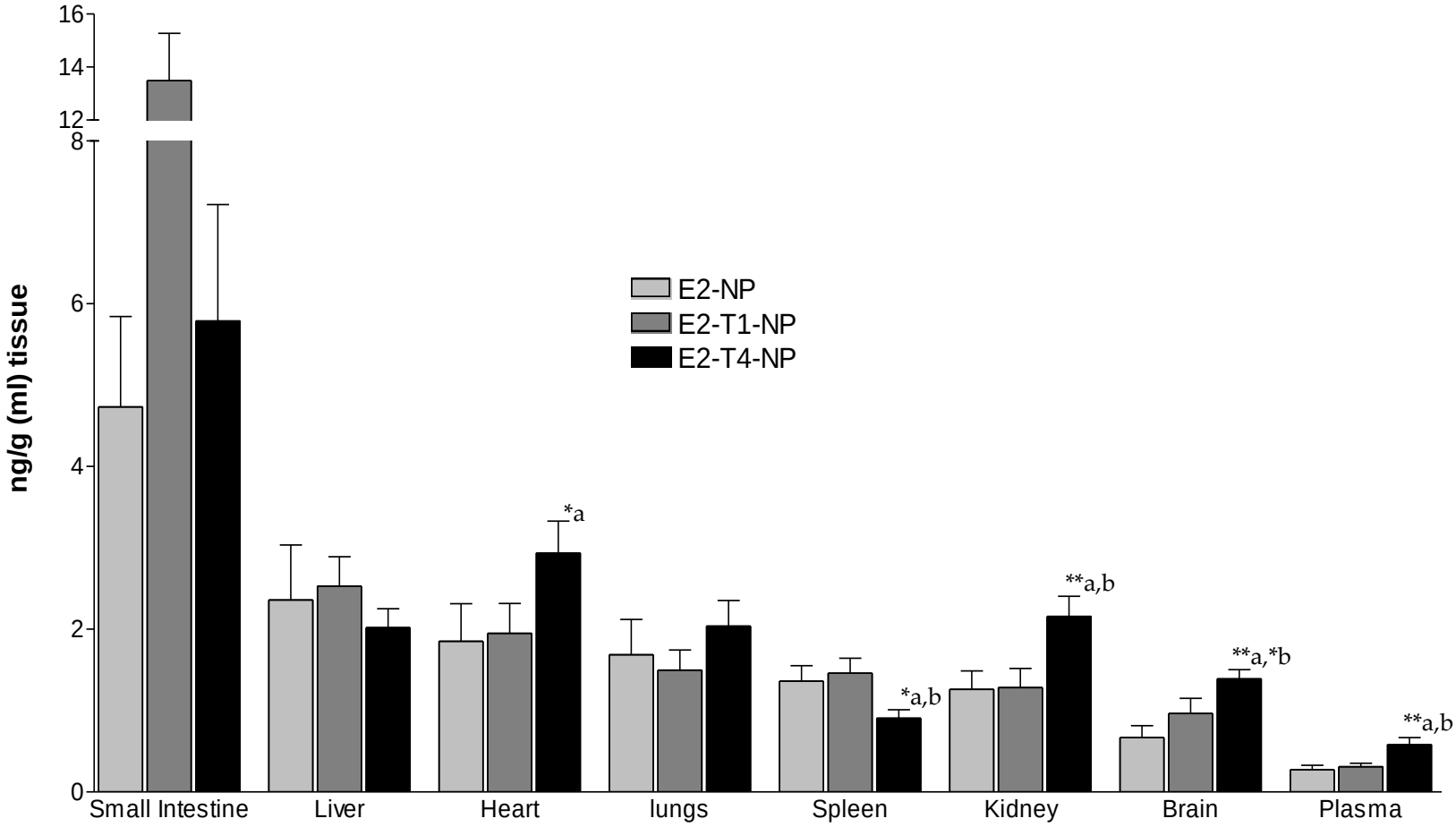

Fig. 4.5a Oestradiol levels in various organs 24 h after oral administration at a dose of 100 μg/rat. Data represented as Mean ± SD (n=3). * $p<0.05$; ** $p<0.01$; *** $p<0.001$; a vs E2-NP, b vs E2-T1-NP.

(b)

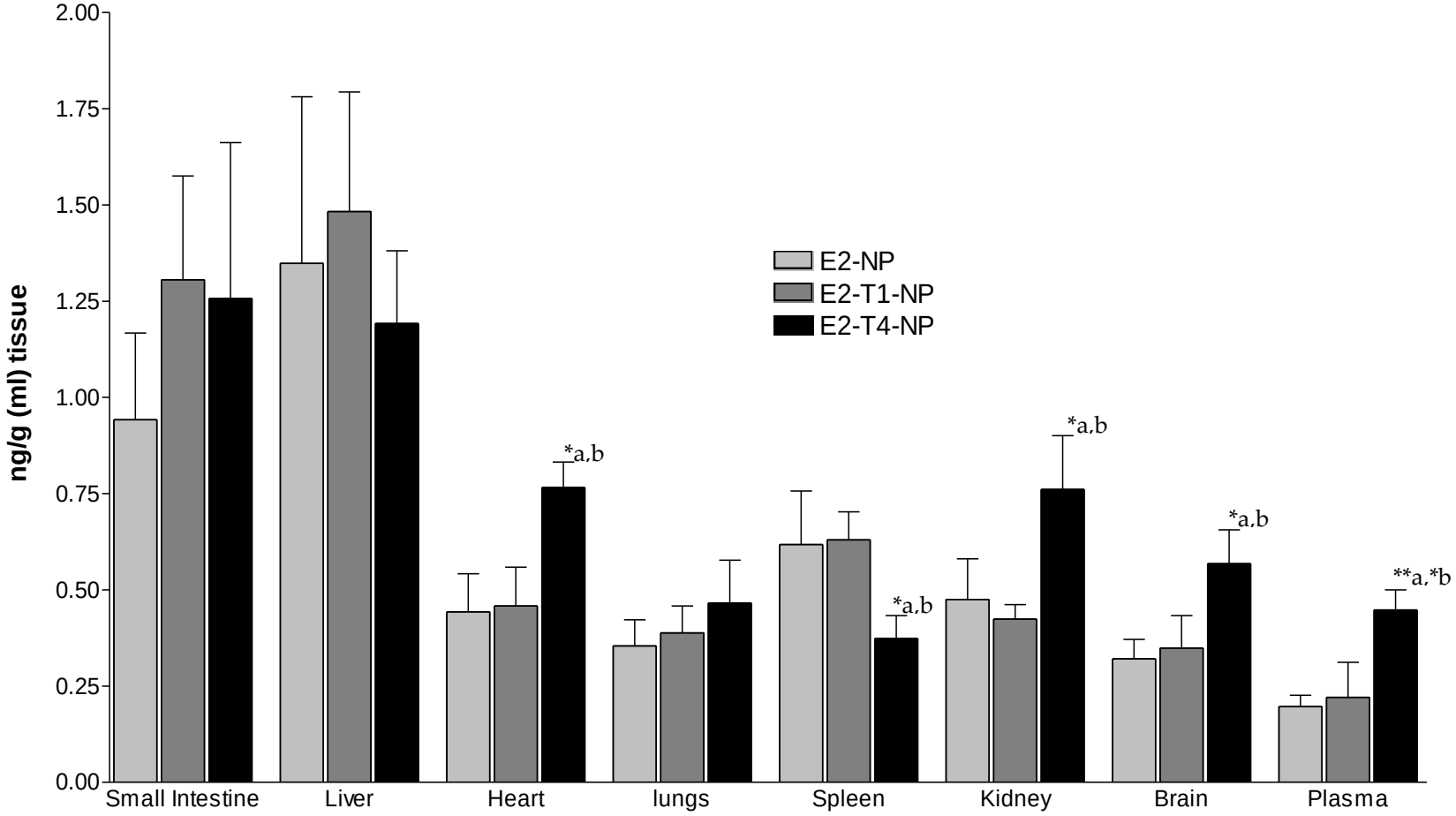

Fig. 4.5b Oestradiol levels in various organs 48 h after oral administration at a dose of 100 μg/rat. Data represented as Mean ± SD (n=3). * $p<0.05$; **$p<0.01$; ***$p<0.001$; a vs E2-NP, b vs E2-T1-NP.

(c)

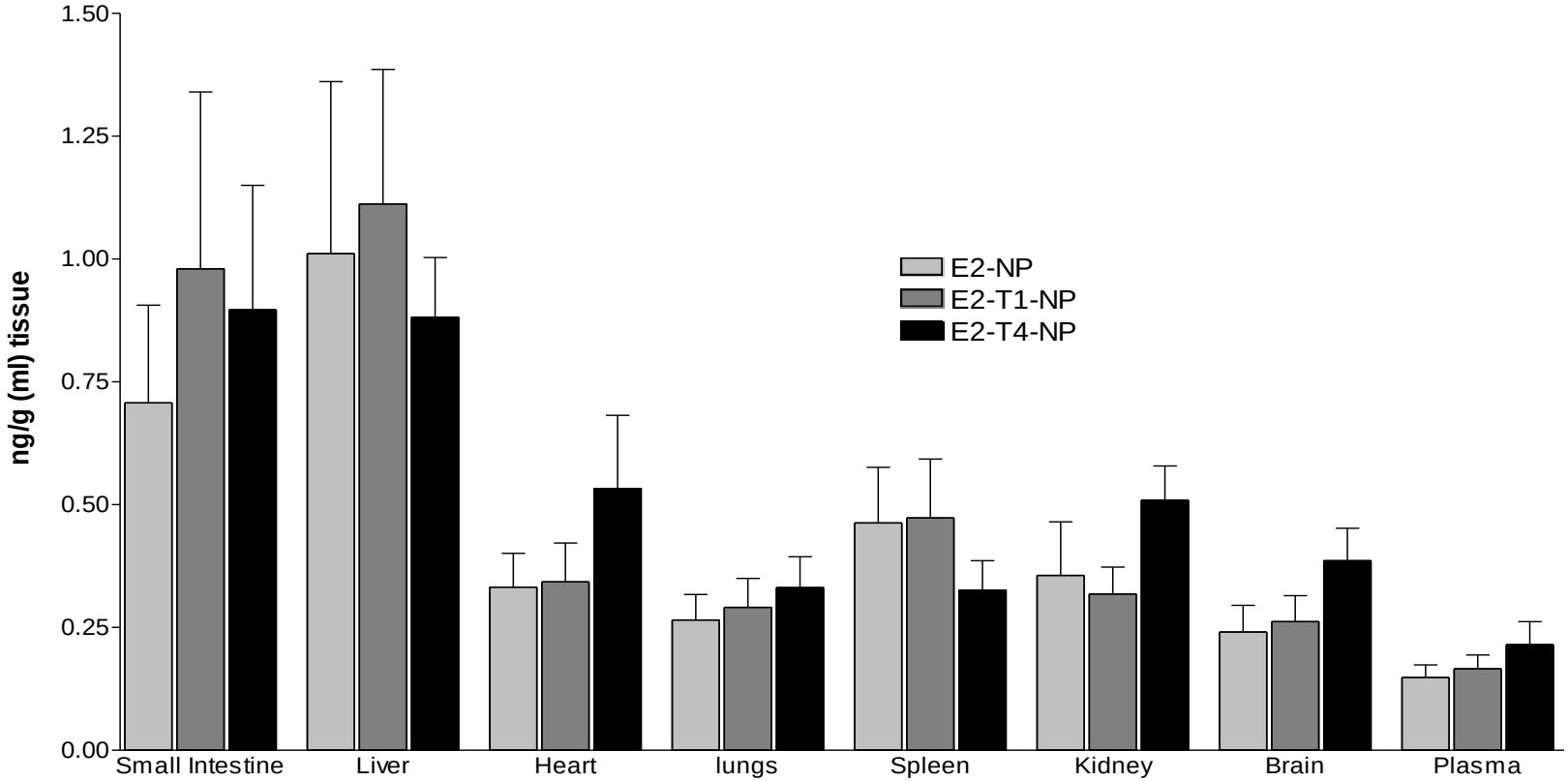

Fig. 4.5c Oestradiol levels in various organs 72 h after oral administration at a dose of 100 μg/rat. Data represented as Mean ± SD (n=3).

and this effect was found to remain even 48 h post-dosing ($p<0.05$) (Fig. 4.5 b). Also, drug levels in the spleen ($p<0.05$) and liver (non-significant) were lower in comparison to E2-NP and E2-T1-NP groups, indicating the stability of surface coating while crossing the gastrointestinal barrier and the role of surface modification in biodistribution of particulate carriers. Surprisingly, E2-T4-NP formulation also resulted in significantly higher ($p<0.05$) oestradiol levels in the heart as compared to E2-NP, which needs further investigation of these higher tissue levels from pharmacological/toxicological viewpoint. Higher doses (200 and 400 μg/rat) of nanoparticulate groups (E2-NP, E2-T1-NP, and E2-T4-NP) were also given by the oral route (Figs. 4.6 & 4.7) to achieve the brain drug levels obtained after administration of 200 μg/rat of drug suspension via the intramuscular route (Fig. 4.8). With both higher doses also, nanoparticulate group prepared with 4% T-80 (E2-T4-NP) showed significantly higher brain values of oestradiol as compared to corresponding uncoated (E2-NP) and 1% T-80 surface coated (E2-T1-NP) group, which again signify the specific function of T-80 coating in brain targeting. Oral administration of E2-T4-NP at a dose of 200 μg/rat resulted in similar brain drug levels obtained after administration of 200 μg/rat of drug suspension via intramuscular route and therefore, should show the same effect as the intramuscular injection does in the reported study (Hua *et al*., 2007).

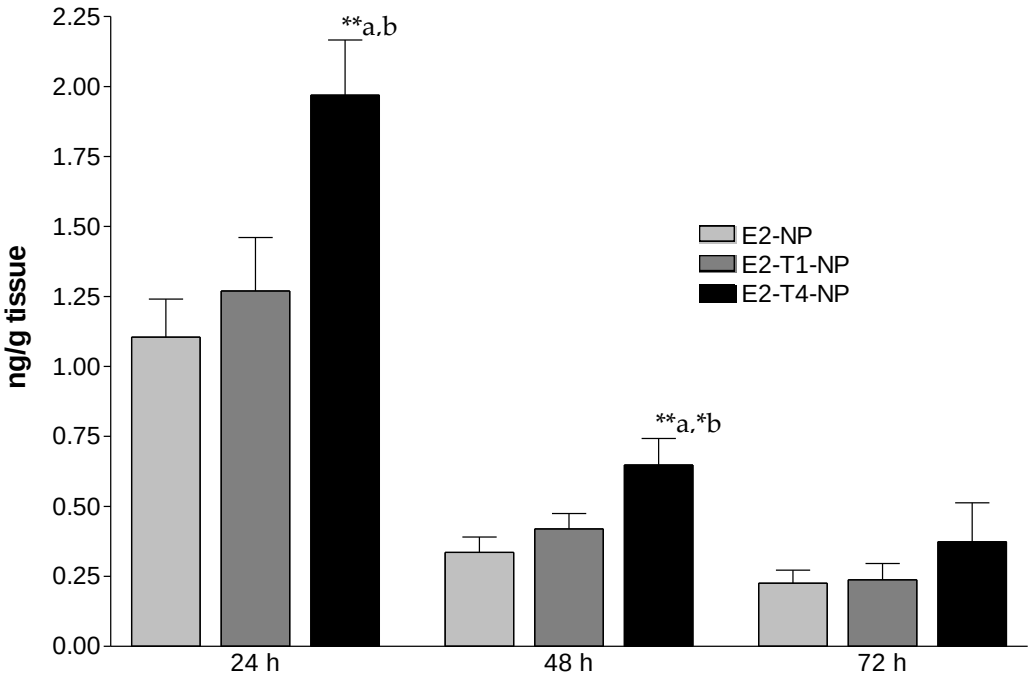

Fig. 4.6 Brain drug levels 24 h, 48 h and 72 h after oral administration of different nanoparticulate groups at a dose of 200 μg/rat. Data represented as Mean ± SD (n=3). *p<0.05; **p<0.01; ***p<0.001.
a vs E2-NP
b vs E2-T1-NP

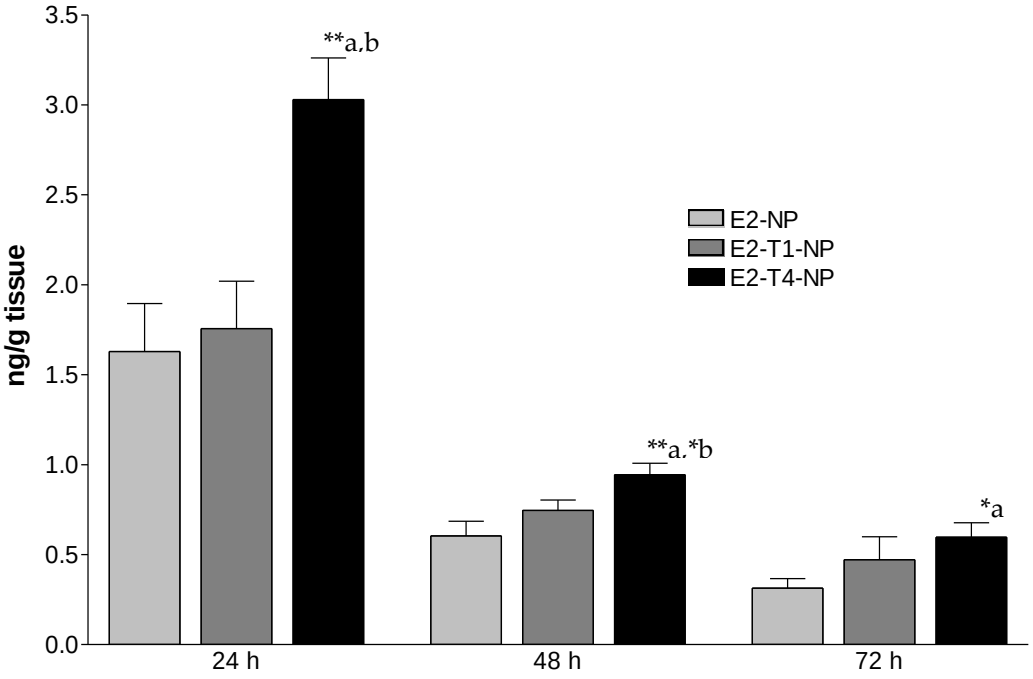

Fig. 4.7 Brain drug levels 24 h, 48 h and 72 h after oral administration of various nanoparticulate groups at a dose of 400 μg/rat. Data represented as Mean ± SD (n=3). *p<0.05; **p<0.01; ***p<0.001.
a vs E2-NP
b vs E2-T1-NP

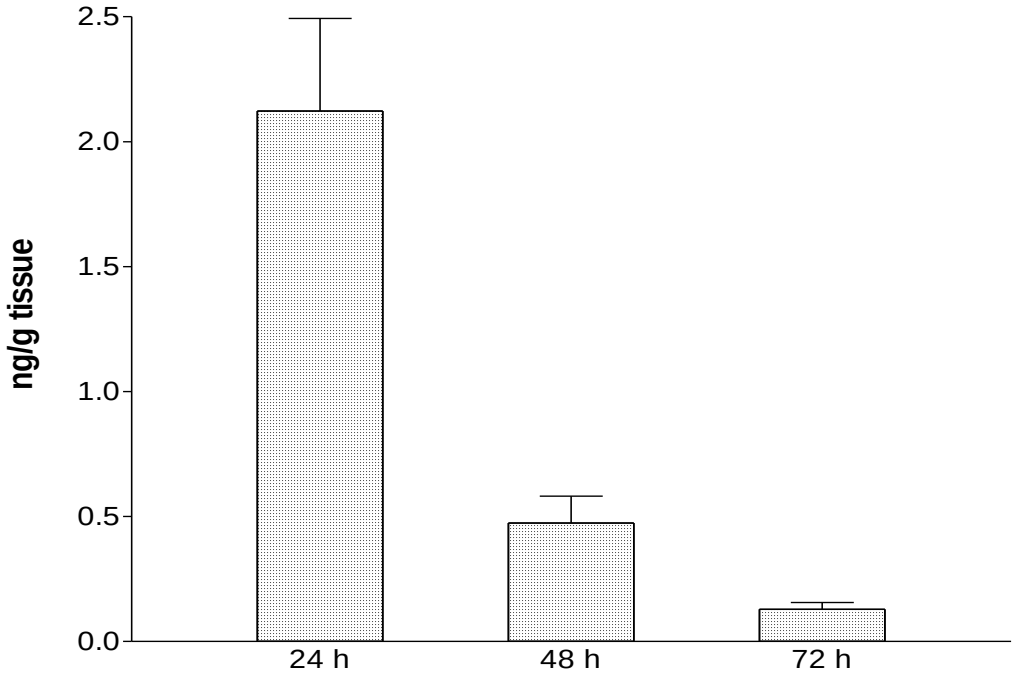

Fig. 4.8 Brain drug levels obtained after administration of 200 μg/rat of drug suspension (E2) via intramuscular route. Data represented as Mean ± SD (n=3).

4.5 Conclusions

The data suggests that oral drug delivery to brain is possible and a clear role of T-80 coating was evident. The *in vitro* data in simulated fluids suggests that T-80 coating is stable during transit and appears to be concentration dependent. The formulation developed could also reduce the peripheral adverse effects of oestradiol by increasing the relative dose of drug reaching the brain and thereby, reducing the total dose required for the therapy as compared to currently available conventional oral formulations.

Chapter-5

Evaluation of oral oestradiol nanoparticles in a rat model of Alzheimer's disease

5.1 Introduction

Alzheimer's disease (AD) is a fatal neurodegenerative disorder of the central nervous system (CNS) associated with the progressive worsening of symptoms ranging from memory loss to declining cognitive ability. The neuropathological hallmarks of AD are characterized by extracellular deposition of the amyloid beta (Aβ) peptide in senile plaques, presence of intracellular neurofibrillary tangles (NFTs), and neuronal loss (Srinivas, 1999; Selkoe, 2000; Cummings, 2004; Parihar and Hemnani, 2004). The first clinical feature of AD is disturbances in short-term memory. Some other clinical symptoms of AD include confusion, anxiety, memory impairment, problems with attention and spatial orientation, language difficulties, and mood swings (Kirk and Kertesz, 1991; Price *et al*., 1993; Green *et al*., 1996). The average time elapsed between diagnosis of AD and death is 10 years, with a range of 3-20 years (Small *et al*., 1997). Women are two times more likely than men to have AD (Bodor and Buchwald, 2006). Deprivation of endogenous oestrogen after the menopause has been implicated as a risk factor in the pathogenesis of AD in post-menopausal women (Henderson, 1997; Behl, 1999; Casetta *et al*., 2005; Casadesus *et al*., 2008; Craig and Murphy, 2009). The neuroprotective actions of oestrogens on the brain have been very well documented in the literature (Brinton, 2001; Behl, 2003; Nilsen, 2008; Simpkins and Singh, 2008; Vasudevan and Pfaff, 2008) and many clinical studies suggest that post-menopausal ERT may reduce the risk or delay the onset of AD (Ohkura *et al*., 1995; Yaffe *et al*., 1998; Sherwin, 1999; Dykens *et al*., 2005). However, conventional oral oestradiol formulations increase the risk of peripheral adverse effects, most notably being breast cancer. An approximately 30% increase in the risk of breast cancer has been reported in post-menopausal women taking oestrogens, which may rise to 50% if taken

for more than 10 years and this forms the main reason why most post-menopausal women avoid traditional hormonal therapy (Bodor and Buchwald, 2006). Therefore, we developed surface modified polymeric nanoparticles for oral delivery of oestradiol to the brain that could reduce the peripheral drug burden without compromising the patient compliance.

Selection of animal model**:** A number of animal models have been developed to mimic the pathological features of AD. For example, long-term oestrogen deprivation by ovariectomy resulted in reversible learning/memory impairment in female SD rats (Simpkins *et al*., 1997; Gibbs, 1998). Similarly, many studies have demonstrated that long-term injection of D-galactose (D-gal) can lead to excessive reactive oxygen species (ROS) formation, neuronal damage and cognitive and memory deterioration in the treated rats or mice (Xu and Zhao, 2002; Holden *et al*., 2003; Wei *et al*., 2005; Chen *et al*., 2006; Cui *et al*., 2006). Unfortunately none of these animal models can completely mimic the behavioural disturbances, or neuropathological abnormalities observed in AD patients. Recently, a paper was published in which a new animal model for AD has been developed by long-term (6 weeks) intraperitoneal administration of D-gal in OVX rats (Hua *et al*., 2007). D-gal at high levels in the body can be turned into aldose and hydroperoxide under the catalysis of galactose oxidase, leading to the formation of free radicals such as superoxide anion. This paper reported that oestrogen deprivation and oxidative stress synergistically enhance the development and progression of AD, as six weeks later the OVX and D-gal injected rats exhibited a higher degree of cognitive and memory impairment. This was accompanied by cholinergic neuronal loss in the basal forebrain and synaptic degeneration in the hippocampus and cerebral cortex. The typical histopathological changes of AD like deposition of Aβ peptide and

appearance of NFTs were also observed in the hippocampus of OVX and D-gal injected rats. Overall, it was shown that model completely mimics the neuropathological and behavioural alterations observed in the AD condition and therefore we adopted this AD rat model to test the efficacy of our nanoparticulate formulation.

5.2 Experimental

5.2.1 Animal groups

Ovariectomized and sham operated female SD rats were purchased from Charles River, UK. All animals were 18 week old at the time of surgery and were received one week after surgery. Animals were housed in cages under conditions of controlled illumination (12:12 h light/dark cycle), humidity, and temperature (18-22 °C). They were divided into four groups (n=10 per group): the sham operated group (Sham), the OVX and D-gal injected group (OVX+D gal), the OVX, D-gal and oestradiol nanoparticles administered group (OVX+D gal+ENPs), and the OVX, D-gal and oestradiol suspension injected group (OVX+D gal+ES). After one week acclimatization to the home cages, pre-treatment behavioural tests were carried out on 20 week old rats weighing 300-350 g. After the behavioural tests, rats in the OVX+D gal+ENPs group received D-gal (20 mg in 2 ml 0.9% saline, intraperitoneal injection every day) and T-80 coated (4%, E2-T4-NP) oestradiol nanoparticles (0.2 mg in 0.4 ml water, via oral route every third day) for 6 weeks, while rats in the OVX+D gal+ES group were given D-gal (20 mg in 2 ml 0.9% saline, intraperitoneal injection every day) and oestradiol (0.2 mg in 0.1 ml sesame oil, intramuscular injection every third day) for 6 weeks. The OVX+D gal rats followed the same experimental procedures as the OVX+D gal+ES group except that the latter injection contained only sesame oil. Rats in the sham group were injected with saline and sesame oil. All procedures were carried out under as Project Licence issued by the UK Home Office under the Animals (Scientific Procedures) Act 1986.

5.2.2 Behavioural tests

Before and after 6 weeks of treatment, animals (n=10) were subjected to

several behavioural tests to assess different kinds of behaviours such as locomotor activity, exploratory pattern, anxiety, learning and memory abilities etc. through the measurement of various behavioural parameters.

5.2.2.1 Open field

The open field test was used to measure the locomotor activity and exploratory behaviour of the animals. The rats were placed in the centre of a locomotor activity arena (dimensions 41 x 41 x 30 cm) and allowed to move freely for a period of 15 min. During this time, activity was monitored by automated video tracking system (EthoVision Pro software, Noldus). The behavioural parameters recorded were: total distance travelled, number of centre entries and time spent in the centre of arena (centre being defined as an inner square covering 1/3 of the box area).

5.2.2.2 Elevated plus maze

Elevated plus maze testing was carried out in a plus-shaped black Perspex maze consisting of two open arms (without walls) and two closed arms (with 15 cm high walls) positioned at right angle to each other and at a height of 1 m above the ground. Each arm of the maze was 44 cm long and 9 cm wide. The rats were placed individually at the junction between the open and closed arms of the plus maze (designated the centre of the maze) and allowed to explore freely for 10 min, during which time behaviour was recorded using automated video tracking system. Behavioural parameters measured using EthoVision Pro software (Noldus) include total distance travelled, time spent at the centre, and number of entries into and time spent in open and closed arms of the maze.

5.2.2.3 Novel object recognition

The test chamber consisted of a black Perspex box (dimensions 41 x 41 x 30 cm). Initially, two identical objects (spaced evenly in the chamber) were placed into the test arena, and rats were allowed to explore the objects and the chamber for 10 min. After a delay of one hour, animals were reintroduced into same arena having one familiar object and one novel object. Rats were then allowed to explore the objects and chamber again for 10 min. Positions of the familiar and novel objects in the chamber were changed randomly between testing of different rats. Behaviour was recorded using the video tracking system (Noldus). Videos were later scored manually using EthoVision Pro software to quantify frequency and time spent exploring the novel object.

5.2.2.4 Prepulse inhibition (PPI)

The startle experiments were performed in a PPI apparatus (Med Associates Inc.) consisting of a sound attenuated box with an amplifier, a loudspeaker, a recording platform and a dim red light. Each rat was put inside an acrylic plastic holder (7.6 cm internal diameter) that was screwed to the recording platform. Signals were routed through the ANL-025C power amplifier. The high-frequency speaker delivered a white noise acoustic stimulus which provided the continuous background noise, prepulses and startle stimuli. The animals were placed in the PPI boxes and allowed to acclimatise for an initial 5 min period. After this, a block of 6 startle stimuli of 120 decibel (dB) alone, above the background noise level of 65dB was carried out. The second block of testing consisted of 52 pseudo-randomised trials, split as follow: 10 X 4dB, 10 X 8dB and 10 X 16dB, prepulse above the background noise level of 65dB. The remaining trials were 12 X 120dB pulse alone, and 10 trials that consisted of no stimulus. Finally, a third block of 6 X 120dB pulse alone

completed the test. The startle stimulus occurred 100ms after the prepulse and recording duration was 65ms after the startle stimulus. The vibrations in the plastic holder due to response of the animal caused the displacement of the recording platform, producing an analogue signal that was recorded by the software as the startle response and stored by the computer. % PPI was calculated as:

$$\% \text{ PPI} = \{(\text{Response}_{(\text{startle stimulus})} - \text{Response}_{(\text{prepulse + startle stimulus})}) / (\text{Response}_{(\text{startle stimulus})})\} \times 100$$

External factors such as background noise and odour may affect the behaviour. Therefore, all the above mentioned tests were carried out without the presence of the experimenter, so as to cause minimal disruption to the normal behaviour and also, apparatus was cleaned with 70% alcohol after testing of each rat.

5.2.3 Histology

5.2.3.1 Termination and tissue processing

Rats (n=5) were deeply anaesthetized and perfused through the heart with physiological (0.9%) saline followed by 4% paraformaldehyde. Subsequently, the whole heads and then the dissected out brains were post-fixed in 4% paraformaldehyde for 24 h. Brains were stored in phosphate buffer saline (PBS) solution at 4 °C until processing. Brains were placed in cassettes and processed with an automated tissue processor (Shandon Citadel 1000; Thermo Scientific, IL, USA) using a prepared protocol (Table 5.1). Following processing, the brains were embedded in plastic base moulds with melted paraffin wax and then allowed to harden.

5.2.3.2 Tissue sectioning

6 μm coronal sections of the forebrains (approximately -2.5 mm to -3.5 mm from Bregma) were cut on a microtome (RM2125; Leica Microsystems,

Table 5.1
The processing protocol for rat brains.

Station	Treatment	Duration (h)	Temperature (°C)
1.	70% alcohol	2	35
2.	80% alcohol	3	35
3.	96% alcohol	4	35
4.	Absolute alcohol	4	35
5.	Absolute alcohol	5	35
6.	Absolute alcohol	5	35
7.	Absolute alcohol	6	35
8.	Histoclear/ absolute alcohol	4	35
9.	Histoclear	5	35
10.	Histoclear	5	35
11.	Paraffin wax	5	60
12.	Paraffin wax	5	60

Wetzlar, Germany). The sections were carefully floated in a 50 °C warm water bath and gently picked up with slides. All tissue sections were mounted onto Superfrost Ultra Plus glass slides (Thermo Scientific) with one section per slide.

5.2.3.3 Immunohistochemistry

Immunohistochemistry was performed to visualize Aβ42 and glial fibrillary acidic protein (GFAP) in the brain tissue. Briefly, tissue sections were first deparaffinized with histoclear and then rehydrated through ethanol to distilled water. 0.3% hydrogen peroxide (H_2O_2) was applied to inhibit endogenous peroxidase activity. All tissues have some degree of endogenous peroxidase enzymatic activity that could potentially react with the diaminobenzidine (DAB) solution in place of the horseradish peroxidase (HRP) to produce non specific chromogen and therefore, saturating the slides with H_2O_2 inactivates the endogenous peroxidase. Tissue fixation alters epitope binding sites and promotes cross linking of unrelated proteins to the antigen of interest. So, antigen retrieval in pressure cooker with heated citrate buffer (pH 6) was performed to expose a greater number of obscured binding sites. Thereafter, sections were pre-incubated with normal goat serum (NGS) in order to block the non-specific adhesion of primary antibody. This was followed by incubation for 1 h at room temperature with a rabbit polyoclonal anti-Aβ42 antibody (1:500; Sigma, Saint Louis, Missouri, USA) or mouse monoclonal anti-GFAP antibody (1:100, Sigma, Saint Louis, Missouri, USA). After rinsing in PBS, the sections were further incubated with biotinylated goat anti-rabbit (or mouse) (1:100, Vector Laboratories, Burlingame, CA, USA) for 1 h at room temperature, followed with streptavidin-HRP (Vector Laboratories) incubation for 20 min. Visualization was achieved by incubation with DAB solution (Dako). Finally, sections were

dehydrated and slides were cover-slipped using DPX mounting solution. The immunohistochemistry protocol is detailed in Table 5.2.

5.2.3.4 Congo red staining

Congo red (Sigma-Aldrich, Egham, UK) was used for staining amyloid in tissue sections; kit manufacturer's instructions were followed.

5.2.4 Western blotting for GFAP

Western blotting was performed using the NuPAGE® electrophoresis system (XCell SureLock; Invitrogen Corporation, Carlsbad, CA, USA). Rats (n=5) were sacrificed and their brains were dissected out. After that, hippocampus region of brains were separated and homogenized. The samples were then loaded onto pre-cast 4-12% Bis-Tris gel cassettes (NuPAGE® Novex). The proteins were electrophoretically transferred onto nitrocellulose membrane (0.45 μm pore size, Invitrogen Corporation). After being blocked for 1 h at room temperature, the blotting membranes were incubated overnight with mouse monoclonal anti-GFAP antibody (1:5000; Sigma, Saint Louis, Missouri, USA) at 4 °C and then with secondary HRP linked donkey anti-mouse IgG antibody (1:10000; Jackson ImmunoResearch Laboratories, Baltimore, PA, USA) for 2 h at room temperature. The proteins were visualized using the ECL Western blotting substrate (Thermo Scientific Pierce, Rockford, IL, USA). The intensity of blots was quantified by using a densitometer (GS-800; Bio-Rad Laboratories Ltd, UK). Glyceraldehyde 3 phosphate dehydrogenase (GAPDH) was used as an internal control.

5.2.5 Quantitative evaluation

Each GFAP immunolabelled section was observed at x400 magnification and numbers of normal and reactive astrocytes were manually counted in one microscopic field of CA1 and dentate gyrus (DG) regions of hippocampus.

Table 5.2

Immunohistochemistry procedure for paraffin embedded tissue.

	Step	Treatment	Duration	Purpose
Tissue Preparation	1.	60 °C oven	30min	To melt wax from the tissue
	2.	Histoclear	3 x 5min	To dissolve remaining wax
	3.	100% alcohol	2 x 5min	To rehydrate tissue
	4.	Distilled water	2min	To rehydrate tissue
	5.	0.3% H_2O_2	10min	To block endogenous peroxidase activity
	6.	PBS	5min	To rinse
	7.	Preheat citrate buffer (pH 6) in Microwave at 900W	13min	To retrieve antigens
	8.	Microwave at 900W with tissue sections in pressure cooker containing preheated 10 mM citrate buffer (pH 6)	7min	To retrieve antigens
	9.	Water	1min	To rinse
	10.	PBS	5min	To rinse
	11.	Encircle each section with wax pen		To allow solutions to pool over sections
	12.	20% v/v NGS (made in 5% bovine serum albumin in PBS)	20min	To block the non-specific adhesion of primary antibody
Primary Antibody	1.	Primary antibody in blocking solution	1h	To bind to the antigen of interest in the tissue
	2.	PBS	3 x 5min	To rinse
Secondary Antibody	1.	1:100 biotinylated secondary antibody in PBS	1h	To bind to the primary antibody
	2.	PBS	3 x 5min	To rinse
DAB Staining	1.	streptavidin-HRP	20min	To bind to the biotinylated secondary antibody
	2.	PBS	5min	To rinse
	3.	DAB reagent	5-10min	To produce a brown chromogen from the reaction with peroxidase
	4.	Distilled water	5min	To rinse
Dehydration	1.	70% alcohol	2min	To dehydrate tissue
	2.	90% alcohol	2min	To dehydrate tissue
	3.	100% alcohol	2min	To dehydrate tissue
	4.	Histoclear	2 x 2min	To remove wax pen
	5.	Coverslip with DPX mounting medium		To protect the sections

Astrocytes having small cell bodies with short and slender processes were considered as normal ones while those having enlarged cell bodies with long, thick and branched processes were counted as reactive astrocytes. Only process-bearing astrocytes with their cell bodies in the plane of the section were considered. Thereafter, ratio of reactive astrocytes to total astrocytes (%) was calculated and applied as index of astrocytosis. Counting was carried out by the observer blinded to treatment groups.

5.2.6 Statistical analysis

Statistical analysis was carried out by one-way ANOVA and subsequent Tukey post-hoc test for multiple comparisons. However, for PPI two-way ANOVA was applied where factors were 'PPI levels' (within groups) and 'treatment' (between the groups). In all cases, statistical significance was defined as $p<0.05$.

5.3 Results and Discussion

5.3.1 Behavioural tests

Pre-treatment behavioural tests did not show any difference among the groups confirming that there was no behavioural deficit before start of the treatment and all the following behavioural results and discussion is based only on the post-treatment behavioural tests outcome.

5.3.1.1 Open field

The open field test is used to examine the motor functions by means of measuring spontaneous activity of the animal in an open field (Hua *et al*., 2007). Also, anxiety-like behaviour can be measured by determining the exploratory pattern of the animals as the propensity to remain close the walls is higher in anxious animals. Therefore, number of centre entries and time

spent at the centre was used as a measure of anxiety. Spontaneous motor activity and exploratory behaviour of the rats was not found to be impaired as data from open field testing showed that Sham and OVX+D gal rats had similar total locomotor activity ($p=0.998$) in the open field (Fig. 5.1 a). Similarly, analysis of the number of centre entries ($F(3,36)=1.664$ $p=0.192$) and time spent at the centre ($F(3,36)=1.185$ $p=0.329$) did not show any significant difference among the groups; although, groups with OVX rats exhibited on average only about 50% of the numbers of entries and time spent at the centre as compared to Sham group, indicating the possibility of higher level of anxiety in the OVX animals (Fig. 5.1 b & c).

5.3.1.2 Elevated plus maze

The elevated plus maze test is carried out to measure fear or anxiety (Pellow *et al*., 1985). Rodents have a natural tendency to avoid the open arms of the maze and spend more time in the confined closed arm milieu and therefore, the ratio of open arm entries to total entries (including centre entries) (%) and also, the ratio of time spent in open arm to that of total time (including time spent at centre) (%) was calculated and applied as an index of anxiety. OVX+D gal group rats did not show any statistical difference in open arm entries (Fig. 5.2 a) and time spent in open arm (Fig. 5.2 b) compared to Sham and drug treated groups. However, most marked difference was observed with OVX+D gal animals as they spent least amount of time (~5.1%) in the open arm as compared to Sham controls (~9.1%) and drug treatment groups i.e. OVX+D gal+ENPs (~8.2%) and OVX+D gal+ES (~7.9%). Total arm entries, an indirect measure of locomotor activity, also showed no significant difference among the groups ($F(3,36)=1.275$ $p=0.298$), but again OVX+D gal group was found to have least number of total arm entries compared to other groups (Fig. 5.2 c), indicating the impairment of motor activity. A significant

(a)

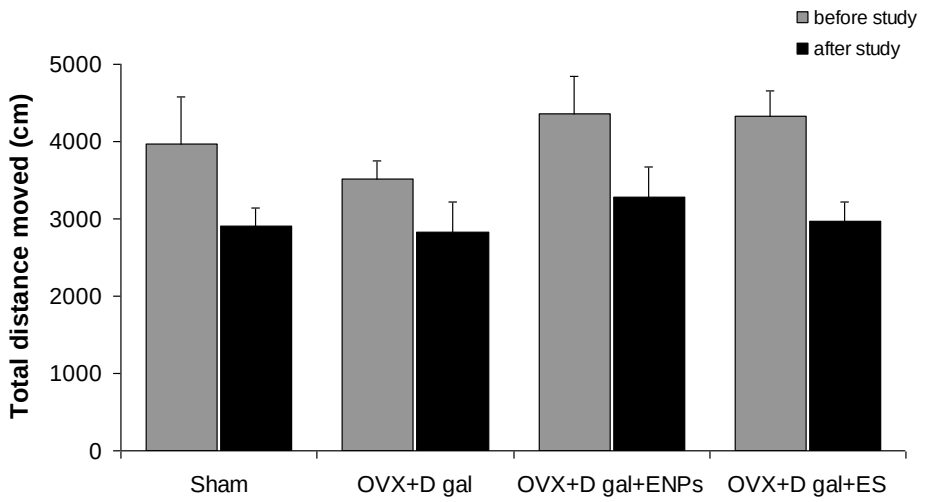

(b)

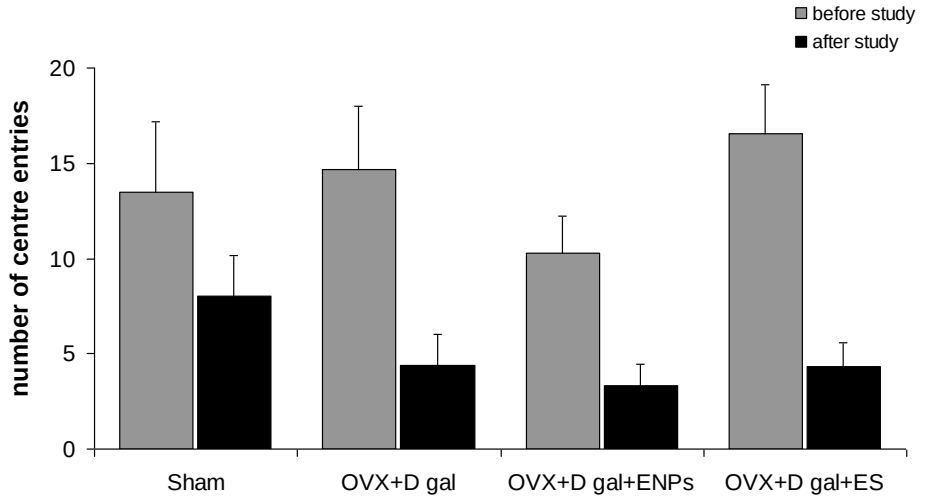

(c)

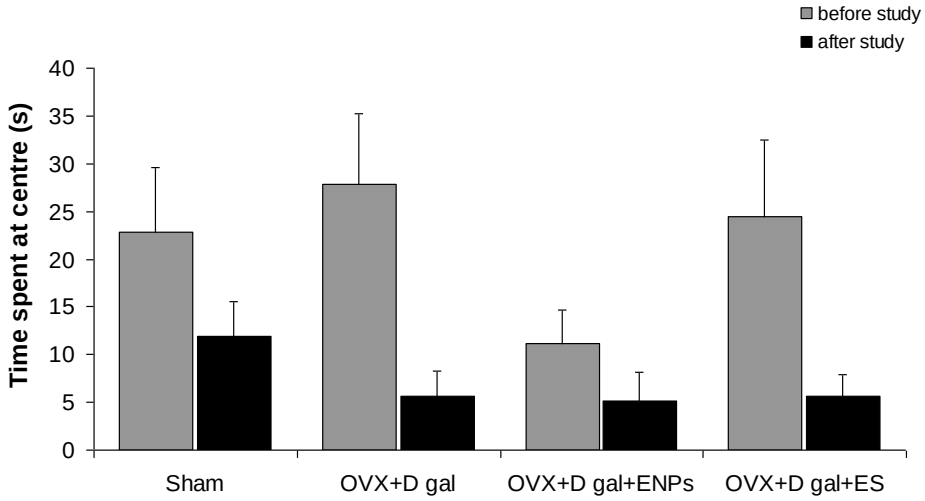

Fig. 5.1 Open field test (a) Total locomotor activity (b) number of centre entries and (c) time spent in central part of the arena. No significant difference between the groups was observed. Diagrams represent Mean ± SEM (n=10).

decrease in time spent at centre was obtained with OVX+D gal animals as compared to Sham (p=0.030) group. This so called "central platform behaviour" suggests the anxious nature of OVX+D gal animals as the decrease in time spent at centre was associated with increase in time spent in the closed arms (Lee and Rodgers, 1990; Lee and Rodgers, 1991). However, this impairment in anxiety-related behaviour was markedly attenuated with nanoparticle treated (OVX+D gal+ENPs, p=0.050) and suspension treated (OVX+D gal+ES, p=0.095) group (Fig. 5.2 d). Overall, OVX+D gal animals exhibited higher degree of anxiety in the elevated plus maze model and oestradiol treatment was found to be effective in preventing/attenuating the impairment, reflecting its neuroprotective action on brain.

5.3.1.3 Novel object recognition

Novel object recognition test is a working memory test based on the rat's natural tendency to investigate the novel objects more than the familiar ones. The preference for the novel object reflects the use of learning and memory processes. Therefore, to test the deficits in working/nonspatial memory, rats were initially allowed to explore the two identical objects during the sample phase. Recognition memory for a familiar object was then tested by replacing one of the original objects with a novel object. If rat remembers the object they have previously explored, they will prefer exploring the novel object in the choice phase (Ennaceur and Delacour, 1988). However, none of the groups under study showed differences in the time spent with novel object (Fig. 5.3) and most surprisingly, even Sham controls did not show any preference for the novel object, suggesting the probable role of sex differences (male vs. female) in novelty-preferences and needs further investigation.

(a)

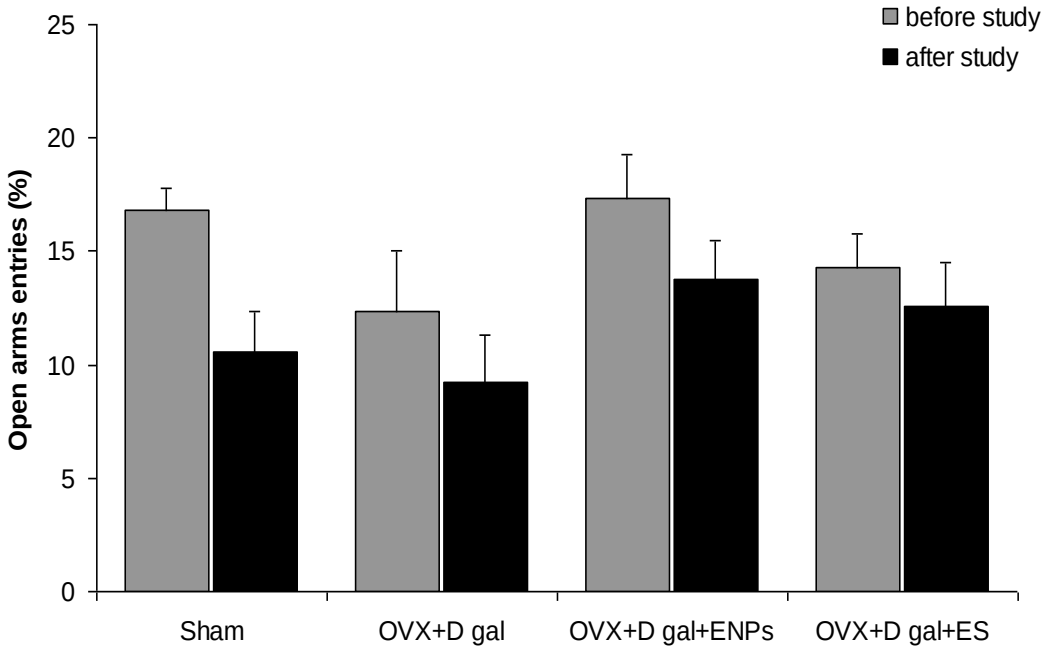

(b)

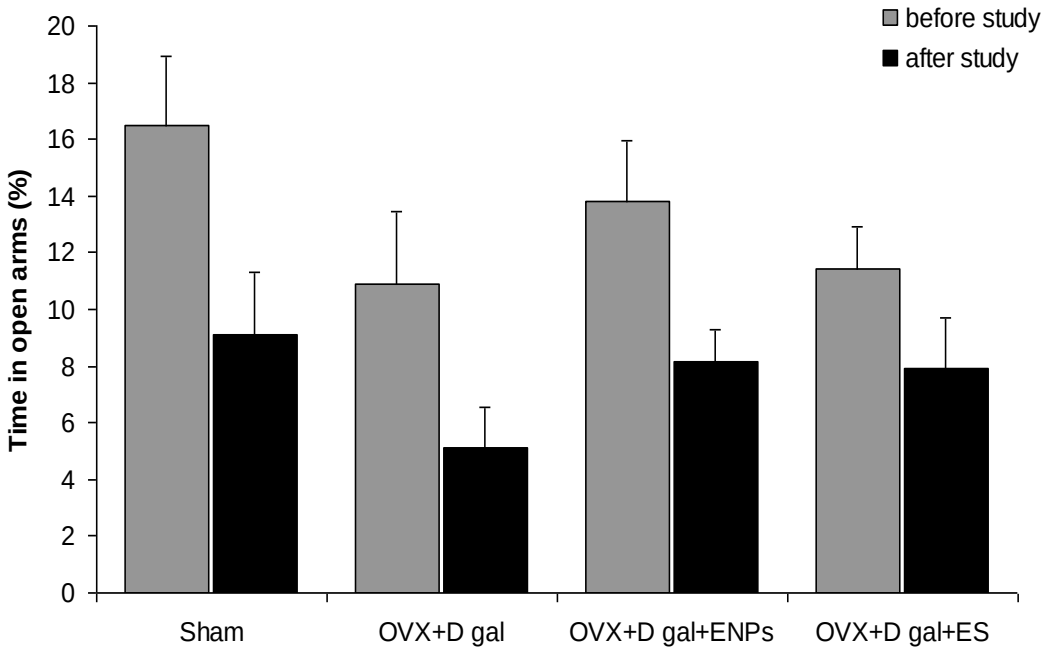

Fig. 5.2a&b Behaviour in the elevated plus maze (a) % open arm entries (b) % time spent in open arms. All bar graphs show Mean ± SEM (n=10).

(c)

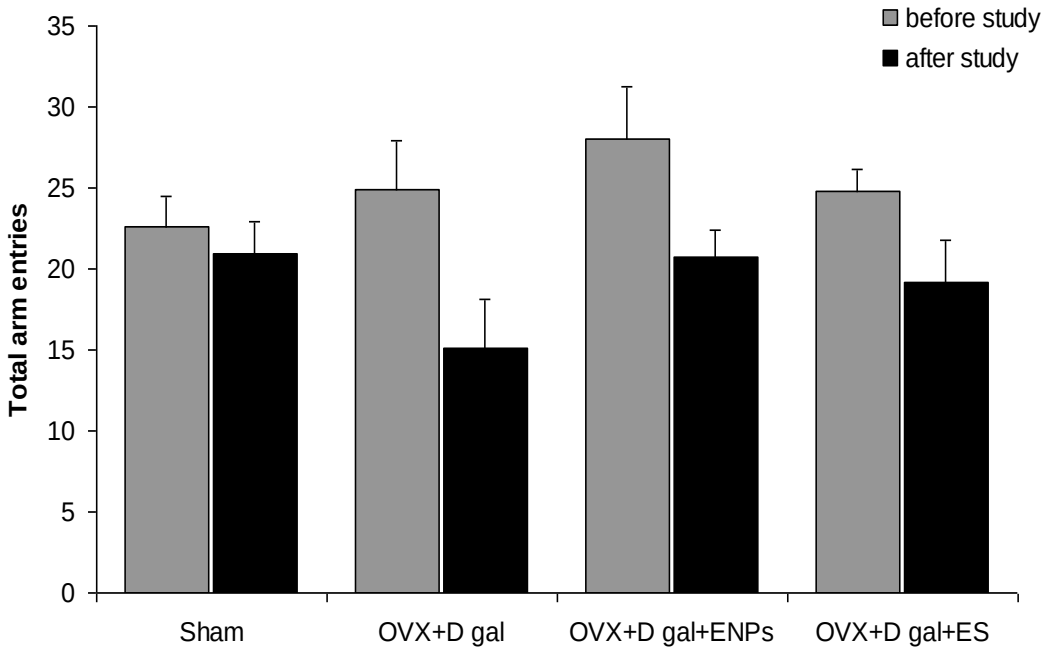

(d)

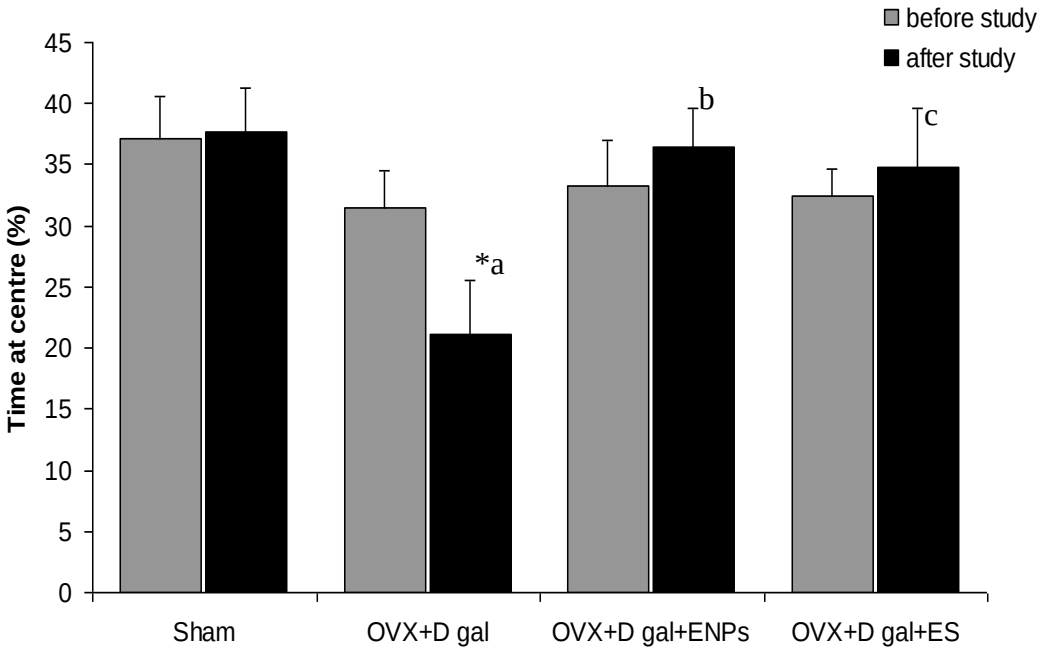

Fig. 5.2c&d Behaviour in the elevated plus maze (c) total arm entries (d) time in the centre of the maze. All bar graphs show Mean ± SEM (n=10). *p<0.050; a vs Sham (p=0.030), b vs OVX+D gal (p=0.050) and c vs OVX+D gal (p=0.095).

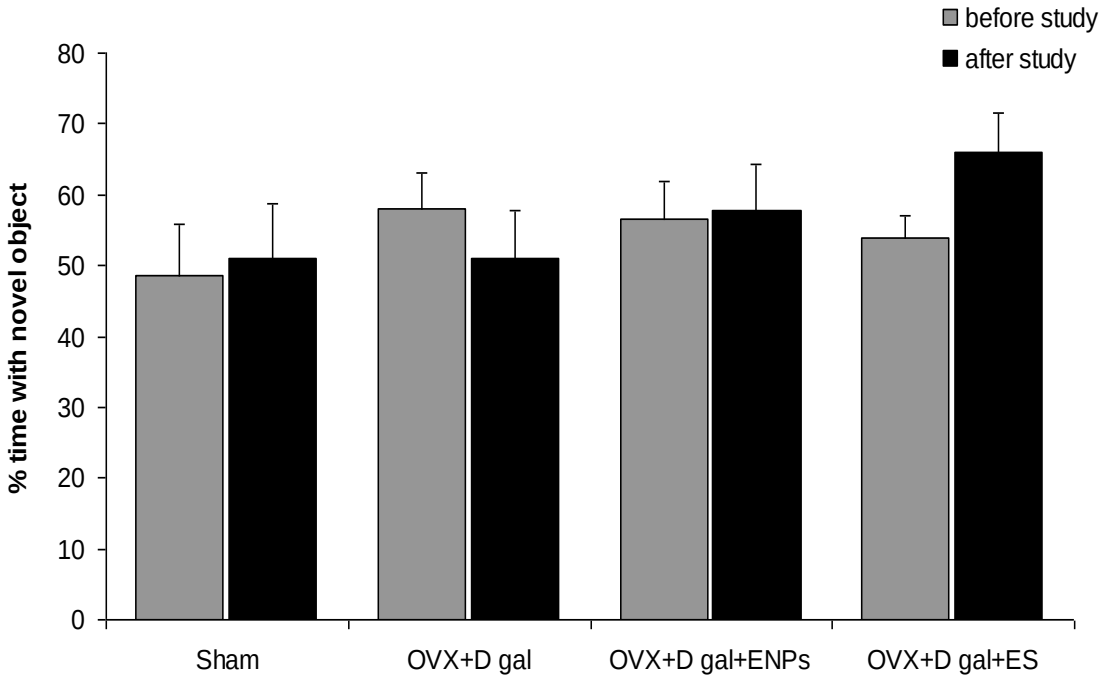

Fig. 5.3 Novel object recognition test. Both before and after the study, even Sham controls did not show any preference for the novel object, suggesting the probable role of sex differences (male vs female) in novelty-preferences and needs further investigation. Bar graph show Mean ± SEM (n=10).

5.3.1.4 PPI

The PPI test is conducted to measure sensorimotor gating deficits in patients with certain neuropsychiatric disorders such as schizophrenia. PPI refers to inhibition of the reflexive motor response to a startling auditory stimulus (pulse) due to presentation of a preceding subthreshold stimulus (prepulse). It is considered to reflect the ability to filter out the unnecessary information and disturbed PPI has been related to impairment in sustained attention and greater distractibility (Geyer *et al*., 2001). The hippocampus and entorhinal cortex, structures which are affected in AD, are involved in the regulation of PPI and studies have demonstrated reduced sensory gating in AD (Jessen *et al*., 2001; McCool *et al*., 2003; Ueki *et al*., 2006). However, current data showed no significant difference in PPI among the groups ($F(3,36)=0.669$ $p=0.577$) and there was also no prepulse level and group interaction ($F(6,72)=2.149$ $p=0.058$), though an increase in prepulse intensity produced a significant increase in prepulse inhibition ($F(6,72)=49.175$ $p<0.001$) (Fig. 5.4 a). The startle response also was found to be similar in all the groups (Fig. 5.4 b). One possible reason for the lack of PPI deficits in the present study could be that the severity of the neurodegenerative changes perhaps was not sufficient to affect the circuitry of prepulse inhibition and therefore, a final conclusion can be drawn only after knowing the status of pathological changes at the cellular level in the brain.

5.3.2 Neuropathological examination

The effect of oestradiol deprivation (OVX) and long term D-gal injection on pathological Aβ42 deposition was probed in the brain using an immunohistochemical technique. OVX+D gal rats exhibited considerable amounts of region-specific intraneuronal Aβ42 immunoreactivity (Fig. 5.5 C

(a)

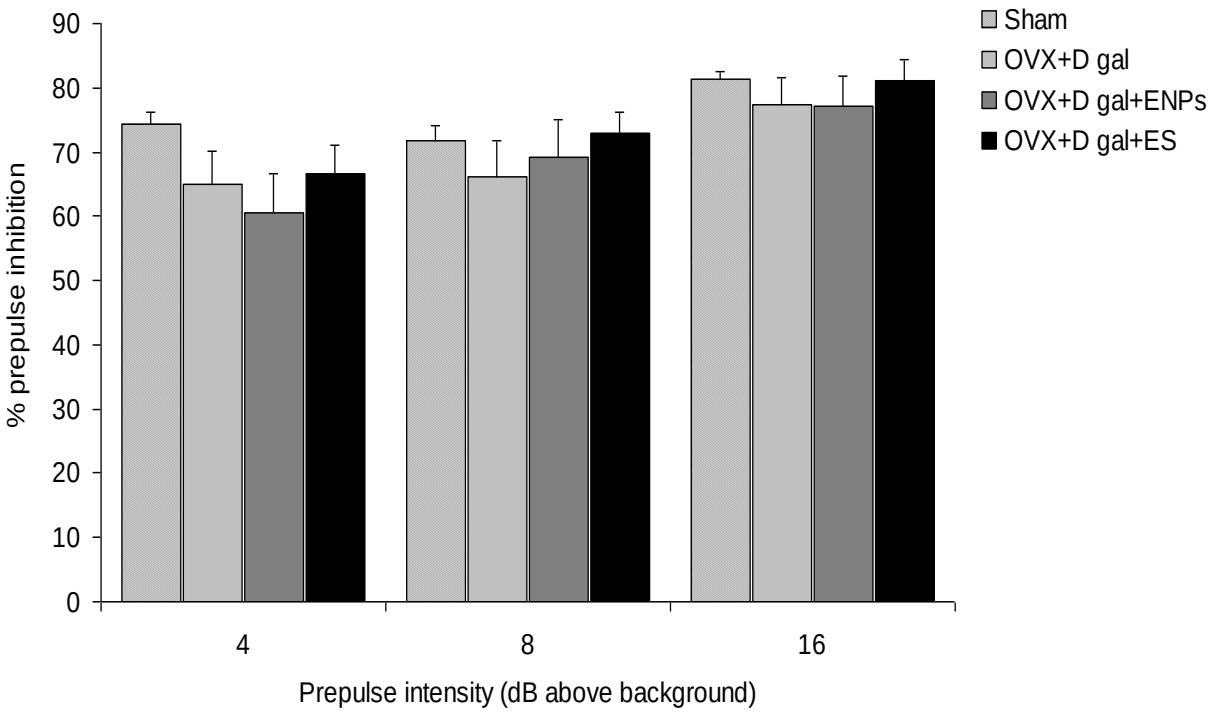

(b)

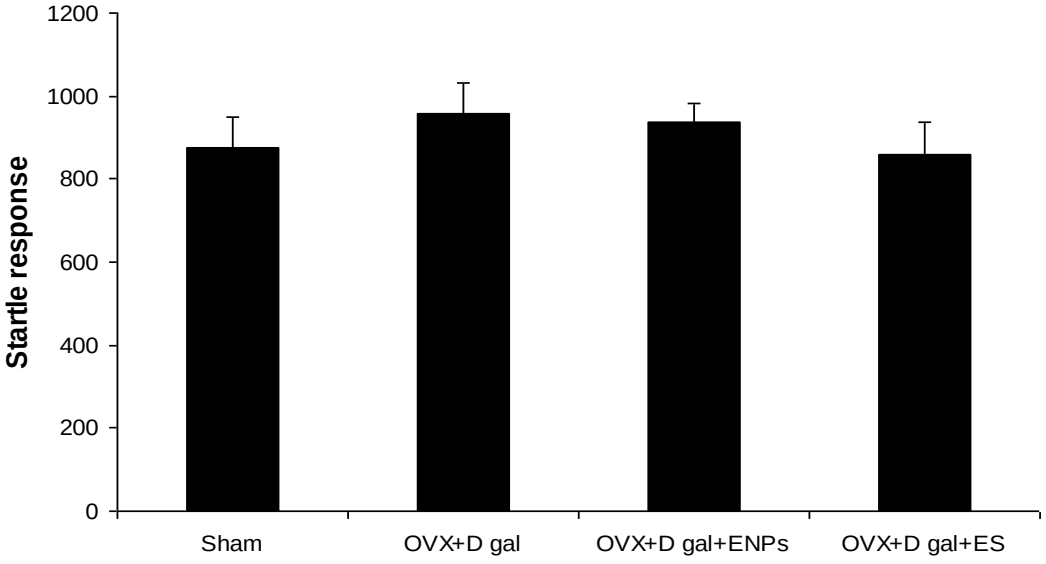

Fig. 5.4 (a) Prepulse inhibition (%) for each prepulse level above background and, (b) startle response to 120dB stimulus. No significant difference in PPI and startle response was found between the groups. Bar graphs show Mean ± SEM (n=10).

and D). This intraneuronal Aβ42 staining was particularly apparent in the CA1 to CA4 pyramidal neurons of hippocampus. On the other hand, no Aβ42 immunoreactive neurons were detected in the Sham control group (Fig. 5.5 A and B), while nanoparticles (Fig. 5.5 E and F) and suspension (Fig. 5.5 G and H) treated animals also displayed no or very few Aβ42 positive neurons These results suggest that oxidative stress due to lack of endogenous oestrogen after menopause enhances the amyloidogenic processing of APP and thereby, plays a major role in the etiology of AD, whereas post-menopausal oestradiol treatment can prevent/reduce this APP processing into amyloidogenic peptide (Aβ42) through its antioxidant neuroprotective action. However, no extracellular Aβ42 fibrillar plaques were detected in the present study and these results were consistent with the findings obtained in the same animal model reported earlier (Hua *et al*., 2007). The results were further supported by the absence of apple green birefringence with Congo red (fibril specific dye) staining under polarized light, which also indicated the non-β-pleated (non-fibrillar) nature of obtained intracellular Aβ42 accumulation. Until lately, only extracellular Aβ deposition was considered to be the hallmark neuropathological sign of AD. But over the last few years, intracellular accumulation of the Aβ peptide and its role in AD pathology has been a subject of investigation. Increasing evidence indicates that accumulation of intraneuronal Aβ is an early stage in the progression of AD, preceding the formation of extracellular Aβ deposits (Echeverria and Cuello, 2002; Wirths *et al*., 2004; Giménez-Llort *et al*., 2007; LaFerla *et al*., 2007). An excessive load of intraneuronal Aβ triggers a cascade of pathological events (proteasome and mitochondrial dysfunction, calcium dyshomeostasis and hyperphosphorylation of tau) leading to neurodegeneration (Casas *et al*., 2004; Oakley *et al*., 2006). Therefore, intraneuronal Aβ accumulation seems to

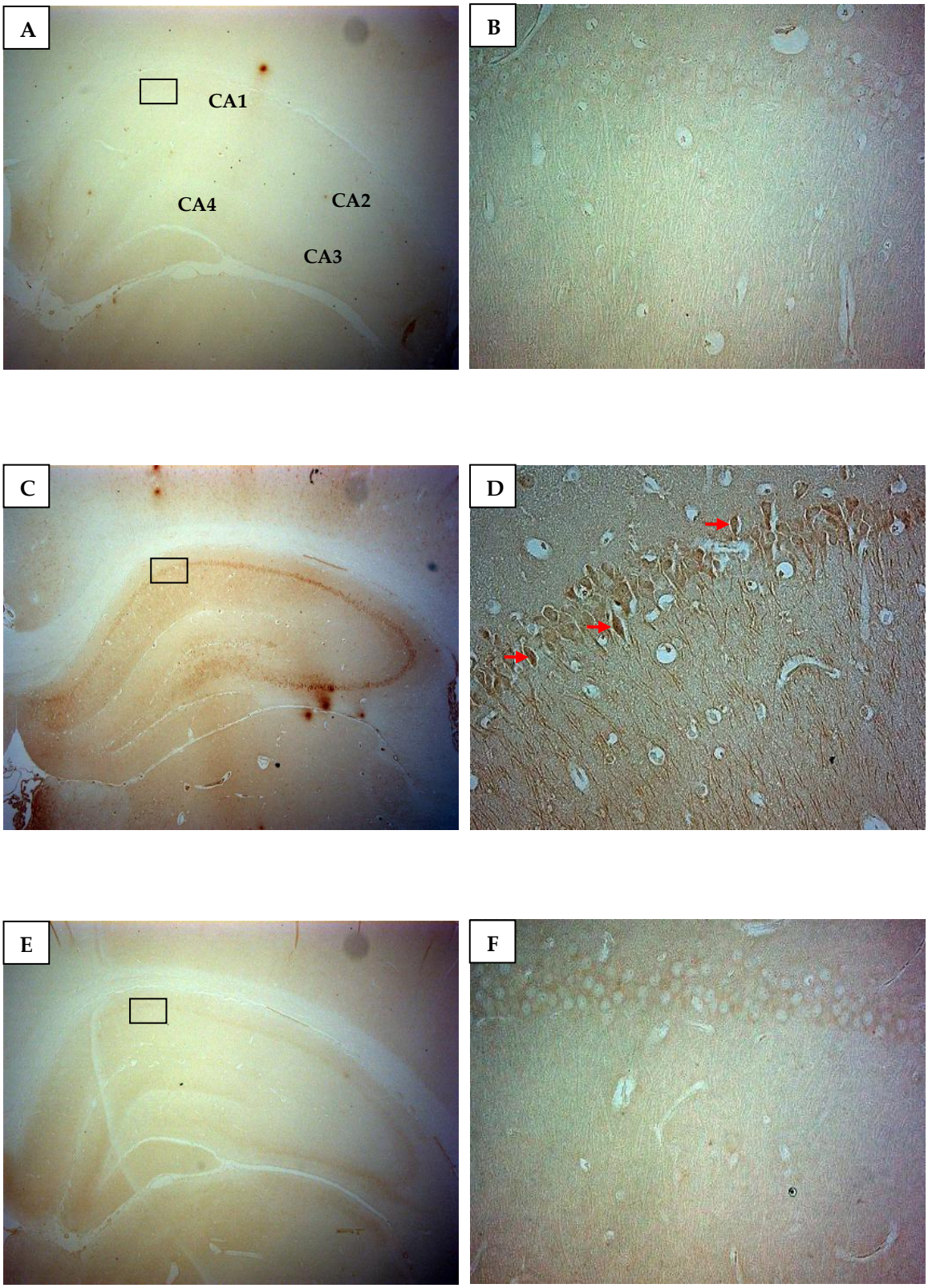
A
CA1
CA4
CA2
CA3
B
C
D
E
F

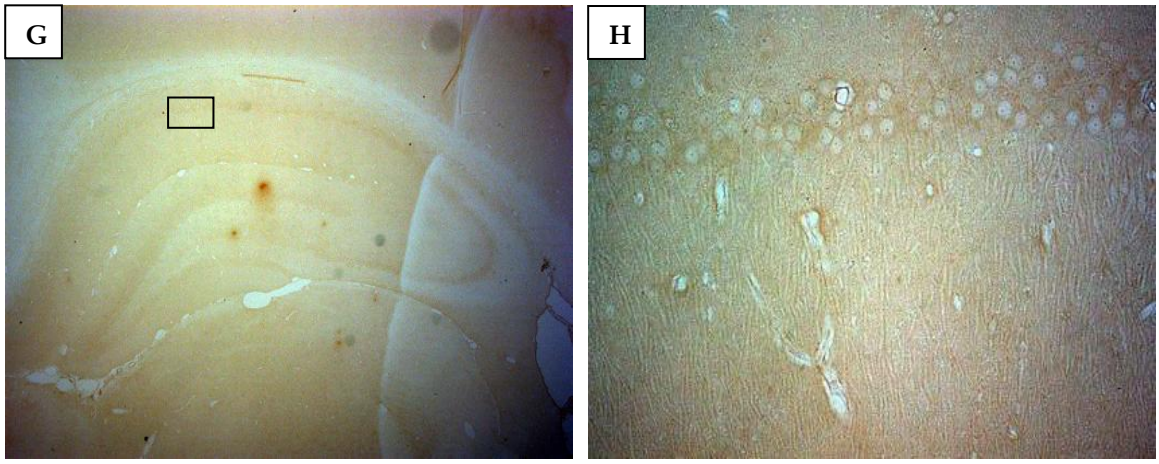

Fig. 5.5 Representative images of immunohistochemistry for Aβ42 expression in the rat hippocampus. OVX+D gal rats (C and D) exhibited strong expression of intraneuronal Aβ42 immunoreactivity (arrows) in the CA1 to CA4 pyramidal neurons of hippocampus. No Aβ42 expression was detected in Sham control (A and B) and oestradiol treated animals i.e. OVX+D gal+ENPs (E and F) and OVX+D gal+ES (G and H). Images A, C, E and G are x25 and boxes shown in them are zoomed at x200 in the subsequent images B, D, F and H respectively.

play an important pathological role in AD. Accumulation of intraneuronal Aβ has been observed in the brains of AD patients (LaFerla *et al*., 1997; Gouras *et al*., 2000; Mochizuki *et al*., 2000; D'Andrea *et al*., 2001; D'Andrea *et al*., 2002a), Down's syndrome (DS) individuals (Gyure *et al*., 2001; Mori *et al*., 2002) and AD animal models (Shie *et al*., 2003; Magrané *et al*., 2005; Cruz *et al*., 2006; Lord *et al*., 2006; Van *et al*., 2008), suggesting a potential contribution of intraneuronal Aβ in AD pathology. Moreover, studies have demonstrated that there is a dynamic correlation between intracellular and extracellular pools of Aβ, where extracellular Aβ plaques develop from an initial intraneuronal pool of Aβ and an inverse relationship exists between intraneuronal Aβ immunoreactivity and extracellular amyloid plaques (Gouras *et al*., 2000; D'Andrea *et al*., 2001; Gyure *et al*., 2001; Mori *et al*., 2002; Oddo *et al*., 2006). There is also evidence which has confirmed the role of intraneuronal Aβ in synaptic dysfunction and profound impairments in long-term potentiation (LTP), thereby leading to cognitive and other behavioural deficits before deposition of extracellular Aβ plaques (Oddo *et al*., 2003; Billings *et al*., 2005; Knobloch *et al*., 2007). However, in spite of large number of immunohistochemical studies on AD brains, which all showed consistent Aβ-staining in diffuse or dense plaques, there are relatively very few reports showing intraneuronal Aβ immunoreactivity. This may be due to different techniques of immunohistochemical staining, as it was shown that prominent intracellular Aβ42 in pyramidal neurons can be detected by heat-induced antigen retrieval but not just by enzymatic pre-treatment. Whereas treatment with formic acid is well suited for the detection of extracellular amyloid plaques, the enhancement of Aβ-immunoreactivity by heat induced methods is more appropriate for the detection of intraneuronal Aβ (D'Andrea *et al*., 2002b; D'Andrea *et al*., 2003).

Apart from Aβ deposition, another key feature of AD neuropathology is astrocytosis, also known as reactive gliosis (Ryu *et al*., 2004; Oide *et al*., 2006; Mohri *et al*., 2007). Astrocytes are the characteristic star-shaped glial cells present in CNS. They perform many important functions in brain including dynamic regulation of synaptic transmission and neuronal electrical activity, and maintenance of extracellular ion balance and of the blood–brain barrier (BBB) (Ransom *et al*., 2003; Abbott *et al*., 2006). Astrocytosis is not limited to AD only, but also implicated in the neuropathology of other neurodegenerative diseases as well such as Huntington's disease, Parkinson's disease, multiple sclerosis, dementia, and stroke (Eddleston and Mucke, 1993; Seifert *et al*., 2006). Astrocytes and microglial cells are the brain phagocytic cells and their activation is considered to be a part of the brain's inflammatory reaction in response to neurodegeneration. But it has been reported that microglia become activated first as a result of neuronal loss and then secrete cytokines (tumour-necrosis factor-α, interleukine-1β) that further activate astrocytes (Abraham, 2001). Reactive astrocytes could be involved in the pathomechanisms leading to AD by favouring oxidative neuronal damage and Aβ toxicity (Schubert *et al*., 2001). Thus, astrocyte activation also might be implicated in AD pathogenesis. Astrocyte activation is generally evidenced by the over-expression of GFAP, the main 8-9 nm intermediate filament of astrocyte. All astrocytes express GFAP, however in response to a CNS injury, they exhibit cellular hypertrophy (enlargement of cell body and increased growth of cell processes) and elevated levels of GFAP. To analyze the activation of astrocytes following oestradiol deprivation (OVX) and long term D-gal injection, GFAP expression in the hippocampus was determined by Western blotting. Surprisingly and contrary to the findings reported earlier with the same animal model (Hua *et al*., 2008), quantitative

densitometric analysis showed no significant difference in the GFAP levels among the groups (Fig. 5.6). Similarly, immunohistochemical staining for GFAP in hippocampus demonstrated that OVX+D gal rats had no difference in the number of reactive (hypertrophic) astrocytes compared to Sham controls and drug treated groups (Figs. 5.7 and 5.8). Unexpectedly, activated astrocytes were also seen in the Sham control animals (Fig. 5.8 B) which could be a normal aging effect as various reports suggest that rodents (Lindsey *et al*., 1979; Kordula *et al*., 2000), monkeys (Sloane *et al*., 2000) and humans (Hansen *et al*., 1987) possess some level of astrocytic reactivity as a function of normal aging.

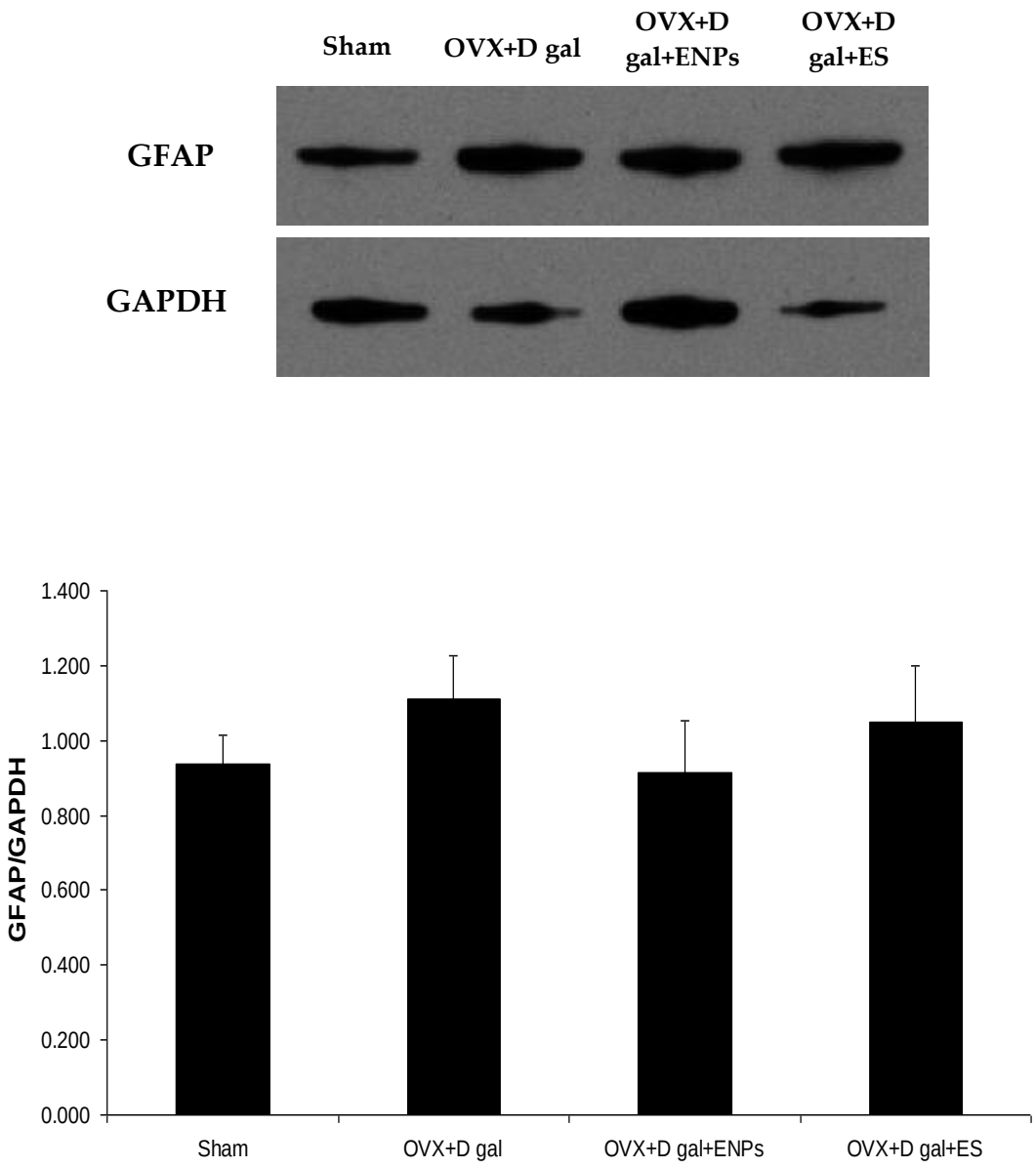

Fig. 5.6 Western blotting and quantitative densitometry analysis of the expression of GFAP proteins. No significant difference in the GFAP levels was observed among the groups. Data expressed as Mean ± SEM (n=5).

(a)

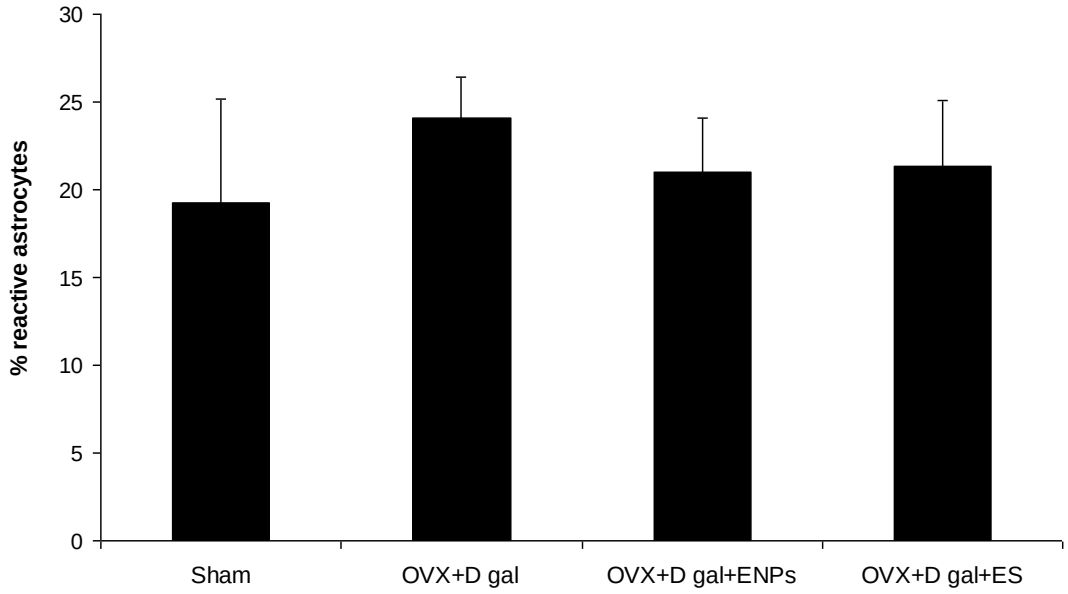

(b)

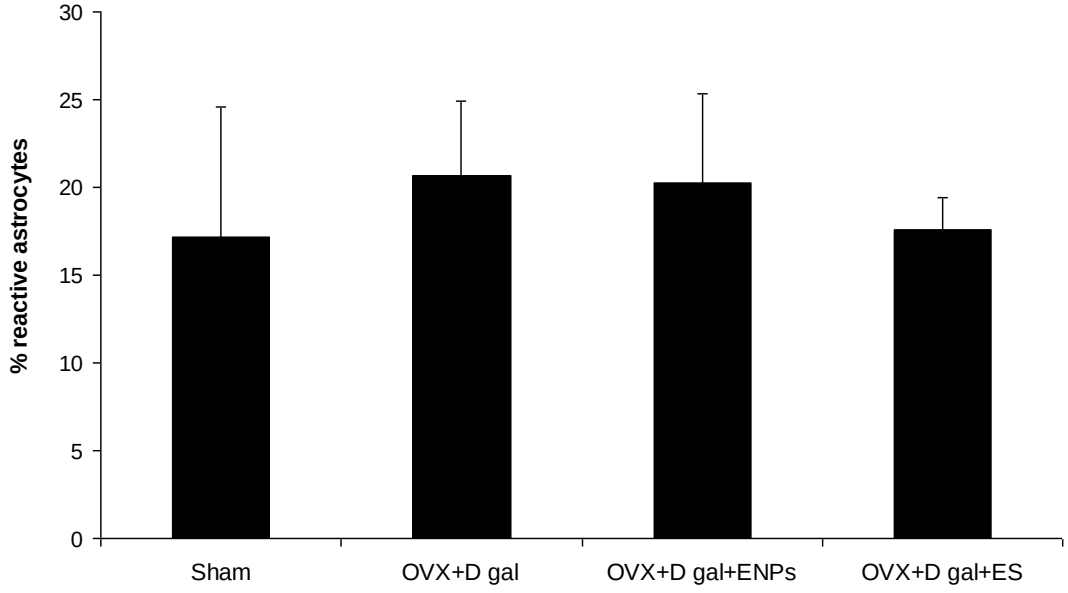

Fig. 5.7 Quantitative analysis of GFAP immunolabelled astrocytes in the (a) CA1 and (b) DG regions of hippocampus. No significant difference in the reactive astrocytes was observed among the groups. Data expressed as Mean ± SEM (n=5).

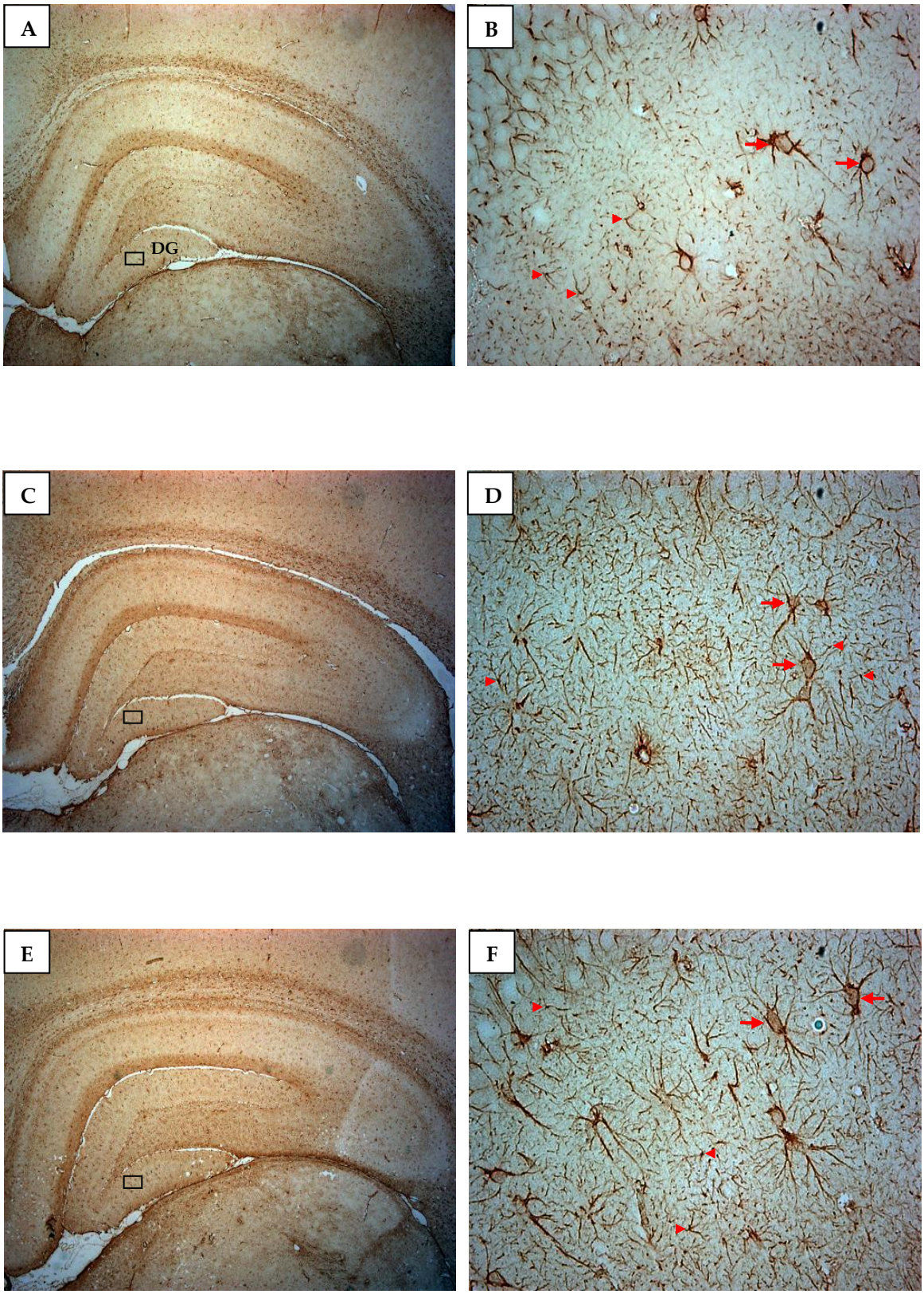
A
DG
B
C
D
E
F

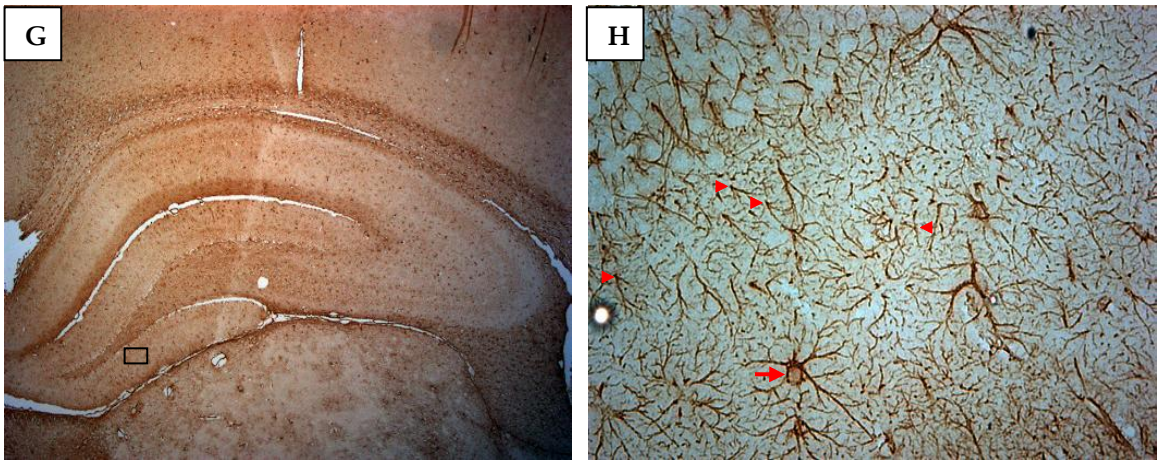

Fig. 5.8 Representative images of immunohistochemistry for GFAP expression in the rat hippocampus. OVX+D gal rats did not show any difference in reactive (hypertrophic) astrocytes (C and D) compared to Sham controls (A and B), and drug treated animals i.e. OVX+D gal+ENPs (E and F) and OVX+D gal+ES (G and H). Images A, C, E and G are x25 and boxes shown in them are zoomed at x400 in the subsequent images B, D, F and H respectively. The arrows are showing the examples of reactive astrocytes as evidenced by the enlarged cell bodies with long, thick and branched processes while arrowheads are pointing towards the normal astrocytes having small cell bodies with short and slender processes.

5.4 Conclusions

From the forgoing studies it is evident that oxidative stress due to the OVX and long term D-gal injection was sufficient to initiate the AD pathology as indicated by intraneuronal Aβ42 accumulation, but perhaps was not adequate to cause severe neurodegeneration in the given period of time i.e. 6 weeks. Thus, lack of severity of neurodegeneration forms the most likely reason of not achieving profound behavioural deficits and astrocyte activation in the present study. These deviations in results from the earlier reported observations with the same animal model could be due to biological variation, suggesting the need for a reconsideration of the model in terms of its robustness. The interesting feature of this study, drawn from our descriptive analysis of the Aβ42 immunostaining, indicates that orally administered T-80 coated oestradiol nanoparticles were as effective as intramuscular drug injection in preventing/reducing the pathological development of AD and therefore, with the added benefits of patient compliance and reduced peripheral drug burden, could be a prospective therapeutic approach in post-menopausal AD.

6. General conclusions & Future work

The major objective of this dissertation to deliver oestradiol orally at the lowest effective dose with the aid of polymeric nanoparticles was successfully achieved. The particles prepared were in the size range of 100-150 nm, ideal for oral drug delivery. The pharmacokinetics of oestradiol demonstrated the potential of polymeric nanoparticles in improving the oral bioavailability and sustaining the release of oestradiol. The dose-proportionality further offers the possibility of dose titration. This exercise further testifies that drug is homogeneously distributed in the nanoparticle matrix as well as the ease of formulation dilution to obtain such small doses administered in the study. The evaluation of oral oestradiol PLGA nanoparticles in a rat model of hyperlipidaemia showed therapeutic efficacy at three times reduced dose and frequency than simple oral drug suspension, indicating the substantial role of polymeric nanoparticles in enhancing the oral delivery aspects of oestradiol. A further possibility of coating the nanoparticles with T-80 for improved brain levels of oestradiol proved feasible. These T-80 coated nanoparticles exhibited a different tissue distribution to that of uncoated nanoparticles. T-80 coating improved brain levels of oestradiol and reduced liver and spleen burden in contrast to uncoated particles, strongly suggesting the role of surface properties in dictating the *in vivo* fate of nanoparticles. Furthermore, the effectiveness of these surface modified oestradiol nanoparticles in preventing the pathological development of AD in a rat model was elegantly demonstrated. Therefore, the nanoparticles developed in this study (uncoated as well as those coated with 4% T-80) could be efficient in alleviating the adverse effects of conventional oral oestradiol treatment and maximize the therapeutic potential of oestradiol.

As we have seen that 6 weeks intraperitoneal administration of D-gal into OVX rats failed to produce the profound AD pathology (behavioural deficits and astrocyte activation) in our case. Moreover, extracellular Aβ deposition was also not found in the present study. It is possible that a period of six weeks and/or D-gal concentration (20 mg in 2 ml saline) was probably insufficient to cause severe neurodegeneration and extracellular Aβ deposition. Therefore, another study using same animal model with modifications of more than six weeks treatment duration and/or higher D-gal concentration can be carried out in future to understand the molecular mechanism of estrogen deprivation and oxidative stress in the pathological development of AD and at the same time to determine the efficacy of our developed orally administered T-80 nanoparticulate formulation in preventing/attenuating the behavioural and neuropathological impairments observed in the AD condition. Further, the oestradiol loaded nanoparticles can also be evaluated for various other therapeutic indications (like stroke, osteoporosis) using appropriate animal models to get an insight of their therapeutic potential in preventing/treating these diseases.

The formulation aspect in the future work should focus on optimization of the freeze-drying process for both, uncoated as well as T-80 (4% v/v) coated oestradiol loaded nanoparticles to overcome the physical (aggregation or particle fusion) and chemical (hydrolysis of polymer material, drug leakage from nanoparticles and chemical reactivity of the drug during the storage) instability problems of these aqueous suspensions on long-term storage. Various types of lyoprotectants/cryoprotectants (eg. trehalose, sucrose, and mannitol) should be screened at different concentrations to get the freeze-dried product having ease of reconstitution and same particle characteristics (size, appearance and drug content uniformity) after reconstitution as before

the freeze-drying process. Thereafter, long-term stability studies (as per ICH guidelines) should be considered to determine the influence of a variety of environmental factors such as temperature, humidity and light and to establish a shelf life for the drug product and recommend storage conditions. Finally, scale up and regulatory toxicological study of the formulations should be carried out before they are taken forward to clinical trials.

References

Abbey, M., Owen, A., Suzakawa, M., Roach, P., Nestel, P.J., 1999. Effect of menopause and hormone replacement therapy on plasma lipids, lipoproteins and LDL-receptor activity. Maturitas, 33, 259-269.

Abbott, N.J., Rönnbäck, L., Hansson, E., 2006. Astrocyte–endothelial interactions at the blood–brain barrier. Nat. Rev. Neurosci., 7, 41-53.

Abdel-Rahman, S.M. and Kauffman, R.E., 2004. The integration of pharmacokinetics and pharmacodynamics: Understanding dose-response. Annu. Rev. Pharmacol. Toxicol., 44, 111-136.

Abraham, C.R., 2001. Reactive astrocytes and α1-antichymotrypsin in Alzheimer's disease. Neurobiol. Aging, 22, 931-936.

Ackerman, G.E. and Carr, B.R., 2002. Estrogens. Rev. Endocr. Metab. Disord., 3, 225-230.

Aggarwal, P., Hall, J.B., McLeland, C.B., Dobrovolskaia, M.A., McNeil, S.E., 2009. Nanoparticle interaction with plasma proteins as it relates to particle biodistribution, biocompatibility and therapeutic efficacy. Adv. Drug Deliv. Rev., 61, 428-437.

Allémann, E., Gurny, R., Doelker, E., 1992. Preparation of aqueous polymeric nanodispersions by a reversible salting-out process: influence of process parameters on particle size. Int. J. Pharm., 87, 247-253.

Allémann, E., Gurny, R., Doelker, E., 1993a. Drug loaded nanoparticles: Preparation methods and drug targeting issues. Eur. J. Pharm. Biopharm., 39, 173-191.

Allémann, E., Leroux, J.C., Gurny, R., Doelker, E., 1993b. *In vitro* extended release properties of drug-loaded poly(DL-lactic acid) nanoparticles produced by a salting out procedure. Pharm. Res., 10, 1732-1737.

Allémann, E., Leroux, J.C., Gurny, R., 1998. Polymeric nano- and microparticles for the oral delivery of peptides and peptidomimetics. Adv. Drug Deliv. Rev., 34, 171-189.

Anderson, G.L., Limacher, M., Assaf, A.R., Bassford, T., Beresford, S.A., Black, H., Bonds, D., Brunner, R., Brzyski, R., Caan, B., Chlebowski, R.,

Curb, D., Gass, M., Hays, J., Heiss, G., Hendrix, S., Howard, B.V., Hsia, J., Hubbell, A., Jackson, R., Johnson, K.C., Judd, H., Kotchen, J.M., Kuller, L., LaCroix, A.Z., Lane, D., Langer, R.D., Lasser, N., Lewis, C.E., Manson, J., Margolis, K., Ockene, J., O'Sullivan, M.J., Phillips, L., Prentice, R.L., Ritenbaugh, C., Robbins, J., Rossouw, J.E., Sarto, G., Stefanick, M.L., Van Horn, L., Wactawski-Wende, J., Wallace, R., Wassertheil-Smoller, S., 2004. Effects of conjugated equine estrogen in postmenopausal women with hysterectomy: the Women's Health Initiative randomized controlled trial. JAMA, 291, 1701-1712.

Ankola, D.D., Boomi, V., Bhardwaj, V., Ramarao, P., Kumar, M.N.V.R., 2007. Development of potent oral nanoparticulate formulation of coenzyme Q10 for treatment of hypertension: can the simple nutritional supplements be used as first line therapeutic agents for prophylaxis/therapy? Eur. J. Pharm. Biopharm., 67, 361-369.

Bachmann, G.A., 1999. Vasomotor flushes in menopausal women. Am. J. Obstet. Gynecol., 180, S312-S316.

Bachmann, G.A., 2005. Menopausal vasomotor symptoms: a review of causes, effects and evidence-based treatment options. J. Reprod. Med., 50, 155-165.

Badeau, M., Adlercreutz, H., Kaihovaara, P., Tikkanen M.J., 2005. Estrogen A-ring structure and antioxidative effect on lipoproteins. J. Steroid Biochem. Mol. Biol., 96, 271-278.

Bala, I., Hariharan, S., Kumar, M.N.V.R., 2004. PLGA nanoparticles in drug delivery: the state of the art. Crit. Rev. Ther. Drug Carrier Syst., 21, 387-422.

Beato, M., 1989. Gene regulation by steroid hormones. Cell, 56, 335-344.

Behl, C., 1999. Alzheimer's disease and oxidative stress: implications for novel therapeutic approaches. Prog. Neurobiol., 57, 301-323.

Behl, C., 2003. Estrogen can protect neurons: modes of action. J. Steroid Biochem. Mol. Biol., 83, 195-197.

Bennink, H.J.T.C., 2004. Are all estrogens the same? Maturitas, 47, 269-275.

Beral, V., 2003. Breast cancer and hormone-replacement therapy in the Million Women Study. Lancet, 362, 419-427.

Berliner, J.A. and Heinecke, J.W., 1996. The role of oxidized lipoproteins in atherogenesis. Free Radic. Biol. Med., 20, 707-727.

Berry, M., Metzger, D., Chambon, P., 1990. Role of the two activating domains of the estrogen receptor in the cell-type and promoter context dependent agonistic activity of the anti-estrogen 4-hydroxytamoxifen. EMBO J., 9, 2811-2818.

Beyer, C., 1999. Estrogen and the developing brain. Anat. Embryol., 199, 379-390.

Bhardwaj, V., Ankola, D. D., Gupta, S. C., Schneider, M., Lehr, C.M., Kumar M.N.V.R., 2009. PLGA nanoparticles stabilized with cationic surfactant: Safety studies and application in oral delivery of Paclitaxel to treat chemical-induced breast cancer in rat. Pharm. Res., 26, 2495-2503.

Bhardwaj, V., Hariharan, S., Bala, I., Lamprecht, A., Kumar, N., Panchagnula R., Kumar, M.N.V.R., 2005. Pharmaceutical aspects of polymeric nanoparticles for oral delivery. J. Biomed. Nanotechnol., 1, 235-258.

Billings, L.M., Oddo, S., Green, K.N., McGaugh, J.L., LaFerla, F.M., 2005. Intraneuronal Aβ causes the onset of early Alzheimer's disease-related cognitive deficits in transgenic mice. Neuron, 45, 675-688.

Birkhauser, M.H., 1996. Chemistry, physiology, and pharmacology of sex steroids. J. Cardiovasc. Pharmacol., 28(Suppl 5), S1-S13.

Birnbaum, D.T., Kosmala, J.D., Henthorn, D.B., Brannon-Peppas, L., 2000. Controlled release of β-estradiol from PLAGA microparticles: The effect of organic phase solvent on encapsulation and release. J. Control. Release, 65, 375-387.

Bjork, E., Isaksson, U., Edman, P., Artursson, P., 1995. Starch microspheres induce pulsatile delivery of drugs and peptides across the epithelial barrier by reversible separation of the tight junctions, J. Drug Target., 2, 501-507.

Bodor, N., Prokai, L., Wu, W.M., Farag, H.H., Jonnalagadda, S., Kawamura, M., Simpkins, J., 1992. A strategy for delivering peptides into the central nervous system by sequential metabolism. Science, 257, 1698-1700.

Bodor, N. and Buchwald, P., 1999. Recent advances in the brain targeting of neuropharmaceuticals by chemical delivery systems. Adv. Drug Deliv. Rev., 36, 229-254.

Bodor, N. and Buchwald, P., 2006. Brain-targeted delivery of estradiol: therapeutic potential and results obtained with a chemical delivery system approach. American J. Drug Deliv., 3, 161-175.

Bottner, M. and Wuttke, W., 2006. Chronic treatment with physiological doses of estradiol affects the GH-IGF-1 axis and fat metabolism in young and middle-aged ovariectomized rats. Biogerontology, 7, 91-100.

Brightman, M.W., 1977. Morphology of blood–brain barrier. Exp. Eye Res., 25, 1-25.

Brinton, R.D., 2001. Cellular and Molecular Mechanisms of estrogen regulation of memory function and neuroprotection against Alzheimer's disease: Recent insights and remaining challenges. Learn. Mem., 8, 121-133.

Brown, E.G. and Hayes, T.J., 1955. The absorptiometric determination of polyethyleneglycol mono-oleate. Analyst, 80, 755-767.

Bruce, D. and Rymer. J., 2009. Symptoms of the menopause. Best Pract. Res. Clin. Obstet. Gynaecol., 23, 25-32.

Casadesus, G., Rolston, R.K., Webber, K.M., Atwood, C.S., Bowen, R.L., Perry, G., Smith, M.A., 2008. Menopause, estrogen, and gonadotropins in Alzheimer's disease. Adv. Clin. Chem., 45, 139-53.

Casas, C., Sergeant, N., Itier, J.M., Blanchard, V., Wirths, O., van der Kolk, N., Vingtdeux, V., van de Steeg, E., Ret, G., Canton, T., Drobecq, H., Clark, A., Bonici, B., Delacourte, A., Benavides, J., Schmitz, C., Tremp, G., Bayer, T.A., Benoit, P., Pradier, L., 2004. Massive CA1/2 neuronal loss with intraneuronal and N-terminal truncated Aβ42 accumulation in a novel Alzheimer transgenic model. Am. J. Pathol., 165, 1289-1300.

Casetta, I., Govoni, V., Granieri, E., 2005. Oxidative stress, antioxidants and neurodegenerative diseases. Curr. Pharm. Des., 11, 2033-2052.

Chabbert-Buffet, N. and Bouchard, P., 2002. The normal human menstrual cycle. Rev. Endocr. Metab. Disord., 3, 173-183.

Chen, C.F, Lang, S.Y., Zuo, P.P., Yang, N., Wang, X.Q., Xia, C., 2006. Effects of D-galactose on the expression of hippocampal peripheral-type benzodiazepine receptor and spatial memory performances in rats. Psychoneuroendocrinology, 31, 805-811.

Chen, H. and Langer, R., 1998. Oral particulate delivery: status and future trends. Adv. Drug Deliv. Rev., 34, 339-350.

Ciccone, C.D., 1995. Basic pharmacokinetics and the potential effect of physical therapy interventions on pharmacokinetic variables, Phys. Ther., 75, 343-351.

Clark, M.A., Hirst, B.H., Jepson, M.A., 2000. Lectin-mediated mucosal delivery of drugs and microparticles. Adv. Drug Deliv. Rev., 43, 207-223.

Clarke, I.J., 1995. Evidence that the switch from negative to positive feedback at the level of the pituitary gland is an important timing event for the onset of the preovulatory surge in LH in the ewe. J. Endocrinol., 145, 271-282.

Cohen, S., Alonso, M.J., Langer, R., 1994. Novel approaches to controlled release antigen delivery. Int. J. Technol. Assessment Health Care, 10, 121-130.

Craig, M.C. and Murphy, D.G., 2009. Alzheimer's disease in women. Best Pract. Res. Clin. Obstet. Gynaecol., 23, 53-61.

Crook, D., 2001. Do we need clinical trials to test the ability of transdermal HRT to prevent coronary heart disease? Curr. Control Trials Cardiovasc. Med., 2, 211-214.

Cruz, J.C., Kim, D., Moy, L.Y., Dobbin, M.M., Sun, X., Bronson, R.T., Tsai, LH., 2006. p25/cyclin-dependent kinase 5 induces production and intraneuronal accumulation of amyloid β *in vivo*. J. Neurosci., 26, 10536-10541.

Cui, X., Zuo, P., Zhang, Q., Li, X., Hu, Y., Long, J., Packer, L., Liu, J., 2006. Chronic systemic D-galactose exposure induces memory loss, neurodegeneration, and oxidative damage in mice: protective effects of R-alpha-lipoic acid. J. Neurosci. Res., 83, 1584-1590.

Cummings, J.L., 2004. Alzheimer's disease. N. Engl. J. Med., 351, 56-57.

D'Andrea, M.R., Nagele, R.G., Wang, H.Y., Peterson, P.A. Lee, D.H., 2001. Evidence that neurones accumulating amyloid can undergo lysis to form amyloid plaques in Alzheimer's disease. Histopathology, 38, 120-134.

D'Andrea, M.R., Nagele, R.G., Gumula, N.A., Reiser, P.A., Polkovitch, D.A., Hertzog, B.M., Andrade-Gordon, P., 2002a. Lipofuscin and Aβ42 exhibit distinct distribution patterns in normal and Alzheimer's disease brains. Neurosci. Lett., 323, 45-49.

D'Andrea, M.R., Nagele, R.G., Wang, H.Y., Lee, D.H., 2002b. Consistent immunohistochemical detection of intracellular beta-amyloid42 in pyramidal neurons of Alzheimer's disease entorhinal cortex. Neurosci. Lett., 333, 163-166.

D'Andrea, M.R., Reiser, P.A., Polkovitch, D.A., Gumula, N.A., Branchide, B., Hertzog, B.M., Schmidheiser, D., Belkowski, S., Gastard, M.C., Andrade-Gordon, P., 2003. The use of formic acid to embellish amyloid plaque detection in Alzheimer's disease tissues misguides key observations. Neurosci. Lett., 342, 114-118.

Dalle-Donne, I., Rossi, R., Colombo, R., Giustarini, D., Milzani, A., 2006. Biomarkers of Oxidative Damage in Human Disease. Clin. Chem., 52, 601-623.

Das, D. and Lin, S., 2005. Double-coated poly (butylcynanoacrylate) nanoparticulate delivery systems for brain targeting of dalargin via oral administration. J. Pharm. Sci., 94, 1343-1353.

Deady, J., 2004. Clinical monograph: hormone replacement therapy. J. Manag. Care Pharm., 10, 33-47.

Delie, F. and Blanco-Prieto, M.J., 2005. Polymeric Particulates to Improve Oral Bioavailability of Peptide Drugs. Molecules, 10, 65-80.

Delie, F., 1998. Evaluation of nano- and microparticle uptake by the gastrointestinal tract. Adv. Drug Deliv. Rev., 34, 221-233.

des Rieux A., Fievez V., Garinot M., Schneider Y-J., Préat V., 2006. Nanoparticles as potential oral delivery systems of proteins and vaccines: A mechanistic approach. J. Control. Release, 116, 1-27.

Desai, M.P., Labhasetwar, V., Amidon, G.L., Levy, R.J., 1996. Gastrointestinal uptake of biodegradable microparticles: effect of particle size. Pharm. Res., 13, 1838-1845.

Desai, M.P., Labhasetwar, V., Walter, E., Levy, R.J., Amidon, G.L., 1997. The mechanism of uptake of biodegradable microparticles in Caco-2 cells is size dependent, Pharm. Res., 14, 1568-1573.

Devineni, D., Klein-Szanto, A., Gallo, J.M., 1995. Tissue distribution of methotrexate following administration as a solution and as a magnetic microsphere conjugate in rats bearing brain tumors. J. Neurooncol., 24, 143-152.

Dhanikula, R.S., Dhanikula, A.B., Panchagnula, R., 2008. Thermoreversible liposomal poloxamer gel for the delivery of paclitaxel: dose proportionality and hematological toxicity studies. Pharmazie, 63, 439-445.

Dingemanse, J. and Appel-Dingemanse, S., 2007. Integrated pharmacokinetics and pharmacodynamics in drug development. Clin. Pharmacokinet., 46, 713-737.

Dollery, C. (Ed.), 1991. Therapeutic Drugs, 1st edition, Vol. 2, Churchill Livingstone, pp. O4-O9.

Dykens, J.A., Moos, W.H., Howell, N., 2005. Development of 17alpha-estradiol as a neuroprotective therapeutic agent: rationale and results from a phase I clinical study. Ann. N. Y. Acad. Sci., 1052, 116-135.

Echeverria, V. and Cuello, A.C., 2002. Intracellular A-Beta Amyloid, A Sign for Worse Things to Come? Mol. Neurobiol., 26, 299-316.

Eddleston, M. and Mucke, L., 1993. Molecular profile of reactive astrocytes implications for their role in neurologic disease. Neuroscience, 54, 15-36.

Ennaceur, A. and Delacour, J., 1988. A new one-trial test for neurobiological studies of memory in rats. 1: Behavioural data. Behav. Res., 31, 47-59.

Esterbauter, H., Gebicki, J., Puhl, H., Jurgens, G., 1992. The role of lipid peroxidation and antioxidants in oxidative modification of LDL. Free Radic. Biol. Med., 13, 341-390.

Ettinger, B., Genant, H.K., Steiger, P., Madvig, P., 1992. Low dosage micronized 17β-estradiol prevents bone loss in post-menopausal women. Am. J. Obstet. Gynecol., 166, 479-488.

Evans, R.M., 1988. The steroid and thyroid hormone superfamily. Science, 240, 889-895.

Ferenczy, A. and Bergeron, C., 1991. Histology of the human endometrium: from birth to senescence. Ann. N. Y. Acad. Sci., 622, 6-27.

Fessi, H., Puisieux, F., Devissaguet, J.P., Ammoury, N., Benita, S., 1989. Nanocapsule formation by interfacial polymer deposition following solvent displacement. Int. J. Pharm., 55, R1-R4.

Filicori, M., 1999. The role of luteinizing hormone in folliculogenesis and ovulation induction. Fertil. Steril., 71, 405-414.

Filicori, M. and Cognigni, G.E., 2001. Clinical reviews 126: Roles and novel regimens of luteinizing hormone and follicle-stimulating hormone in ovulation induction. J. Clin. Endocrinol. Metab., 86, 1437-1441.

Findlay, J.K. and Drummond, A.E., 1999. Regulation of the FSH receptor in the ovary. Trends Endocrinol. Metab., 10, 183-188.

Fishman, J., Bradlow, H.L., Gallagher, T.F., 1960. Oxidative metabolism of estradiol. J. Biol. Chem., 235, 3104-3107.

Florence, A.T., 1997. The oral absorption of micro- and nanoparticulates: neither exceptional nor unusual. Pharm. Res., 14, 259-266.

Freedman, R.R., 2001. Physiology of hot flashes. Am. J. Hum. Biol., 13, 453-464.

Galindo-Rodriguez, S.A., Allémann, E., Fessi, H., Doelker, E., 2005. Polymeric nanoparticles for oral delivery of drugs and vaccines: a critical

evaluation of *in vivo* studies, Crit. Rev. Ther. Drug Carr. Syst., 22, 419-464.

Gao, K. and Jiang, X., 2006. Influence of particle size on transport of methotrexate across blood brain barrier by polysorbate 80-coated polybutylcyanoacrylate nanoparticles. Int. J. Pharm., 310, 213-219.

Geyer, M.A., Krebs-Thomson, K., Braff, D.L., Swerdlow, N.R., 2001. Pharmacological studies of prepulse inhibition models of sensorimotor gating deficits in schizophrenia: A decade in review. Psychopharmacology, 156, 117-154.

Gibbs, R.B., 1998. Impairment of basal forebrain cholinergic neurons associated with aging and long-term loss of ovarian function. Exp. Neurol., 151, 289-302.

Giménez-Llort, L., Blázquez, G., Cañete, T., Johansson, B., Oddo, S., Tobeña, A., LaFerla, F.M., Fernández-Teruel, A., 2007. Modeling behavioral and neuronal symptoms of Alzheimer's disease in mice: A role for intraneuronal amyloid. Neurosci. Biobehav. Rev., 31, 125-147.

Gorodeski, G.I., 2002. Update on cardiovascular disease in postmenopausal women. Best Pract. Res. Clin. Obstet. Gynaecol., 16, 329-355.

Gouras, G.K., Tsai, J., Naslund, J., Vincent, B., Edgar, M., Checler, F., Greenfield, J.P., Haroutunian, V., Buxbaum, J.D., Xu, H., Greengard, P., Relkin, N.R., 2000. Intraneuronal Aβ42 accumulation in human brain. Am. J. Pathol., 156, 15-20.

Govender, T., Stolnik, S., Garnett, M.C., Illum, L., Davis, S.S., 1999. PLGA nanoparticles prepared by nanoprecipitation: drug loading and release studies of a water soluble drug. J. Control. Release, 57, 171-185.

Green, J.D., Baddelay, A.D., Hodge,s J.R., 1996. Analysis of the episodic memory deficit in early Alzheimer's disease: evidence from the doors and people test. Neuropsychologia, 34, 537-551.

Grodstein, F. and Stampfer, M., 1995. The epidemiology of coronary heart disease and estrogen replacement in postmenopausal women. Prog. Cardiovasc. Dis., 38, 199–210.

Grodstein, F., Stampfer, M.J., Manson, J.E., Colditz, G.A., Willett, W.C., Rosner, B., Speizer, F.E., Hennekens, C.H., 1996. Postmenopausal estrogen and progestin use and the risk of cardiovascular disease. N. Engl. J. Med., 335, 453-461.

Grodstein, F., Newcomb, P.A., Stampfer, M.J., 1999. Postmenopausal hormone therapy and the risk of colorectal cancer: a review and meta-analysis. Am. J. Med., 106, 574-582.

Gurny, R., Peppas, N.A., Harrington, D.D., Banker, G.S., 1981. Development of biodegradable and injectable latices for controlled release of potent drugs. Drug Dev. Ind. Pharm., 7, 1-25.

Gyure, K.A., Durham, R., Stewart, W.F., Smialek, J.E., Troncoso, J.C., 2001. Intraneuronal Aβ-amyloid precedes development of amyloid plaques in Down syndrome. Arch. Pathol. Lab. Med., 125, 489-492.

Hall, J.M., Couse, J.F., Korach, K.S., 2001. The multifaceted mechanisms of estradiol and estrogen receptor signaling. J. Biol. Chem., 276, 36869-36872.

Hansen, L.A., Armstrong, D.M., Terry, R.D. 1987. An immunohistochemical quantification of fibrous astrocytes in the aging human cerebral cortex. Neurobiol. Aging, 8, 1-6.

Hariharan, S., Bhardwaj, V., Bala, I., Sitterberg, J., Bakowasky, U., Kumar M.N.V.R., 2006. Design of estradiol loaded PLGA nanoparticulate formulations: a potential oral delivery system for hormone therapy. Pharm. Res., 23, 184-195.

Henderson, V.W., 1997. Estrogen, Cognition, and a Woman's Risk of Alzheimer's Disease. Am. J. Med., 103, 11S-18S.

Hillery, A.M. and Florence A.T., 1996. The effect of adsorbed poloxamer 188 and 407 surfactants on the intestinal uptake of 60-nm polystyrene particles after oral administration in the rat. Int. J. Pharm., 132, 123-130.

Holden, H.M., Rayment, I., Thoden, J.B., 2003. Structure and function of enzymes of the Leloir pathway for galactose metabolism. J. Biol. Chem., 278, 43885-43888.

Hua, X., Lei, M., Zhang, Y., Ding, J., Han, Q., Hu, G., Xiao, M., 2007. Long-term D-galactose injection combined with ovariectomy serves as a new rodent model for Alzheimer's disease. Life Sci., 80, 1897-1905.

Hua, X., Lei, M., Ding, J., Han, Q., Hu, G., Xiao, M., 2008. Pathological and biochemical alterations of astrocytes in ovariectomized rats injected with D-galactose: A potential contribution to Alzheimer's disease processes. Exp. Neurol., 210, 709-718.

Hulley, S., Furberg, C., Barrett-Connor, E., Cauley, J., Grady, D., Haskell, W., Knopp, R., Lowery, M., Satterfield, S., Schrott, H., Vittinghoff, E., Hunninghake, D., 2002. Noncardiovascular disease outcomes during 6.8 years of hormone therapy: Heart and Estrogen/progestin Replacement Study follow-up (HERS II), JAMA, 288, 58-66.

Huwyler, J., Wu, D., Pardridge, W.M., 1996. Brain delivery of small molecules using immunoliposomes. Proc. Natl. Acad. Sci. USA, 93, 14164-14169.

Jain, R.A., 2000. The manufacturing techniques of various drug loaded biodegradable poly(lactide-co-glycolide) (PLGA) devices. Biomaterials, 21, 2475-2490.

Jaiswal, J., Gupta, S.K., Kreuter, J., 2004. Preparation of biodegradable cyclosporine nanoparticles by high-pressure emulsification-solvent evaporation process. J. Control. Release, 96, 169-178.

Jalil, R. and Nixon, J.R., 1990. Biodegradable poly(lactic acid) and poly(lactide-co-glycolide) microcapsules: problems associated with preparative techniques and release properties. J. Microencapsulation, 7, 297-325.

Jani, P.U., Halbert, G.W., Langridge, J., Florence, A.T., 1989. The uptake and translocation of latex nanospheres and microspheres after oral administration to rats. J. Pharm. Pharmacol., 41, 809-812.

Jani, P.U, Halbert, G.W., Langridge, J., Florence, A.T., 1990. Nanoparticle uptake by the rat gastrointestinal mucosa: quantitation and particle size dependency. J. Pharm. Pharmacol., 42, 821-826.

Jani, P.U., Florence, A.T., McCarthy, D.E., 1992a. Further histological evidence of the gastrointestinal absorption of polystyrene nanospheres in the rat. Int. J. Pharm., 84, 245-252.

Jani, P.U., McCarthy, D.E., Florence, A.T., 1992b. Nanospheres and microsphere uptake via Peyer's patches: observation of the rate of uptake in the rat after a single oral dose. Int. J. Pharm., 86, 239-246.

Jessen, F., Kucharski, C., Fries, T., Papassotiropoulos, A., Hoenig, K., Maier, W., Heun, R., 2001. Sensory gating deficit expressed by a disturbed suppression of the P50 event-related potential in patients with Alzheimer's disease, Am. J. Psychiatry, 158, 1319-1321.

Jung, T., Kamm, W., Breitenbach, A., Kaiserling, E., Xiao, J.X., Kissel, T., 2000. Biodegradable nanoparticles for oral delivery of peptides: is there a role for polymers to affect mucosal uptake? Eur. J. Pharm. Biopharm., 50, 147-160.

Katzenellenbogen, J.A. and Katzenellenbogen, B.S., 1996. Nuclear hormone receptors: ligand-activated regulators of transcription and diverse cell responses. Chem. Biol., 3, 529–536.

Keep, P.A.V., 1990. The history and rationale for hormone replacement therapy. Maturitas, 12, 163-170.

Kirk, A. and Kertesz, A., 1991. On drawing impairment in Alzheimer's disease. Arch. Neurol., 48, 73-77.

Knobil, E. and Hotchkis, J., 1988. The menstrual cycle and its neuroendocrine control. In: Knobil, E. and Neill, J.D. (Eds.), The Physiology of reproduction. Vol. 2, Raven Press, New York, pp. 1971-1994.

Knobloch, M., Konietzko, U., Krebs, D.C., Nitsch, R.M., 2007. Intracellular Aβ and cognitive deficits precede β-amyloid deposition in transgenic arcAβ mice. Neurobiol. Aging, 28, 1297-1306.

Kordula, T., Bugno, M., Rydel, R.E., Travis, J., 2000. Mechanism of interleukin-1- and tumor necrosis factor alpha-dependent regulation of the alpha-1-antichymotrypsin gene in human astrocytes. J. Neurosci. 20, 7510-7516.

Kraus, W.L., Mcinerney, E.M., Katzenellenbogen, B.S., 1995. Ligand-dependent transcriptionally productive association of the amino- and carboxy-terminal regions of a steroid hormone nuclear receptor. Proc. Natl. Acad. Sci. USA, 92, 12314-12318.

Kreuter, J., Petrov, V.E., Kharkevich, D.A., Alyautdin, R.N., 1997. Influence of the type of surfactant on the analgesic affects induced by the peptide dalargin after its delivery across the blood–brain barrier using surfactant-coated nanoparticles. J. Control. Release, 49, 81-87.

Kreuter, J., 2001. Nanoparticulate systems for brain delivery of drugs. Adv. Drug Deliv. Rev., 47, 65-81.

Kreuter, J., 2005. Application of nanoparticles for the delivery of drugs to the brain. Int. Congr. Ser., 1277, 85-94.

Kriwet, B. and Kissel, T., 1996. Poly (acrylic acid) Microparticles widen the intercellular spaces of Caco-2 cell monolayers: An examination by confocal laser scanning microscopy. Eur. J. Pharm. Biopharm., 42, 233-240.

Kuhl, H., 2004. Mechanisms of sex steroids. Future developments. Maturitas, 47, 285–291.

Kumar, M.N.V.R., Bakowsky, U., Lehr, C.M., 2004. Preparation and characterization of cationic PLGA nanospheres as DNA carriers. Biomaterials, 25, 1771-1777.

Kwon, H.Y., Lee, J.Y., Sung, W.C., Jang, Y., 2001. Preparation of PLGA nanoparticles containing estrogen by emulsification-diffusion method. Colloids Surf. A Physicochem. Eng. Asp., 182, 123-130.

LaFerla, F.M., Troncoso, J.C., Strickland, D.K., Kawas, C.H., Jay, G., 1997. Neuronal cell death in Alzheimer's disease correlates with apoE uptake and intracellular Aβ stabilization. J. Clin. Invest., 100, 310-320.

LaFerla, F.M., Green, K.N., Oddo, S., 2007. Intracellular amyloid-β in Alzheimer's disease. Nat. Rev. Neurosci., 8, 499-509.

Lamprecht, A., Ubrich, N., Perez, M.H., Lehr, C.M., Hoffman, M., Maincent, P., 1999. Biodegradable monodispersed nanoparticles prepared by pressure homogenization-emulsification. Int. J. Pharm., 184, 97-105.

Lavelle, E.C., Sharif, S., Thomas, N.W., Holland, J., Davis, S.S., 1995. The importance of gastrointestinal uptake of particles in the design of oral delivery systems. Adv. Drug Deliv. Rev., 18, 5-22.

le Nestour, E., Marraoui, J., Lahlou, N., Roger, M., de Ziegler, D., Bouchard, P., 1993. Role of estradiol in the rise in follicle-stimulating hormone levels during the luteal-follicular transition. J. Clin. Endocrinol. Metab., 77, 439-442.

Lee, C. and Rodgers, R.J., 1990. Antinociceptive effects of elevated plus-maze exposure: influence of opiate receptor manipulations. Psychopharmacology, 102, 507-513.

Lee, C. and Rodgers, R.J., 1991. Effects of benzodiazepine antagonist, flumazenil, on antinociceptive and behavioural responses to the elevated plus-maze in mice. Neuropharmacology, 30, 1263-1267.

Lehr, C.M., Bouwstra, J.A., Tukker, J.J., Junginger, H.E., 1990. Intestinal transit of bioadhesive microspheres in an in situ loop in the rat-a comparative study with copolymer and blends on poly(acrylic acid). J. Control. Release, 13, 51-62.

Lemieux, C., Ge´linas, Y., Lalonde, J., Labrie, F., Richard, D., Deshaies, Y., 2006. Hypocholesterolemic action of the selective estrogen receptor modulator acolbifene in intact and ovariectomized rats with diet-induced hypercholesterolemia. Metab. Clin. Exp., 55, 605-613.

Leroux, J.C., Allémann, E., Doelker, E., Gurny, R., 1995. New approach for the preparation of nanoparticles by an emulsification-diffusion method. Eur. J. Pharm. Biopharm., 41, 14-18.

Lewis, D.H., 1990. Controlled release of bioactive agents from lactide/glycolide polymers. In: Chasin, M. and Langer, R. (Eds.), Biodegradable polymers as drug delivery systems. Vol. 45, Marcel Dekker, New York, pp. 1-41.

Lin, J.H., 1994. Dose-dependent pharmacokinetics: Experimental observations and theoretical considerations. Biopharm. Drug Dispos., 15, 1-31.

Lindsey, J.D., Landfield, P.W., Lynch, G., 1979. Early onset and topographical distribution of hypertrophied astrocytes in hippocampus of aging rats: a quantitative study. J. Gerontol., 34, 661-671.

Liu, M.L., Xu, X., Rang, W.Q., Li, Y.J., Song, H.P., 2004. Influence of ovariectomy and 17β-estradiol treatment on insulin sensitivity, lipid metabolism and post-ischemic cardiac function. Int. J. Cardiol., 97, 485-493.

Livingstone, C. and Collison, M., 2002. Sex steroids and insulin resistance. Clin. Sci., 102, 151-166.

Lobo, R.A., 1995. Benefits and risks of estrogen replacement therapy. Am. J. Obstet. Gynecol., 173, 982-989.

Lokind, K.B. and Lorenzen, F.H., 1996. Oral bioavailability of beta estradiol and prodrugs tested in rats, pigs and dogs. Int. J. Pharm., 127, 155-164.

Loose-Mitchell, D.S. and Stancel, G.M., 2001. Estrogens and progestins. In: Hardman, J.G., Limbird, L.E., Gilman, A.G. (Eds.), Goodman and Gilman's-The pharmacological basis of therapeutics, 10th edition, McGraw-Hill, pp. 1597-1634.

Lord, A., Kalimo, H., Eckman, C., Zhang, X.Q., Lannfelt, L., Nilsson, L.N., 2006. The Arctic Alzheimer mutation facilitates early intraneuronal Aβ aggregation and senile plaque formation in transgenic mice. Neurobiol. Aging, 27, 67-77.

Lundeen, S.G., Carver, J.M., Mckean, M.L., Winneker, R.C., 1997. Characterization of the Ovariectomized Rat Model for the Evaluation of Estrogen Effects on Plasma Cholesterol Levels. Endocrinology, 138, 1552-1558.

Lyrenas, S., Carlstrom, K., Backstrom, T., von Schoultz, B., 1981. A comparison of serum estrogen levels after percutaneous and oral administration of estradiol-17β. Br. J. Obstet. Gynaecol., 88, 181-187.

Magrané, J., Rosen, K.M., Smith, R.C., Walsh, K., Gouras, G.K., Querfurth, H.W., 2005. Intraneuronal β-amyloid expression down regulates the Akt survival pathway and blunts the stress response. J. Neurosci., 25, 10960-10969.

Mangelsdorf, D.J., Thummel, C., Beato, M., Herrlich, P., Schotz, G., Umesono, K., Blumberg, B., Kastner, P., Mark, M., Chambon, P., Evans, R.M., 1998. The nuclear receptor superfamily: the second decade. Cell, 83, 835-839.

Martucci, C.P. and Fishman, J., 1993. P450 enzymes of estrogen metabolism. Pharmacol. Ther., 57, 237-257.

Maurus, P.B. and Kaeding, C.C., 2004. Bioabsorbable Implant Material Review. Oper. Tech. Sports Med., 12, 158-160.

Mazzuoli, G., Acca, M., Pisani, D., Diacinti, D., Scarda, A., Scarnecchia, L., Pacitti, M.T., D'Erasmo, E., Minisola, S., Bianchi, G., Manfredi, G., 2000. Annual skeletal balance and metabolic bone marker changes in healthy early postmenopausal women: results of a prospective study. Bone, 26, 381–386.

McAllister, J.M., Kerin, J.F.P., Trant, J.M., Estabrook, R.W., Mason, J.I., Waterman, M.R., Simpson, E.R., 1989. Regulation of cholesterol side-chain cleavage and 17-hydroxylase/lyase activities in proliferating human theca internal cells in long term monolayer culture. Endocrinology, 125, 1959-1966.

McCool, M.F., Varty, G.B., Del Vecchio, R.A., Kazdoba, T.M., Parker, E.M., Hunter, J.C., Hyde, L.A., 2003. Increased auditory startle response and reduced prepulse inhibition of startle in transgenic mice expressing a double mutant form of amyloid precursor protein. Brain Res., 994, 99-106.

McCullough, L.D. and Hurn, P.D., 2003. Estrogen and ischemic neuroprotection: an integrated view. Trends Endocrinol. Metab., 14, 228-235.

McGee, E.A. and Hsueh, A.J., 2000. Initial and cyclic recruitment of ovarian follicles. Endocr. Rev., 21, 200-214.

Mcinerney, E.M. and Katzenellenbogen, B.S., 1996. Different regions in activation function-1 of the human estrogen receptor required for antiestrogen- and estradiol-dependent transcription activation. J. Biol. Chem., 271, 24172-24178.

Meena, A.K., Ratnam, D.V., Chandraiah, G., Ankola, D.D., Ramarao, P., Kumar, M.N.V.R., 2008. Oral Nanoparticulate Atorvastatin Calcium is

More Efficient and Safe in Comparison to Lipicure® in Treating Hyperlipidemia. Lipids, 43, 231-241.

Mehvar, R., 2001. Principles of nonlinear pharmacokinetics. Am. J. Pharm. Educ., 65, 178-184.

Mellman, I., 1996. Endocytosis and molecular sorting. Annu. Rev. Cell Dev. Biol., 12, 575-625.

Mestecky, J., Moldoveanu, Z., Michalek, S.M., Morrow, C.D., Compans, R.W., Schafer, D.P., Russell, M.W., 1997. Current options for vaccine delivery systems by mucosal routes. J. Control. Release, 48, 243-257.

Misra, A., Ganesh, S., Shahiwala, A., Shah, S.P., 2003. Drug delivery to the central nervous system: a review. J. Pharm. Pharmaceut. Sci., 6, 252-273.

Mittal, G., Sahana, D.K., Bhardwaj, V., Kumar, M.N.V.R., 2007. Estradiol loaded PLGA nanoparticles for oral administration: Effect of polymer molecular weight and copolymer composition on release behavior *in vitro* and *in vivo*. J. Control. Release, 119, 77-85.

Mittal, G. and Kumar, M.N.V.R., 2009. Impact of polymeric nanoparticles on oral pharmacokinetics: A dose-dependent case study with estradiol. J. Pharm. Sci., 98, 3730-3734.

Mochizuki, A., Tamaoka, A., Shimohata, A., Komatsuzaki, Y., Shoji, S., 2000. Aβ42-positive nonpyramidal neurons around amyloid plaques in Alzheimer's disease. Lancet, 355, 42-43.

Mohri, I., Kadoyama, K., Kanekiyo, T., Sato, Y., Kagitani-Shimono, K., Saito, Y., Suzuki, K.,Kudo, T., Takeda, M., Urade,Y.,Murayama, S., Taniike, M., 2007. Hematopoietic prostaglandin D synthase and DP1 receptor are selectively upregulated in microglia and astrocytes within senile plaques from human patients and in a mouse model of Alzheimer disease. J. Neuropathol. Exp. Neurol., 66, 469-480.

Mori, C., Spooner, E.T., Wisniewsk, K.E., Wisniewski, T.M., Yamaguch, H., Saido, T.C., Tolan, D.R., Selkoe, D.J., Lemere, C.A., 2002. Intraneuronal Aβ42 accumulation in Down syndrome brain. Amyloid, 9, 88-102.

Mueck, A.O., Seeger, H., Lippert, T.H., 2002. Estradiol metabolism and malignant disease. Maturitas, 43, 1-10.

Murakami, H., Kawashima, Y., Niwa, T., Hino, T., Takeuchi, H., Kobayashi, M., 1997. Influence of the degrees of hydrolyzation and polymerization of poly(vinylalcohol) on the preparation and properties of poly(-lactide-co-glycolide) nanoparticle. Int. J. Pharm., 149, 43-49.

Nanda, K., Bastian, L.A., Hasselblad, V., Simel, D.L., 1999. Hormone replacement therapy and the risk of colorectal cancer: a meta-analysis. Obstet. Gynecol., 93, 880-888.

Nelson, L.R. and Bulun, S.E., 2001. Estrogen production and action. J. Am. Acad. Dermatol., 45, S116-S124.

Newcomb, P.A. and Storer, B.E., 1995. Postmenopausal hormone use and risk of large-bowel cancer. J. Natl. Cancer Inst., 87, 1067-1071.

Nilsen, J., 2008. Estradiol and neurodegenerative oxidative stress. Front. Neuroendocrinol., 29, 463-475.

Nilsson, S., Makela, S., Treuter, E., Tujague, M., Thomsen, J., Andersson, G., Enmark, E., Pettersson, K., Warner, M., Gustafsson, J., 2001. Mechanisms of estrogen action. Physiol. Rev., 81, 1535–1565.

Norris, D.A., Puri, N., Sinko, P.J., 1998. The effect of physical barriers and properties on the oral absorption of particulates. Adv. Drug Deliv. Rev., 34, 135-154.

Oakley, H., Cole, S.L., Logan, S., Maus, E., Shao, P., Craft, J., Guillozet-Bongaarts, A., Ohno, M., Disterhoft, J., Van Eldik, L., Berry, R., Vassar, R., 2006. Intraneuronal β-amyloid aggregates, neurodegeneration, and neuron loss in transgenic mice with five familial Alzheimer's disease mutations: potential factors in amyloid plaque formation. J. Neurosci., 26, 10129-10140.

Oddo, S., Caccamo, A., Shepherd, J.D., Murphy, M.P., Golde, T.E., Kayed, R., Metherate, R., Mattson, M.P., Akbari, Y., LaFerla, F.M., 2003. Triple-transgenic model of Alzheimer's disease with plaques and tangles: intracellular Aβ and synaptic dysfunction. Neuron, 39, 409-421.

Oddo, S., Caccamo, A., Smith, I.F., Green, K.N., LaFerla, F.M., 2006. A Dynamic Relationship between Intracellular and Extracellular Pools of Aβ. Am. J. Pathol., 168, 184-194.

O'Hagan, D.T., 1990. Intestinal translocation of particulates–implications for drug and antigen delivery. Adv. Drug Deliv. Rev., 5, 265-285.

Ohkawa, H., Ohishi, N., Yagi, K., 1979. Assay for lipid peroxides in animal tissues by thiobarbituric acid reaction. Anal. Biochem., 95, 351-358.

Ohkura, T., Isse, K., Akazawa, K., Hamamoto, M., Yaoi, Y., Hagino, N., 1995. Long-term estrogen replacement therapy in female patients with dementia of the Alzheimer type: 7 case reports. Dementia, 6, 99-107.

Oide, T., Kinoshita, T., Arima, K., 2006. Regression stage senile plaques in the natural course of Alzheimer's disease. Neuropathol. Appl. Neurobiol., 32, 539-556.

Okamoto, C.T., 1998. Endocytosis and transcytosis, Adv. Drug Deliv. Rev., 29, 215-228.

Owen, J.A., 1975. Physiology of the menstrual cycle. Am. J. Clin. Nutr., 28, 333-338.

Owens, D.E. and Peppas, N.A., 2006. Opsonization, biodistribution, and pharmacokinetics of polymeric nanoparticles. Int. J. Pharm., 307, 93-102.

Paganini-Hill, A., 1995. Estrogen replacement therapy and stroke. Prog. Cardiovasc. Dis., 38, 223-242.

Panyam, J., Dali, M.M., Sahoo, S.K., Ma, W., Chakravarthi, S.S., Amidon, G.L., Levy, R.J., Labhasetwar, V., 2003. Polymer degradation and *in vitro* release of a model protein from poly(D,L-lactide-co-glycolide) nano- and microparticles. J. Control. Release, 92, 173-187.

Panyam, J., Labhasetwar, V., 2003. Biodegradable nanoparticles for drug and gene delivery to cells and tissue. Adv. Drug Deliv. Rev., 55, 329-347.

Pardridge, W.M., 2005. Drug and gene targeting to the brain via blood–brain barrier receptor-mediated transport systems. Int. Cong. Ser., 49, 49-62.

Pardridge, W.M., Buciak, J.L., Friden, P.M., 1991. Selective transport of an anti-transferrin receptor antibody through the blood–brain barrier *in vivo*. J. Pharmacol. Exp. Ther., 259, 66-70.

Parihar, M.S. and Hemnani, T., 2004. Alzheimer's disease pathogenesis and therapeutic interventions. J. Clin. Neurosci., 11, 456-467.

Parini, P., Angelin, B., Stavreus-Evers, A., Freyschuss, B., H. Eriksson, Rudling, M., 2000. Biphasic effects of the natural estrogen 17β-estradiol on hepatic cholesterol metabolism in intact female rats. Arterioscler. Thromb. Vasc. Biol., 20, 1817-1823.

Peetla, C. and Labhasetwar, V., 2009. Effect of molecular structure of cationic surfactants on biophysical interactions of surfactant modified nanoparticles with a model membrane and cellular uptake. Langmuir, 25, 2369-2377.

Pellow, S., Choplin, P., File, S.E., Briley, M., 1985. Validation of open : closed arms entries in an elevated plus-maze as a measure of anxiety in the rat. J. Neurosci. Methods, 14, 149-167.

Pines, A., 2002. Hormone therapy and the cardiovascular system. Maturitas, 43(Suppl. 1), S3–S10.

Price, B.H., Gurvit, H., Weintraub, S., Geula, C., Leimkuhler, E., Mesulam, M., 1993. Neuropsychological patterns and language deficits in 20 consecutive cases of autopsy-confirmed Alzheimer's disease. Arch. Neurol., 50, 931-937.

Quigley, M.E.T., 1987. Estrogen therapy arrests bone loss in elderly women. Am. J. Obstet. Gynecol., 156, 1516-1523.

Quintanar-Guerrero D., Fessi, H., Allémann E., Doelker, E., 1996. Influence of stabilizing agents and preparative variables on the formation of poly(D,L-lactic acid) nanoparticles by an emulsification-diffusion technique. Int. J. Pharm., 143, 133-141.

Quintanar-Guerrero, D., Allémann, E., Fessi, H., Doelker, E., 1998. Preparation techniques and mechanisms of formation of biodegradable nanoparticles from preformed polymers. Drug Dev. Ind. Pharm., 24, 1113-1128.

Ransom, B., Behar, T., Nedergaard, M., 2003. New roles for astrocytes (stars at last). Trends Neurosci., 26, 520-522.

Ratnam, D.V., Chandraiah, G., Sonaje, K., Boomi, V., Bhardwaj, V., Ramarao, P., Kumar, M.N.V.R., 2008. A potential therapeutic strategy for diabetes and its complications in the form of co-encapsulated antioxidant nanoparticles (NanoCAPs) of ellagic acid and coenzyme Q10:

Preparation and evaluation in streptozotocin induced diabetic rats. J. Biomed. Nanotechnol., 4, 33-43.

Rifici, V.A. and Khachadurian, A.K., 1992. The Inhibition of Low-Density Lipoprotein Oxidation by 17-β estradiol. Metabolism, 41, 1110-1114.

Roney, C., Kulkarni, P., Arora, V., Antich, P., Bonte, F., Wu, A., Mallikarjuana, N.N., Manohar, S., Liang, H.F., Kulkarni, A.R., Sung, H.W., Sairam, M., Aminabhavi, T.M., 2005. Targeted nanoparticles for drug delivery through the blood–brain barrier for Alzheimer's disease. J. Control. Release, 108, 193-214.

Rossouw, J.E., Anderson, G.L., Prentice, R.L., LaCroix, A.Z., Kooperberg, C., Stefanick, M.L., Jackson, R.D., Beresford, S.A., Howard, B.V., Johnson, K.C., Kotchen, J.M., Ockene, J., 2002. Risks and benefits of estrogen plus progestin in healthy postmenopausal women: principal results From the Women's Health Initiative randomized controlled trial, JAMA, 288, 321-333.

Ruggiero, R.J. and Likis, F.E., 2002. Estrogen: Physiology, pharmacology, and formulations for replacement therapy. J. Midwifery Womens Health, 47, 130-138.

Rymer, J. and Morris, E.P., 2000. Extracts from 'clinical evidence'. Menopausal symptoms. Br. M. J., 321, 1516-1519.

Ryu, J.K., Franciosi, S., Sattayaprasert, P., Kim, S.U., McLarnon, J.G., 2004. Minocycline inhibits neuronal death and glial activation induced by beta amyloid peptide in rat hippocampus. Glia, 48, 85-90.

Sah, H., 1997. Microencapsulation techniques using ethyl acetate as a dispersed solvent: Effects of its extraction rate on the characteristics of PLGA microspheres. J. Control. Release, 47, 233-245.

Sahana, D.K., Mittal, G., Bhardwaj, V., Kumar, M.N.V.R., 2008. PLGA nanoparticles for oral delivery of hydrophobic drugs: Influence of organic solvent on nanoparticle formation and release behavior *in vitro* and *in vivo* using estradiol as a model drug. J. Pharm. Sci., 97, 1530-1542.

Sahoo, S.K., Panyam, J., Prabha, S., Labhasetwar, V., 2002. Residual polyvinyl alcohol associated with poly (d,l-lactide-co-glycolide) nanoparticles

affects their physical properties and cellular uptake. J. Control. Release, 82, 105-114.

Schipper, N.G., Olsson, S., Hoogstraate, J.A., de Boer, A.G., Varum, K.M., Artursson, P., 1997. Chitosans as absorption enhancers for poorly absorbable drugs 2: mechanism of absorption enhancement. Pharm. Res., 14, 923-929.

Schroeder, U., Sommerfeld, P., Sabel, B.A., 1998. Efficacy of oral dalargin-loaded nanoparticles delivery across blood–brain barrier. Peptides, 19, 777-780.

Schubert, P., Ogata, T., Marchini, C., Ferroni, S., 2001. Glia-related pathomechanisms in Alzheimer's disease: a therapeutic target? Mech. Ageing Dev., 123, 47-57.

Schwabe, J.W.R., Chapman, L., Finch, J.T., Rhodes, D., 1993. The crystal structure of the estrogen receptor DNA-binding domain bound to DNA: how receptors discriminate between their response elements. Cell, 75, 567–578.

Seifert, G., Schilling, K., Steinhauser, C., 2006. Astrocyte dysfunction in neurological disorders: a molecular perspective. Nat. Rev. Neurosci., 7, 194-206.

Selkoe, D.J., 2000. The origins of Alzheimer's disease: A is for amyloid. JAMA, 283, 615-617.

Shen, B.J., Todaro, J.F., Niaura, R., McCaffery, J.M., Zhang, J., Spiro, A., Ward K.D., 2003. Are metabolic risk factors one unified syndrome? Modeling the structure of the metabolic syndrome x. Am. J. Epidemiol., 157, 701-711.

Sherwin, B.B., 1997. Estrogen effects on cognition in menopausal women. Neurology, 48, S21-S26.

Sherwin, B.B., 1999. Can estrogen keep you smart? Evidence from clinical studies. J. Psych. Neurosci., 24, 315-321.

Shie, F.S., LeBoeuf, R.C. Jin, L.W., 2003. Early intraneuronal Aβ deposition in the hippocampus of APP transgenic mice. Neuroreport., 14, 123-129.

Shinoda, M., Latour, M.G., Lavoie, J.M., 2002. Effects of physical training on body composition and organ weights in ovariectomized and hyperestrogenic rats. Int. J. Obes., 26, 335-343.

Shive, M.S., Anderson, J.M., 1997. Biodegradation and biocompatibility of PLA and PLGA microspheres. Adv. Drug. Deliv. Rev., 28, 5-24.

Simoni, M., Gromoll, J., Neischlag, E., 1997. The follicle-stimulating hormone receptor: biochemistry, molecular biology, physiology, and pathophysiology. Endocr. Rev., 18, 739–773.

Simpkins, J.W., Green, P.S., Gridley, K.E., Singh, M., de Fiebre, N.C., Rajakumar, G., 1997. Role of estrogen replacement therapy in memory enhancement and the prevention of neuronal loss associated with Alzheimer's disease. Am. J. Med., 103, 19S-25S.

Simpkins, J.W. and Singh, M., 2008. More than a decade of estrogen neuroprotection. Alzheimers Dement., 4, S131-S136.

Singh, R. and Lillard Jr. J.W., 2009. Nanoparticle-based targeted drug delivery. Exp. Mol. Pathol., 86, 215-223.

Sitruk-Ware, R., 1990. Estrogen therapy during menopause. Practical treatment recommendations. Drugs, 39, 203-217.

Sloane, J.A., Hollander, W., Rosene, D.L., Moss, M.B., Kemper, T., Abraham, C.R., 2000. Astrocytic hypertrophy and altered GFAP degradation with age in subcortical white matter of the rhesus monkey. Brain Res., 862, 1-10.

Small, G.W., Rabins, P.V., Barry, P.P., Buckholtz, N.S., DeKosky, S.T., Ferris, S.H., Finkel, S.I., Gwyther, L.P., Khachaturian, Z.S., Lebowitz, B.D., McRae, T.D., Morris, J.C., Oakley, F., Schneider, L.S., Streim, J.E., Sunderland, T., Teri, L.A., Tune, L.E., 1997. Diagnosis and treatment of Alzheimer’s disease and related disorders. Consensus statement of the American Association of Geriatric Psychiatry, the Alzheimer’s association and the American Geriatric Society. JAMA, 278, 1363-1371.

Song, C.X., Labhasetwar, V., Murphy, H., Qu, X., Humphrey, W.R., Shebuski, R.J., Levy, R.J., 1997. Formulation and characterization of biodegradable nanoparticles for intravascular local drug delivery. J. Control. Release, 43, 197-212.

Speiser P. and Kreuter J., 1976. *In vitro* studies of poly(metylmethacrylate) adjuvants. J. Pharm. Sci., 65, 1624-1627.

Srinivas, P., 1999. Diagnosis and management of Alzheimer's disease - an update. Med. J. Malaysia, 54, 541-549.

Srinivasan, K., Viswanad, B., Asrat, L., Kaul, C.L., Ramarao, P., 2005. Combination of high-fat diet-fed and low-dose streptozotocin treated rat: a model for type 2 diabetes and pharmacological screening. Pharmacol. Res., 52, 313-320.

Stampfer, M.J. and Colditz, G.A., 1991. Estrogen replacement therapy and coronary heart disease: a quantitative assessment of the epidemiologic evidence. Prev. Med., 20, 47-63.

Stevenson, J.C., 1990. Pathogenesis, prevention and treatment of osteoporosis. Obstet. Gynecol., 75, 36S-41S.

Stevenson, J.C., 1998. Various actions of oestrogens on the vascular system. Maturitas, 30, 5-9.

Stevenson, J.C., 1999. Optimising delivery systems for HRT. Maturitas, 33, S31-S38.

Stevenson, J.C., 2000. Cardiovascular effects of oestrogens. J. Steroid Biochem. Mol. Biol., 74, 387-393.

Stevenson, J.C., 2005. Justification for the use of HRT in the long-term prevention of osteoporosis. Maturitas, 51, 113-126.

Sun, W., Xie, C., Wang, H., Hu, Y., 2004. Specific role of polysorbate 80 coating on the targeting of nanoparticles to the brain. Biomaterials, 25, 3065-3071.

Swaan, P.W., 1998. Recent advances in intestinal macromolecular drug delivery via receptor-mediated transport pathways. Pharm. Res., 15, 826-834.

Tamai, I. and Tsuji, A., 1996. Drug delivery through the blood brain barrier. Adv. Drug Deliv. Rev., 19, 401-424.

Tanna, N., 2003a. Hormone replacement therapy: (1) an overview. Pharm. J., 271, 615-617.

Tanna, N., 2003b. Hormone replacement therapy: (2) risks and benefits. Pharm. J., 271, 646-648.

Tolbert, T. and Oparil, S., 2001. Cardiovascular Effects of Estrogen. Am. J. Hypertens., 14, 186S–193S.

Tsai, M.J. and O'Malley, B.W., 1994. Molecular mechanisms of action of steroid/thyroid receptor superfamily members. Annu. Rev. Biochem., 63, 451-486.

Ueki, A., Goto, K., Sato, N., Iso, H., Morita, Y., 2006. Prepulse inhibition of acoustic startle response in mild cognitive impairment and mild dementia of Alzheimer type. Psychiatry Clin. Neurosci., 60, 55-62.

Umesono, K. and Evans, R.M., 1989. Determinants of target gene specificity for steroid/thyroid hormone. Cell, 57, 1139-1146.

Van, B.B., Vanhoutte, G., Pirici, D., Van, D.D., Wils, H., Cuijt, I., Vennekens, K., Zabielski, M., Michalik, A., Theuns, J., De Deyn, P.P., Van der Linden, A., Van Broeckhoven, C., Kumar-Singh, S., 2008. Intraneuronal amyloid β and reduced brain volume in a novel APP T714I mouse model for Alzheimer's disease. Neurobiol. Aging, 29, 241-252.

Vandervoort, J. and Ludwig, A., 2002. Biocompatible stabilizers in the preparation of PLGA nanoparticles: a factorial design study. Int. J. Pharm., 238, 77-92.

Vasudevan, N. and Pfaff, D.W., 2008. Non-genomic actions of estrogens and their interaction with genomic actions in the brain. Front. Neuroendocrinol., 29, 238-257.

Vauthier, C. and Bouchemal, K., 2009. Methods for the Preparation and Manufacture of Polymeric Nanoparticles. Pharm. Res., 26, 1025-1058.

Warner, M., Nilsson, S., Gustafsson, J.A., 1999. The estrogen receptor family. Curr. Opin. Obstet. Gynecol., 11, 249-254.

Wei, H.F., Li, L., Song, Q.J., Ai, H.X., Chu, J., Li, W., 2005. Behavioural study of the D-galactose induced aging model in C57BL/6J mice. Behav. Brain Res., 157, 245-251.

Weiser, M.J., Foradori, C.D., Handa, R.J., 2008. Estrogen receptor beta in the brain: From form to function. Brain Res. Rev., 57, 309-320.

Wirths, O., Multhaup, G., Bayer, T.A., 2004. A modified β-amyloid hypothesis: intraneuronal accumulation of the b-amyloid peptide – the first step of a fatal cascade. J. Neurochem., 91, 513-520.

Wise, P.M. and Dubal, D.B., 2000. Estradiol Protects Against Ischemic Brain Injury in middle-aged rats. Biol. Reprod., 63, 982-985.

Wise, P.M., Dubal, D.B., Wilson, M.E., Rau, S.W., Liu, Y., 2001. Estrogens: trophic and protective factors in the adult brain. Front. Neuroendocrinol., 22, 33-66.

Wise, P.M., 2006. Estrogen therapy: does it help or hurt the adult and aging brain? Insights derived from animal models. Neuroscience, 138, 831-835.

Wolberg, H. and Lippoldt, A., 2002. Tight junctions of the blood–brain barrier: development, composition and regulation. Vasc. Pharmacol., 38, 323-337.

Xu, X.H. and Zhao, T.Q., 2002. Effects of puerarin on D-galactose-induced memory deficits in mice. Acta Pharmacol. Sin., 23, 587-590.

Yaffe, K., Sawaya, G., Lieberburg, I., Grady, D., 1998. Estrogen therapy in postmenopausal women: effects on cognitive function and dementia. JAMA, 279, 688-695.

Yeh, P-Y., Ellens H., Smith P.L., 1998. Physiological considerations in the design of particulate dosage forms for oral vaccine delivery. Adv. Drug Deliv. Rev., 34, 123-133.

Yen, S.S.C., Martin, P.L., Burnier, A.M., Czekala, N.M., Greaney, M.O., Callantine, M.R., 1975. Circulating estradiol, estrone, and gonadotrophin levels following the administration of orally active 17β-estradiol in postmenopausal women. J. Clin. Endocrinol. Metab., 40, 518-521.

Yin, Y.S., Chen, D.W., Qiao, M.X., Wei, X.Y., Hu, H.Y., 2007. Lectin-conjugated PLGA nanoparticles loaded with thymopentin: Ex vivo bioadhesion and *in vivo* biodistribution. J. Control. Release, 123, 27-38.

Yoncheva, K., Lizarraga, E., Irache, J.M., 2005. Pegylated nanoparticles based on poly(methyl vinyl ether-co-maleic anhydride): preparation and evaluation of their bioadhesive properties, Eur. J. Pharm. Sci., 24, 411-419.

Yoo, J.W. and Lee, C.H., 2006. Drug delivery systems for hormone therapy. J. Control. Release, 112, 1-14.

Zambaux, M.F., Bonneaux, F., Gref, R., Maincent, P., Dellacherie, E., Alonso, M.J., Labrude, P., Vigneron, C., 1998. Influence of experimental parameters on the characteristics of poly(lactic acid) nanoparticles prepared by double emulsion method, J. Control. Release, 50, 31-40.